1967

# Flow distribution in cryogenic heat exchangers

Donald Winston Woodward
*Lehigh University*

# FLOW DISTRIBUTION

# IN

# CRYOGENIC HEAT EXCHANGERS

by

DONALD WINSTON WOODWARD

A THESIS

Presented to the Graduate Faculty

of Lehigh University

in Candidacy for the Degree of

Master of Science

Lehigh University

1967

This thesis is accepted and approved in partial fulfillment of the requirements for the degree of Master of Science.

______________________

______________________
Professor in charge

______________________
Head of the Department

## ACKNOWLEDGMENTS

I would like to acknowledge the valuable assistance I received from Professor A. S. Foust, my thesis advisor, and Professor L. A. Wenzel at Lehigh University.

I am also indebted to Mr. Glenn Kinard and Mr. Lee Gaumer for their advice and assistance while acting as my thesis advisors from Air Products and Chemical Co., Inc.

I would like to thank Air Products and Chemical Co., Inc. for the use of their facilities.

To my faithful wife, Ginny, for her encouragement and many hours spent typing I am forever grateful.

TABLE OF CONTENTS

## LIST OF FIGURES

LIST OF TABLES

## ABSTRACT

The major portion of the text is concerned with developing design procedures for single and two phase flow in the tubeside distribution system. Distribution systems such as buttonhook and ring headers are designed to give minimum flow variations in their branch streams. These flow variations are found by a combination of solving the First Law of Thermodynamics for each branch stream and a special convergence technique. Flow rates in the tube bundle can then be analyzed with respect to variations of tube length and inside diameter, plugged tubes, and phase separation.

The actual exchanger duty can be analyzed dividing the exchanger into many smaller imaginary exchangers each carrying one of the discrete tubeside flows. For each of the imaginary exchangers the shellside flow as a percentage of the total shellside flow is equal to the number of tubes carrying each flow as a percentage of the total number of tubes. Actual exchanger duty is found by plotting cooling curves while maintaining a fixed UA and fixed inlet temperatures of both warming and cooling streams.

A procedure for checking and designing against instability of flow in a system is also presented. This includes slug flow in the distribution system, tube pulsations as a function of time, and the case where tubes operating with equal pressure drops may carry as many as three two-phase flow rates.

To further illustrate the above procedures and to develop "short cuts" a typical cryogenic heat exchanger was analyzed.

## GENERAL NOMENCLATURE

$A$ area ($ft^2$)
$C_p$ specific heat (Btu's/lb °F)
$D$ diameter (inches)
$f$ fanning fraction factor [3]
$G$ total mass flow rate ($lb/ft^2$-hr)
$G'$ gas flow rate ($lb/ft^2$-hr)
$g_c$ gravitational constant ($ft/sec^2$)
$H$ vertical height (ft)
$h$ vertical height (ft)
I.D. inside tube diameter (inches)
$K$ proportionality constant
$K'$ constant in Hughmark's slip correlations [5] (see fig 4)
$K_c$ coefficient of contraction [7] (see fig 6)
$K_e$ coefficient of expansion [8] (see fig 7)
$L$ length (ft)
$L'$ liquid flow rate ($lb/ft^2$-hr)
$L''$ percentage loss of duty
$M$ flow (moles/hr)
MW molecular weight
$m$ flow (lb/sec)
$\bar{m}$ maldistribution of flow (± percentage of mean)
$N$ number of discrete flows
$N_{Fr}$ Froude Number, $12540q^2/D^5$
$N_{Re}$ Reynold Number, $DG/12\mu$
$N_{Re'}$ two phase Reynolds Number with slip, $DG/12(R_L\mu_L + R_G\mu_G)$
NT total number of heat exchange tubes
O. D. outside tube diameter (inches)
$P$ pressure (psi)
$\Delta P^*$ fictitious pressure drop (see p.11)
$Q$ heat transfer (Btu's/hr)
$Q'$ volumetric flow rate ($ft^3/sec$)
$q$ flow rate ($ft^3/sec$)
$R_L$ liquid volume fraction with slip
$R_V$ gas volume fraction with slip
$R_{L'}$ liquid volume fraction without slip
$R_{V'}$ gas volume fraction without slip
$R_{V''}$ $Q'_G/Q'_L$
$S_a$ cross sectional area upstream of an expansion or downstream of a contraction
$S_b$ cross sectional area downstream of an expansion or upstream of a contraction
$T$ temperature (°F)
$\Delta T_{LM}$ log mean temperature difference, $(T_{HIGH} - T_{LOW})/\log(T_{HIGH}/T_{LOW})$
$t$ time (seconds)
$U$ overall outside heat transfer coefficient (Btu's/hr-°F-$ft^2$)
$V$ velocity (ft/sec)

| | |
|---|---|
| $Z$ | Hughmark's hold-up parameter [5], $N_{Re}^{1/6} N_{Fr}^{1/8} R_L^{-\frac{1}{4}}$ (see fig 4) |
| $\gamma$ | surface tension (dynes/cm) |
| $\Delta$ | change |
| $\epsilon$ | pipe roughness factor [10] |
| $\lambda$ | heat of vaporization (Btu's/lb) |
| $\lambda'$ | Baker chart parameter [9] (see fig 8), $((\rho_G/.075)(\rho_L/62.3))^{\frac{1}{2}}$ |
| $\mu$ | viscosity (lb/ft-hr) |
| $\mu'$ | viscosity (cp) |
| $\mu_c$ | critical viscosity (lb/ft-hr) |
| $\pi$ | 3.1416 |
| $\rho$ | density (lb/ft$^3$) |
| $\Psi$ | Baker Chart parameter [9] (see fig 8), $((73/\gamma_L)(\mu_L 62.3/\rho_L)^2)^{1/3}$ |
| $\partial$ | partial derivative |

Subscripts

| | |
|---|---|
| B | refers to branch stream off of ring header |
| f | refers to frictional forces |
| G | refers to gas flow |
| H | refers to ring header |
| L | refers to liquid flow |
| P | refers to symmetrical piping |
| T | refers to tubes |
| TP | refers to two phase flow |
| TS | refers to tube sheet |
| TSH | refers to tube sheet header |

numbers (1, 2, 3 etc.) and lower case letters (a, b, c etc.) refers to specific positions defined in particular section

## FOOTNOTES

Footnotes are denoted by a superscript with a circle ie. [1]. These circled numbers refer to page 108.

## INTRODUCTION

The purpose of this study is to develop a design procedure for the distribution system of a coil wound and plate-fin heat exchanger. Both single and two phase flow are considered. Instabilities which may exist will be discussed with ways to design in a more stable region. A procedure for calculating maldistribution for any system and its effect on the loss of exchanger duty is also presented.

A coil-wound heat exchanger briefly is one in which equilength tubes are wound around a mandrel in layers of alternating direction. For smaller exchangers (see fig. 1) the tubes are connected to buttonhook headers and for the larger exchangers they are connected at the entrance and exit to tubesheets (see fig. 2). Coil wound exchangers have the advantage of operating with very high pressures. Some may be as large as 14 feet in diameter and 75 feet long.

A plate-fin or core heat exchanger is formed by brazing aluminum plates and corrugated aluminum together in a molten salt bath (see fig. 3). It has the advantage of large heat exchange surface area per volume of exchanger (450 $ft^2/ft^3$ of exchanger volume).

## GENERAL DESIGN PROCEDURE

To get maximum performance from a heat exchanger it is desirable to evenly distribute a single stream to numerous heat exchange passages or tubes. The most economical means to this is by a buttonhook header for smaller coil-wound exchangers (see fig. 1) and ring headers for larger models (see fig. 2). The branch streams from the ring headers are connected to tubesheets. If the number of tubesheets is one or two, symmetrical piping is used (see fig. 2). For core exchangers either a straight manifold or symmetrical piping is connected to a passage header (see fig. 3).

It is assumed that a certain amount of pressure drop has been allotted to the heat exchange system. In other words, the entrance and exit pressures are known. One would wish to have as much of this pressure drop as possible in the tube bundle to enhance the heat transfer coefficient. However, as pressure drop is sacrificed from the distribution system to the heat exchange area the maldistribution of flow increases. As the heat transfer coefficient increases, the exchanger duty increases with fixed area. As the maldistribution increases, the exchanger duty decreases again assuming fixed area . A loss of exchange duty will cause a loss of production. In designing the distribution system, the cost of the header plus the cost of the loss of production should be minimized. The cost of the distributor depends on the cost of material, fabrication, insulation, and installation. The design of the distribution system influences maldistribution, which affects loss of duty, which in turn is proportional to loss of production. The total minimum cost for various distribution systems will assure an optimum design.

Since piping is available in discrete diameters the possible combinations of header and branch stream diameters are limited. This allows one to assume a design and calculate the total cost, repeating with a new design until the minimum cost is realized. Any other method of solution would result in fractional pipe sizes of no practical use. One now wishes to find two points in the system where the pressure is common to all branch streams; usually the inlet and outlet. It is now possible to add up all the pressure drops for each branch stream and solve for the flow rate through each branch. The maldistribution is then known from which the loss of exchanger duty may be found.

Pipe sizes between one and three inches are available at every one half inch interval; from four inches on, at every two inch interval. A rough first estimate of header and branch pipe diameter can be obtained from the pipe flow chart in Perry's Chemical Engineers Handbook (1), based on $\Delta P/L$. For frictional pressure drop ($\Delta P_F'/L$) needed in the pipe flow chart, table 1, has been developed for the first trial of the header design. Values for table 1 were obtained by taking several optimum designs and working backwards across the pipe flow chart. If sufficient data is not available for the chart the diameter may be estimated from

$$D = \sqrt{4.734m/\sqrt{\rho}}$$

where D = diameter in inches
m = mass rate in lb/sec
$\rho$ = density in lb/ft$^3$.

Pressure drop equations for each resistance encountered are written. They have all been derived empirically by methods described in the articles of the footnotes. In developing the pressure drop equations, irreversible energy loss due to a flow disturbance caused by change in direction, friction, and turbulence is taken into account plus any reversible energy due to a change in velocity or static head.

Equation 1

$$\Delta P_{12} = 0.000135\rho\left[1.8V_2^2 - 0.368V_1V_2\right] \quad [2]$$

or

$$\Delta P_{12} = 4.5381\rho\left[\frac{1.8q_2^2}{D_2^4} - \frac{0.368q_1q_2}{D_1^2D_2^2}\right]$$

Type of flow - split flow

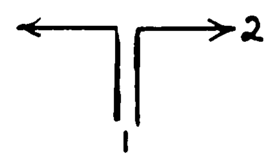


Equation 2

$$\Delta P_{12} = \frac{174fq^2L\rho}{D^5} \quad [3]$$

Type of flow - straight pipe

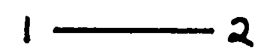


Equation 3

$$\Delta P_{12} = 0.000135\rho\left[1.8V_2^2 - 0.368V_1V_2\right] \quad [2]$$

or

$$\Delta P_{12} = 4.5381\rho\left[\frac{1.8q_2^2}{D_2^4} - \frac{0.368q_1q_2}{D_1^2D_2^2}\right]$$

Type of flow - branch pipe 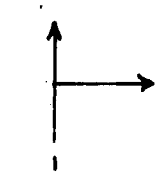

**Equation 4**

$$\Delta P_{12} = \rho \frac{K_e V_1^2}{2g_c} + \frac{(V_2^2 - V_1^2)\rho}{2g_c} \quad ④$$

or

$$\Delta P_{12} = 3.6283\rho\left((K_e - 1)\frac{q_1^2}{D_1^4} + \frac{q_2^2}{D_2^4}\right)$$

Type of flow - sudden expansion 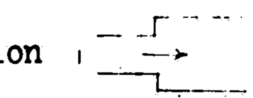

Equation 5

$$\Delta P_{12} = \rho \frac{K_c V_2^2}{2g_c} + \frac{(V_2^2 - V_1^2)\rho}{2g_c} \quad ④$$

or

$$\Delta P_{12} = 3.6283\rho\left((K_c + 1)\frac{q_2^2}{D_2^4} - \frac{q_1^2}{D_1^4}\right)$$

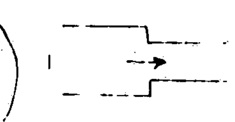

Type of flow - sudden contraction

Equation 6

$$\Delta P_{12} = 0.000135\rho\left\langle 1.36V_2^2 - 0.64V_1^2 - 0.72V_1V_2 \right\rangle \quad ②$$

or

$$\Delta P_{12} = 4.5381\rho\left\langle \frac{1.36q_2^2}{D_2^4} - \frac{0.64q_1^2}{D_1^4} - \frac{0.72q_1q_2}{D_1^2D_2^2} \right\rangle$$

Type of flow - branch flow 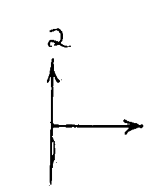

**Equation 7**

$$\Delta P_{12} = 0.000135\rho\left\langle 2V_2^2 - 0.05V_1^2 - 2V_2\left(0.205V_3\frac{q_3}{q_2} \quad V_1\frac{q_1}{q_2}\right) \right\rangle \quad ②$$

or

$$\Delta P_{12} = 4.5381\rho\left\langle \frac{2q_2^2}{D_2^2} - \frac{2.05q_1^2}{D_1^2} - \frac{0.41q_3^2}{D_2^2 D_3^2} \right\rangle$$

Type of flow - join branch

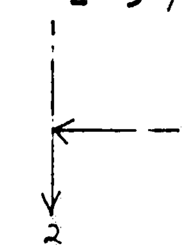


Equation 8

$$\Delta P_{12} = 0.000135\rho\left\langle 2V_2^2 - 0.4V_1^2 - 0.41V_2\left(\frac{V_3q_3}{q_2} + \frac{V_1q_1}{q_2}\right) \right\rangle$$ 2

or

$$\Delta P_{12} = 4.5381\rho\left\langle \frac{2q_2^2}{D_2^4} - \frac{0.4q_1^2}{D_1^4} - \frac{0.82q_1^2}{D_1^2 D_2^2} \right\rangle$$

Type of flow - join flow

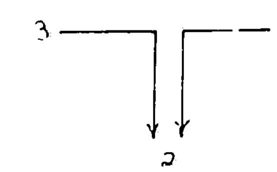


Equation 9

$$\Delta P_{12} = 0.000135\rho\left\langle 2V_2^2 - 0.4V_1^2 - 2V_2\left(\frac{0.205V_1q_1}{q_2} - \frac{V_3q_3}{q_2}\right) \right\rangle$$ 2

or

$$\Delta P_{12} = 4.5381\rho\left\langle \frac{2q_2^2}{D_2^4} - \frac{0.4q_1^2}{D_1^4} - \frac{0.41q_1^2}{D_1^2 D_2^2} - \frac{2q_3^2}{D_2^2 D_3^2} \right\rangle$$

Type of flow - join branch

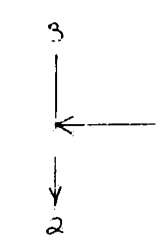


Equation 10

$$\Delta P_{12} = 0.000135\rho\, 1.2V_2^2$$ 2

or

$$\Delta P_{12} = 5.4457\rho\frac{q^2}{D^4}$$

Type of flow - elbows (std.)

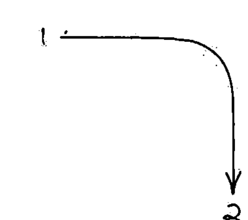

**Equation 11**

$$\Delta P_{12} = 0.000135\rho\left\langle 1.8V_2^2 - 0.368V_1V_2 \right\rangle \quad [2]$$

or

$$\Delta P_{12} = 4.5381\rho\left\langle \frac{1.8q_2^2}{D_2^4} - \frac{0.368q_2^2}{D_2^2 D_1^2} \right\rangle$$

Type of flow - bend with capped tee 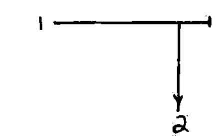

The above equations are especially suited for turbulent flow with appreciable entrance effects. If the change in density is greater than 10%, the equations will lose accuracy. They may also be used for homogeneous two phase flow by using the homogeneous density.

For nonhomogeneous two phase flow the following method should be used for frictional pressure drop in a straight pipe. Calculate the liquid volume fraction in the pipe using slip correlations of Hughmark [5] (see fig. 4).

$$Z = (N_{Re}')^{1/6}(N_{Fr})^{1/8}(R_L')^{-\frac{1}{4}}$$

$N_{Re}'$ = two phase Reynold number

$$= \frac{(6.6 \times 10^5)q\rho}{D(R_L\mu_L + R_G\mu_G)} \text{ or } \frac{DG}{12(R_L\mu_L + R_G\mu_G)}$$

$N_{Fr}$ = Froude number

$$= \frac{12540q^2}{D^5}$$

$R'$ = volume fraction without slip
$R$ = volume fraction with slip
$L$ refers to liquid
$G$ refers to gas
$R_L = 1 - K'R_G'$
$K'$ = constant from fig. 4

One must first assume no slip, find $K'$ from fig. 4, and calculate $R_L$. $R_L$ may be used to calculate a new value for $N_{Re}'$. Repeat this procedure until convergence is reached. If it does not converge, no slip may be assumed. The limits of this correlation are:

$$1 < (N_{Re}')^{1/6}(N_{Fr})^{1/8}(R_L')^{-\frac{1}{4}} < 130.$$

In order to read the two phase pressure drop from the Chenowith-Martin-Lapin-Bauer curves (6), the fictitious single phase pressure drops must first be found. The fictitious liquid pressure drop is calculated by assuming liquid only is flowing in the pipe at a G rate (lb/hr-ft$^2$) equal to that of the two phase fluid. Similarly the fictitious gas pressure drop is calculated by assuming gas only is flowing in the pipe at a G rate (lb/hr-ft$^2$) equal to that of the two phase fluid. The limits of the $\Delta P_{TP}$ correlations are :

$$\Delta P_G^*/\Delta P_L^* < 1000 \text{ or } N_{Re} > 3000.$$

The pressure drop due to the head may be found by looking at differential lengths of pipe or tubing.

$$\Delta P \text{ head} = \sum_{i=0}^{n}(\rho_L R_L + \rho_G R_G)_i(\Delta h_i)/144$$

where i refers to the differential vertical segment, $\Delta h_i$ (ft), and n is the number of segments

For constant gas-liquid ratios this reduces to

$$\Delta P \text{ head} = (\rho_L R_L + \rho_G R_G)H/144$$

where H is the vertical height (ft).

When there exists cooling or heating through tube walls the density of the tubeside fluid will change. With a constant mass flow rate the velocity will therefore change. By Bernoulli's equation this velocity change will be accompanied by a corresponding pressure change.

$$\Delta P_{12} = \frac{(V_2^2 - V_1^2)}{2g_c}\rho$$

or

$$\Delta P_{12} = \frac{3.6282}{D^4}\rho(q_2^2 - q_1^2)$$

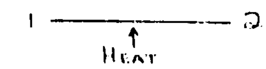


Symbols used in pressure drop equations:

$\Delta P_{12}$ = pressure drop from 1 to 2 (psi)
$D$ = inside diameter (inches)
$V$ = velocity (ft/sec)
$q$ = flow rate ($ft^3$/sec)
$\rho$ = density ($lb/ft^3$)
$N_{Re} = 55004\ qD/\mu$
$f$ = fanning friction factor 3
= $16/N_{Re}$ for $N_{Re} < 2000$
= see ref 3 for $N_{Re} > 3000$
$L$ = pipe length (ft)
$K_e$ = coefficient of expansion 7 (see fig. 6)
$K_c$ = coefficient of contraction 8 (see fig. 7)
$\mu$ = viscosity (lb/ft-hr)
$G$ = mass flow rate ($lb/hr.ft^2$)

The two common pressure points described earlier must now be defined. For ring headers at the entrance and exit of the bundles, the entrance and exit tubesheets are all at different pressures. If one were to choose the inlet and outlet pressures as common points and then sum the pressure drops for each branch stream he would have four unknown diameters in each equation. These diameters are of the inlet header, inlet branch, outlet branch, and outlet header streams. To do a trial and error solution of the pressure drop equations one would have to try a very large number of diameter combinations. In order to avoid this task one may assume a common pressure point at the center of the tube bundle, ie. one half a tube length. This is by no means rigorous. Consider that each entrance tubesheet sees a common average exit tubesheet pressure because of the fact that entrance and exit tubesheets are randomly connected and each tubesheet has approximately the same number of tubes connected to each exit tubesheet. Similiarly each exit tubesheet sees a common average entrance tubesheet pressure. One may get a feel for the fact that most of the tubes are concentrated about a single pressure at the middle of the bundle, assuming pressure drop is a linear function of length. Presented graphically:

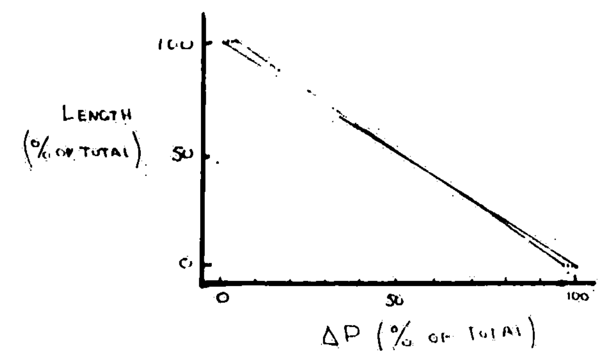


Each point at the 0 and 100% length line represents a tubesheet. Since $\Delta P$ is assumed a linear function of length and each tubesheet is connected to another tubesheet by an equal number of tubes, straight lines may be drawn connecting all combinations of tubesheets. It is apparent that most will cross at a point of 50% length and 50% $\Delta P$. As was stated before this is not rigorous but will make trial and error solution less complicated. Actually the pressure drop at this 50% point assumes a normal distribution.

For any type of symmetrical piping pressure drops are equal in all branches. If one has a ring header at the entrance and symmetrical piping at the outlet, common pressure points exist at the inlet, exit tubesheets and exit.

The common pressure points for most systems have now been defined and the distribution system can now be designed. It has been assumed that the tube bundle or core has already been designed and the average pressure drop across them is known.

For symmetrical piping one assumes equal flow of split streams and estimates pipe diameters as described earlier. Since all streams are equal, one may sum all pressure drops that are applicable from the entrance to exit. New pipe diameters are estimated until the minimum piping cost for the fixed pressure drop is assured. No maldistribution will arise from symmetrical piping.

For ring headers at one end and symmetrical piping at the other one must first assume a header diameter and a branch stream diameter and symmetrical pipe diameters. It is desired to choose flows that will give exactly equal pressure drops for each stream. One must first assume equal flows in all branch streams and sum the total pressure drop in each from entrance to exit. Total pressure drops will differ slightly for each stream. From these pressure drops better flow rates may be estimated and new pressure drops calculated.

$$\Delta P = Kq^2 \qquad\qquad K = \Delta P/q^2$$
$$\partial\Delta P = 2Kq\partial q$$
$$\partial\Delta P = 2\Delta Pq\partial q/q^2 = 2\Delta P\partial q/q$$
$$\partial q = \partial\Delta Pq/2\Delta P$$

where $\Delta P$ = average total pressure drop (psi)
$K$ = constant
$q$ = average flow rate (ft/sec)
$\partial q$ = q new - q old
$\partial\Delta P$ = $\Delta P$ average - $\Delta P$ old

Three or four trials are needed with the above equation to converge to four significant numbers. Maldistribution, loss of duty, and loss of production can be calculated as will be shown later, for the particular design. The cost due to loss of production and the cost of the ring header are summed. New ring headers and branch diameters are chosen and the cost calculated until the minimum cost and optimum design are reached.

The next case will be for ring headers at the inlet and outlet. The method here is slightly more complicated than the others. For symmetrical headers just one semicircle need be considered. The radius of the rings is large enough to assume a straight pipe. First assume header and branch diameters.

Assume a common pressure in the middle of the bundle and by summing pressure drops from the entrance to the middle of the bundle for each branch stream a flow rate for each branch may be found. By knowing the flow rate in each branch the pressures at the inlet tubesheet may be found. The exact same procedure is used on the exit end. One now knows the pressure at all inlet and outlet tubesheets. One can now find discrete flow rates in the bundle between particular tubesheets. Knowing this the flow rates through each branch stream may be calculated and the tubesheet pressures recalculated. This procedure is repeated until convergence is reached. The maldistribution, loss of duty, and loss of production are found and new diameters are assumed until cost is minimized.

For plate-fin exchangers with straight manifolds the situation is very similiar to the wound coil except that the passages are not randomly connected between passage headers and hence one does not get random maldistribution in the passages but a segregated maldistribution. Again assume header and branch diameter and sum pressure drops from entrance to exit to get the flow rate. Pressure drop equations or correlations in the various types of cores may be obtained from the vendors. A method for calculating loss of duty is suggested later. Again the distribution system is optimized by minimizing the cost.

When two phase flow exists in the distribution system one must be careful not to be in the slug flow region. This can easily be checked by referring to a Baker chart. (9) For symmetrical piping at the inlet one may design for annular or dispersed flow. If a small amount of liquid is present an annular entrance pattern might be acceptable. But the loss of duty for the case of extreme liquid maldistribution should be checked for significance. There are two ways of making a two phase stream homogeneous. One is to increase the pressure above the critical pressure of the gas and the other is to increase the velocity to the dispersed flow pattern in which liquid is entrained in the gas phase. For ring, straight, or buttonhook headers at the inlet one must design for a homogeneous or dispersed flow. It is presently common practice to avoid two phase flow by raising the pressure of the gas above the critical pressure to achieve a homogeneous fluid which can then be distributed by a ring or straight header. It may be economically advantageous to increase the velocity of a two phase fluid to a homogeneous fluid. Again one may use the Baker chart (see fig. 8) to get into the dispersed region.

**It should be noted that a ring, straight, or buttonhook header may have to be necked down or tapered so that the homogeneous regime will remain to the end or last branch stream.** For the discharge system one may be in any two phase regime except of course slug flow. Distributing the two phase fluid from the branch streams to the tubesheet or core poses another serious matter as will be shown in the maldistribution section. It is very important the equal gas-liquid ratios are distributed to each tube or each core passage. A conical diffuser seems to be the best method (see fig. 9). If one has annular flow entering the diffuser he should have some sort of conical device upstream to scrape the liquid off the walls and disperse it in the gas.

## INSTABILITIES

Instabilities which may arise in the system could cause a form of maldistribution that could be quite serious, not only effecting loss of duty but loss of equipment as well.

One type of instability is caused by a condensing or evaporating fluid. A plot of mass flow rate (G) versus two phase pressure drop ($\Delta P_{TP}$) may reveal curves similiar to one of the following.

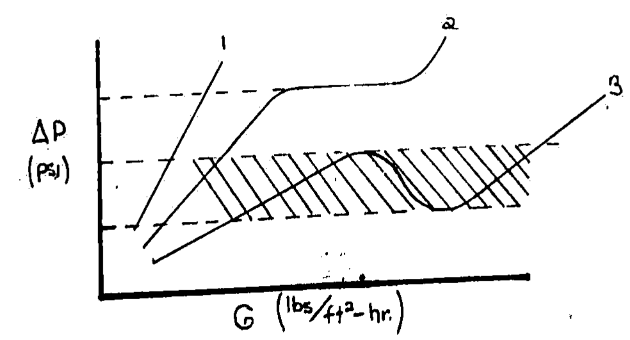

One can see that if the pressure drop is in the shaded region two or three flow rates for curve 3 may exist. In a core or tube bundle one tube or passage may be at a low flow rate while another at a high flow rate. For curve 2 many flow rates may occur at a particular pressure drop. Curve 1 is a single phase fluid which is stable. If one finds he has designed in the unstable region he may either increase the pressure to above the critical pressure to obtain a single phase fluid and get curve 1 or redesign the bundle so a pressure drop outside the unstable region exists. The stability curve may be drawn by first plotting temperature versus duty, the cooling curve. From the equation $q = UA\Delta T_{LM}$ one can plot tube length versus duty. From this liquid condensed versus length is graphed. From Hughmark's slip correlations (5) a plot of liquid volume fraction versus length is made. Using Chenowith - Martin two phase pressure drop correlations (6) pressure drop per length versus length is plotted. The area under this curve is the total pressure drop. One now has a point on the $\Delta P_{TP}$ versus G curve. A new G is assumed and the procedure is repeated until a smooth curve results.

Another type of instability may occur in a tube with non-uniform pressure drop and non-uniform duty and may manifest itself as pulsations. A rigorous analysis of this effect is beyond the scope of this study. To simplify matters one may consider the "worst case" and see if its effect on the loss of duty is appreciable. The "worst case" would be if all duty was exchanged at the tube inlet and all pressure drop occured at the outlet. The tube is adiabatic and frictionless in between. Pressure drop and duty are constant. A plot of mass flow (G) versus time is the desired result of this analysis.

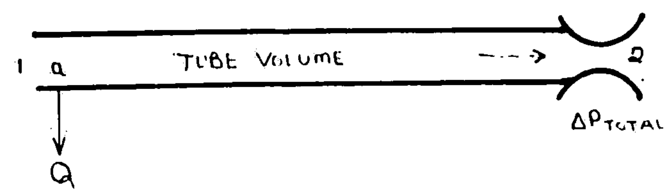


The step wise procedure is:

1. $\Delta P = K\rho_2 V_2^2/2g_c$
2. Find the constant K for the design case
   $K = 2\Delta P g_c/\rho_2 V_2^2$
3. At time (t) = $0^-$ assume no heat flow (Q = 0)
   a) Calculate $V_2 = \sqrt{2\Delta P g_c/\rho_2 K}$
      where $V_2 = V_1$ and $\rho_2 = \rho_1$
   b) Calculate $G_2 = \rho_2 V_2$ and $G_1 = G_2 = \rho_1 V_1$
4. At t = $0^+$ assume heat flow (Q = constant, Btu's/sec)
   a) $\rho_1 V_1 = \rho_a V_a$, always
   b) $V_a = V_2$, always
   c) $V_1 = m_1/\rho_1 A$, always, therefore,
   d) $m_1/\rho_a = V_2 A$, always
      A = tube cross sectional area ($ft^2$)

For the ratio $m_1/\rho_a$ only one value for $m_1$ and one value for $\rho_a$ exists. A graph of $m_1/\rho_a$ versus $m_1$ should be plotted.

$Q = (C_p\Delta T + \Delta R_L\lambda)m_1$ = constant

$C_p$ = specific heat, $f(T)$

$\Delta R_L$ = fraction liquefied or vaporized, $f(T)$

$\lambda$ = heat of vaporization, $f(T)$

$m_1$ = mass flow rate in lb/sec

$Q$ = heat flow (Btu's/sec)

Fill in values for the following list over the temperature range of the design exchanger.

1) $T$ ($^oF$)
2) $C_p$ (Btu's/lb $^oF$)
3) $\lambda$ (Btu's/lb)
4) $\Delta R_L$
5) $\rho_a$ (lb/ft$^3$)
6) $C_p\Delta T + \Delta R_L\lambda$
7) $m_1$

A plot of $m_1/\rho_a$ versus $m_1$ can now be plotted.

e) $m_1$ and $\rho_a$ can now be found for a particular $V_2A$

5. The new density ($\rho_a$) will reach the restriction at $t$ = tube volume/$V_2A$ where $\rho_2 = \rho_a$
   a) $V_2 = 2\Delta P g_c/\rho_2 K$
   b) $m_1/\rho_a = V_2A$
   c) from graph find new $m_1$ and $\rho_a$
6. Repeat step 5 and a plot of $m_1$ versus time can be plotted.

## TWO-PHASE FLOW

Simultaneous gas-liquid flow is frequently encountered. The design problems are much more complicated in two phase flow than that in single phase flow. It is common knowledge that gas-liquid flow in tubes exists in different patterns or regimes depending on the physical and geometric properties of the system. These flow regimes are labled bubble, plug, stratified, wavy, slug, froth, annular, and spray by those knowledgeable in the field of two phase flow. Heat, mass, and momentum transfer as well as hold-up can be predicted with reasonable accuracy only when the flow regimes can be specified.

Prediction of the flow regime offers another problem in two phase flow. The only sure method is by visual observation of the actual flow under investigation through a transparent tube. Even visual observations under certain conditions may cause some doubts to the observer as to what he is seeing. Boundaries between regimes are not well defined and high-speed photography may be necessary. Correlations are numerous given fluid properties, flow rates, and tube dimensions, but are only reasonably accurate. Practically all correlations are based on data obtained from only five systems (air-water, $CO_2$-water, steam-water, air-oil, and $NH_4$-water) using only horizontal and vertical tubes.

Transport coefficients for two phase flow can be predicted from general correlations without regard to regimes but the ranges are limited and accuracy very poor. Even if the flow pattern, geometric dimensions, and fluid properties are known pressure drop from the most reliable correlations can only be predicted with 25% accuracy. Two phase heat transfer coefficients can be found from general correlations using a single phase flow coefficient or using dimensionless groups assuming a liquid film on the wall but again are very inaccurate.

In order to make accurate prediction of transport properties, one needs to know what fluid mechanism exists and how it is caused. Some of those who have done outstanding work are: D. J. Nicklin in vertical slug flow and bubble flow, Calvert and Williams in vertical annular flow, E. S. Kordvban in horizontal slug flow, C. B. Wallis in horizontal bubble flow, Bergelin and Gayley in horizontal wavy and stratified flow, and Russel and Lamb in horizontal annular flow. However, at present the author is not aware of a dependable method of calculating transport properties outside the range of the above investigations.

LOCAL MALDISTRIBUTION AND LOSS OF EXCHANGER DUTY

There exists in practically all systems maldistribution of flow, much of which can not be avoided. This maldistribution affects the exchanger duty and thus causes a loss of production. Given a particular design one would want to know how much loss of duty as a percent of the design duty will occur. There are essentially two types of tubeside flow maldistribution. The first type which will be called local maldistribution results in a cross sectional area of an exchanger having a temperature gradient. The second type will be called random maldistribution which occurs when tubes or flow passages of different flow rates or temperature occur randomly through the bundle or core and a cross section will show a constant shellside temperature.

When local maldistribution occurs the loss of performance due to the entropy gain of mixing streams of different temperature is large. It may also be shown by drawing cooling curves for cross sectional segments of an exchanger that the mean temperature difference between the warming and cooling stream is less than the uniformly distributed case, hence more loss of duty ($Q = UA\Delta T_{LM}$).

Local maldistribution in core exchangers is caused by fluid not being distributed properly in the headers to the individual core passages. One can see from the diagram below that the heavier passages receive more flow because of higher pressure drop due to the momentum of the entry stream. This would be particularly bad for two phase entry.

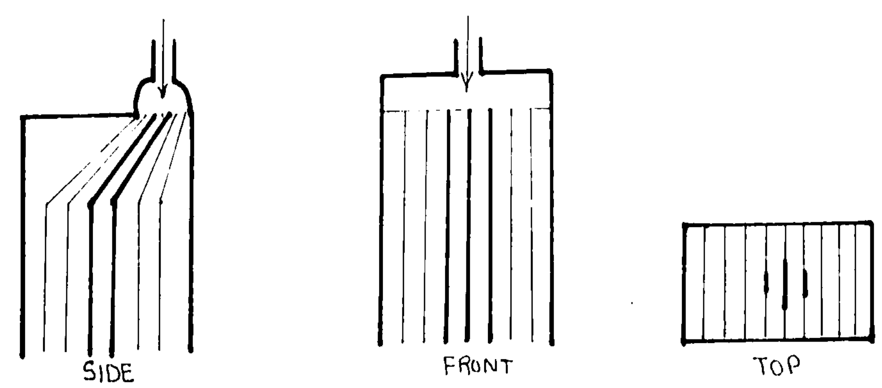

To calculate loss of exchanger duty one must divide the core into two cross sectional areas and make an estimate of the flow each passage is receiving. Let the passages carrying the large flow be one exchanger and the passages carrying the low flow be another. Draw cooling curves for each allowing a proportional amount of original UA for each exchanger and add the duty of each. The design duty less the sum of the two duties is the loss of exchange duty. Local maldistribution in parallel core exchangers may also occur when a straight manifold is used to distribute to each core. Consider three typical manifolding designs for distributing single phase fluid to three identical parallel cores. Fluid velocity in these examples is great enough so that the pressure drop due to friction is negligible compared to the change in pressure due to change in velocity. Noting that for every branch there is a pressure recovery in the inlet header and a pressure loss in the outlet header, one would find distribution patterns conforming with the following sketches.

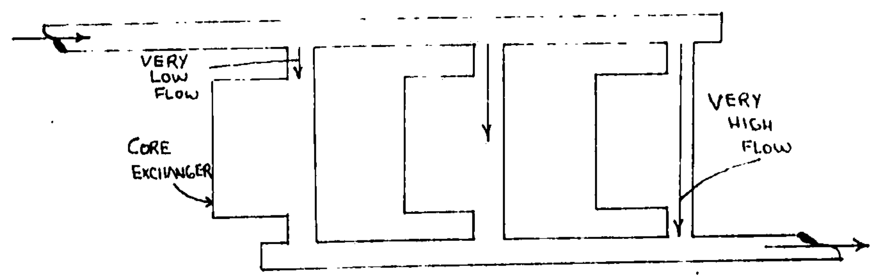


POOR DESIGN

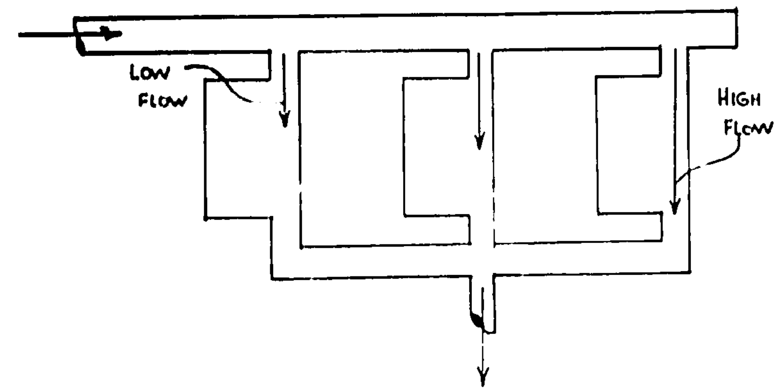


FAIR DESIGN

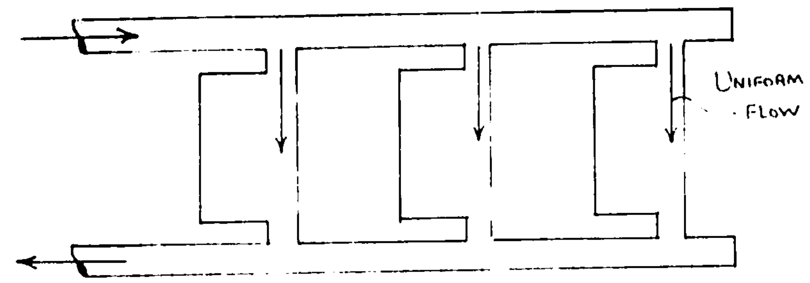


GOOD DESIGN

Cooling curves can be drawn for each individual core as before and the duty of each calculated.

Local maldistribution in large wound coil exchangers is quite complex. The tubes that are wound first on the mandrel are usually connected to the top of the upper tubesheet and to the bottom of the lower tubesheet. If the entrance flow is not homogeneous as in two phase separated flow, liquid will tend to travel in the center of the bundle. The effect this can have on loss of exchanger duty can be quite serious, particularly at high liquid-gas ratios. These tubes are also longer than the tubes which extend from the top of the lower tubesheet to the bottom of the upper one since the actual heat exchange length is the same for all tubes.

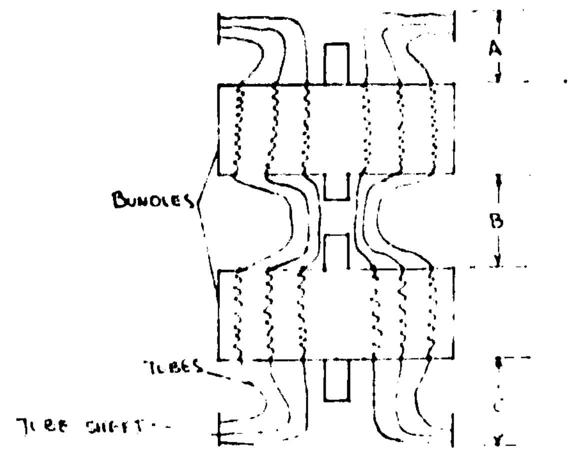


Since the tubes are circumferentially wound in each bundle the tubes outside the bundles lose their identity in the circumferential direction and not in the radial direction. The average tube length per each circumferential segment must be found before and after each bundle. The average lengths in these circumferential segments are directly additive. For instance consider sections A or C. If the tubes were disconnected from the tubesheets and extended vertically the following representation of tube lengths could be made.

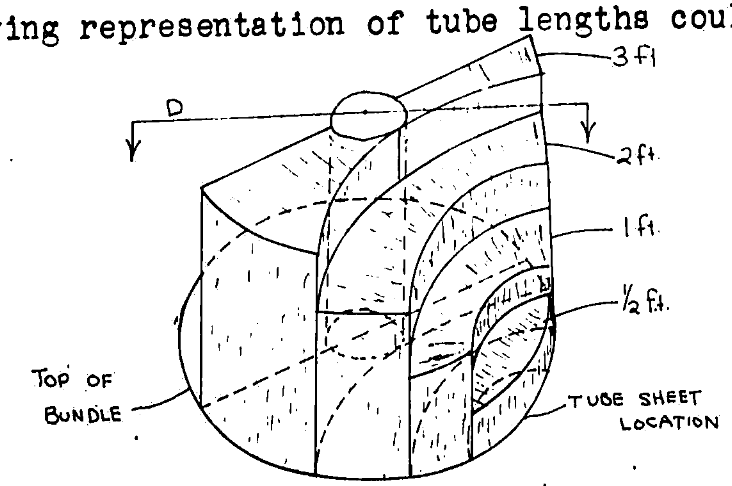

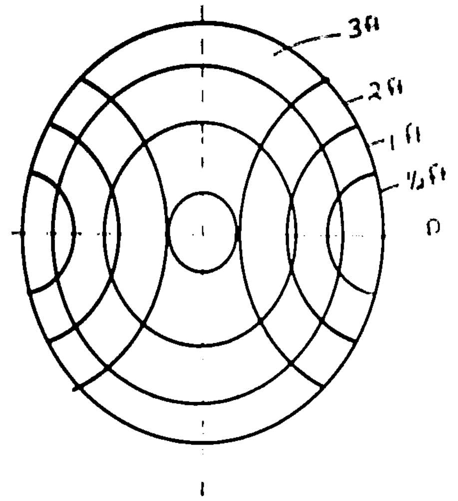


The tube lengths in three equal area concentric segments may then be represented bv the following diagram.

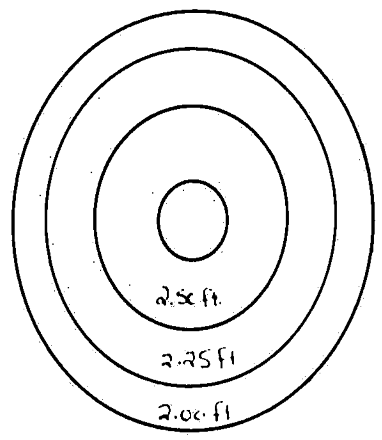


Similiarly for section B, if the tubes are straightened in the vertical direction, it could be represented as

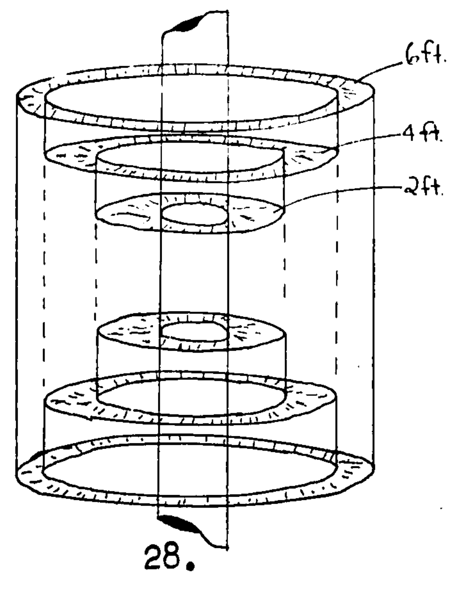

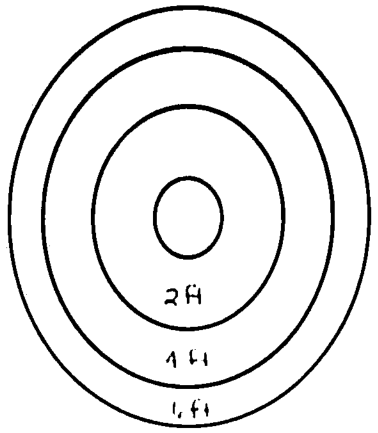


The tube lengths in three equal area concentric segments may then be represented by the following diagram.

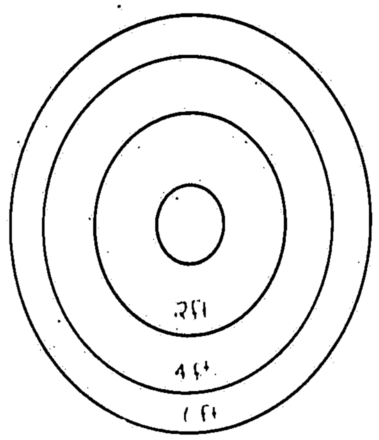


The three concentric segments representations of sections A, B, and C may now be added directly.

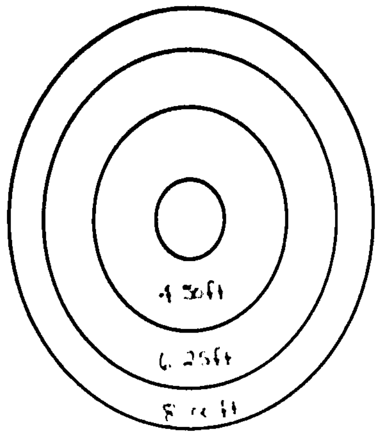


If one has separated two phase flow entering the tubesheets where the liouid is going into the tubes at the bottom of the tubesheet, a distribution of liouid fraction may be:

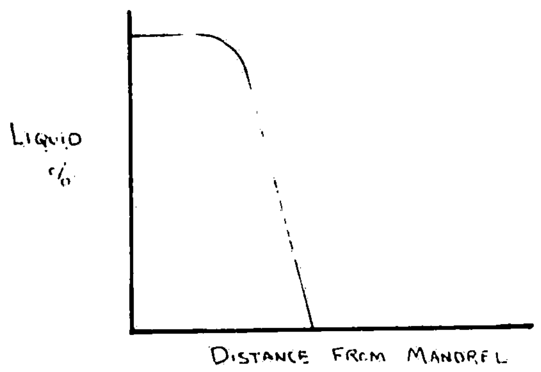


During the winding of the large tube bundles, the tubes which are wound first on the mandrel receive much flexing and distortion. Quite often these tubes crack, leak, and must be plugged. This reduces the effective area of the exchanger. From experience one can estimate how many tubes are going to be plugged in each bundle section.

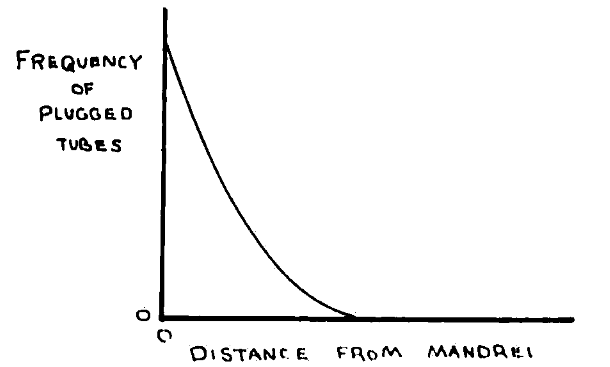


The three major causes of local maldistribution, tube lengths, unequal liquid fractions, and plugged tubes have been discussed. To find the loss of duty caused by local maldistribution divide the bundle into concentric segments of equal annular area.

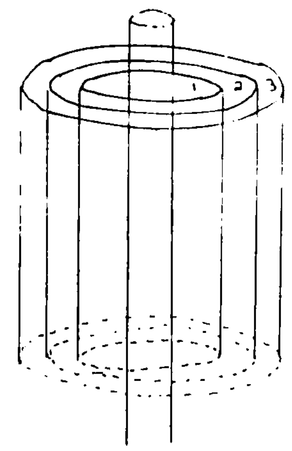

For each segment estimate the average tube length, liquid fraction, and number of plugged tubes. The following assumptions must be made in developing a

**model exchanger:**

1. **no radial shellside liquid mixing**
2. **perfect circumferential shellside mixing**
3. **equal pressure at any level in the exchanger.**

**It is apparent from these assumptions there will be shellside gas mixing. The following model can be used to calculate loss of duty.**

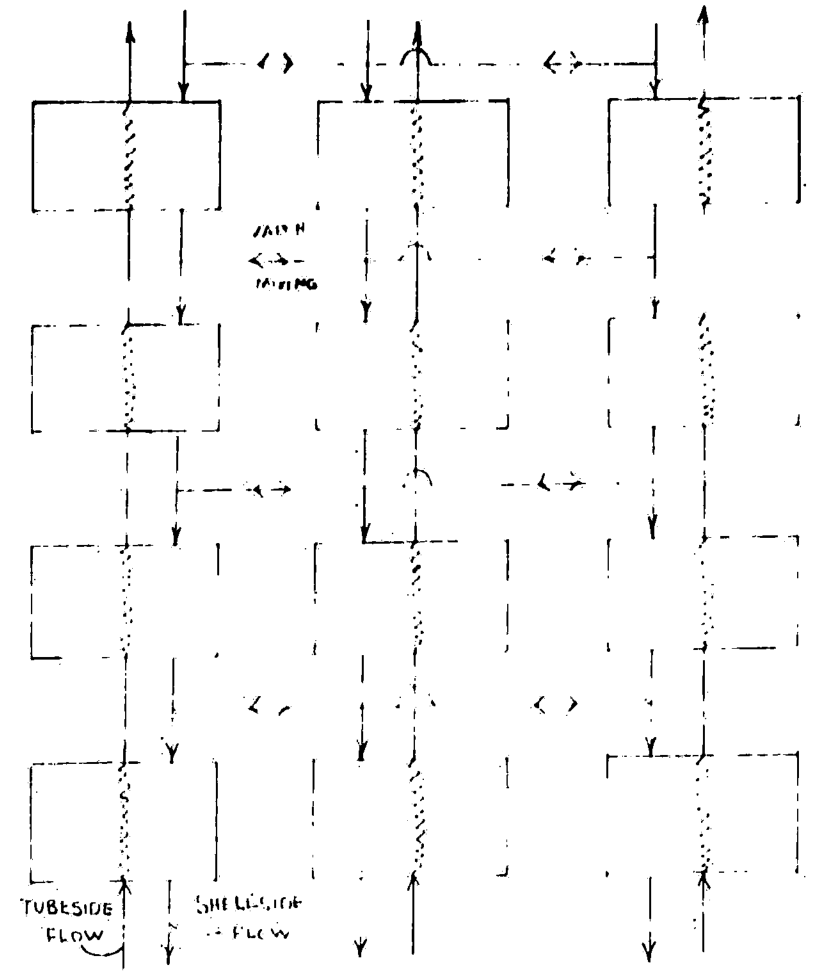


**Each column represents equal surface area concentric bundle segments. Each vertical segment represents equal surface area vertical segment of the exchanger. All inlet conditions are known for each column. The following steps should be followed:**

1. **For a first assumption assume no shellside gas mixing**
2. **Draw cooling curves for each column and keeping UA constant at 1/3 the design value estimate conditions in and out of each vertical segment**
3. Calculate shellside pressure drop through the top section in each exchanger
4. If the $\Delta P$'s are unequal there will be a flow of shellside gas in a particular direction
5. Guess vapor flows between the top sections
6. Guess a new $\Delta H$ across each exchange section
7. Calculate $\Delta T$'s across section and $\Delta T_{lm}$ between tube and shell streams
8. Calculate a cross-sectional area, assume constant U
9. Calculate a new $\Delta H = UA\Delta T_{lm}$
10. Use this new $\Delta H$ in step 6 and repeat until it no longer changes
11. Calculate new pressure drop for each top segment
12. If pressure drops are unequal, guess a new vapor flow and repeat from step 6
13. When pressure drops are equal repeat the entire procedure for the second segment for each column and so on until bottom segment.

Reflecting back to local maldistribution in a single core exchanger in which the corrugated sheets are open in places to the stream next to it in the same layer, a similiar analysis with gas mixing should be done.

One can now draw a cooling curve for each column in the model and calculate the duty of each. Quite often no shellside gas mixing can be assumed which greatly simplifies the analysis.

RANDOM MALDISTRIBUTION AND

CORRESPONDING LOSS OF DUTY

So far random maldistribution has not been taken into account. Random maldistribution exists when tube flow rates different from design are randomly distributed through the bundle. Since the flow variations are randomly distributed, a cross section of the tube bundle will always show a constant shellside temperature assuming no local maldistribution. Maldistribution effects tend to partially cancel and entropy of mixing exists only at the tubeside exit. This type is not as serious as local maldistribution but will present itself in all systems.

One type of random maldistribution has already been discussed and is that caused by instabilities. It will be assumed that the instability which is a function of two phase flow rate has been eliminated and that the effect of the pulsation type is negligible.

The variations of tubesheet pressures due to header $\Delta P$'s cause another type of random maldistribution. Since each exit tubesheet has an equiprobable chance of having tubes connected to an entrance tubesheet, it can be assumed that an equal number of tubes connect all possible combinations and entrance and exit tubesheets. For instance if one has eight entrance tubesheets and four exit tubesheets there are 32 discrete pressure drops in the bundle and therefore 32 discrete flow rates due to variations in tubesheet pressures. There tends to be a normal distribution of pressure drops in the bundle as many of the discrete pressure drops are the same.

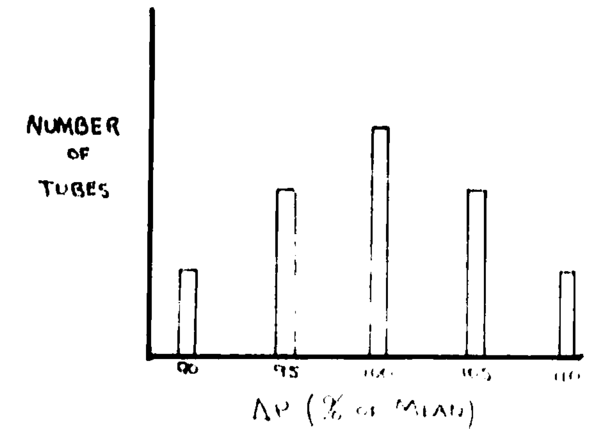


In calculating the actual exchanger duty the above random maldistribution must be combined with the local maldistribution.

The shellside cooling curves for each column have been drawn neglecting random maldistribution. Take one of the three model exchangers and isolate it. Consider each discrete pressure drop due to variations in the tubesheet pressures in the isolated exchanger as a separate exchanger. If there are five discrete pressure drops there are five separate model exchangers each with a different tube side flow and the same shellside flow. This can be done for each of the three concentric segments. We now have 15 separate exchangers representing the bundle. Draw a cooling curve for each of the 15 exchangers keeping the UA of each proportional to the number of tubes in each. Find the duty of each and sum the UA's to check to see if it equals the design UA.

It has been found by past experience that the percent loss of duty "L" is equal to a constant "K", which is particular to a tube bundle, times the percent maldistribution squared ($L'' = Km^2$). The percent maldistribution, m, is defined as the percent of maximum and minimum deviation from the mean when one half of the flow is at the maximum and one half of the flow is at the minimum. For instance if one half of the tubes are flowing at 90% the mean and the other half are 110% the mean the maldistribution is 10%. In the case where the maximum and minimum percent deviations are not equal the largest absolute percent deviation is used as a conservative estimate. The value for K must now be found for each segment.

The cooling curves for each column have been drawn neglecting this random maldistribution. Take one of the three model exchangers and isolate it. Assume some percent maldistribution "m". Consider two exchangers equal to the one we have isolated. Keeping the same shellside cooling curve for each, let one carry the low flow and one carry the high flow and draw a cooling curve for each maintaining the same UA in each case. Find the duty of each and average the two. The difference between this duty and the duty before considering maldistribution is the loss of duty. Find the percent loss of duty "L" and evaluate "K". $K = L''/m^2$. Repeat this for each concentric segment to find a value for K in each.

Another random type of maldistribution must now be incorporated into the analysis. It is caused by variations of tube inside diameter. Tube vendors usually give a maximum and minimum inside diameter. It may be assumed that the diameters are uniformly distributed between these limits because the variations are due to the gradual wearing down of the dies. This means that every tube will have a different diameter of uniform distribution between the maximum and minimum tolerances. With a constant pressure drop through each tube the flow can be approximated as being uniformly distributed. (Actually flow rate is proportional to diameter to the 5/2 power.) We wish to find what this effect has on loss of duty. Consider the following equation $L'' = K\overline{m}^2$ which has already been discussed. This equation is accurate for percent loss of duty when one has discrete flows symmetric about a mean flow rate as indicated below:

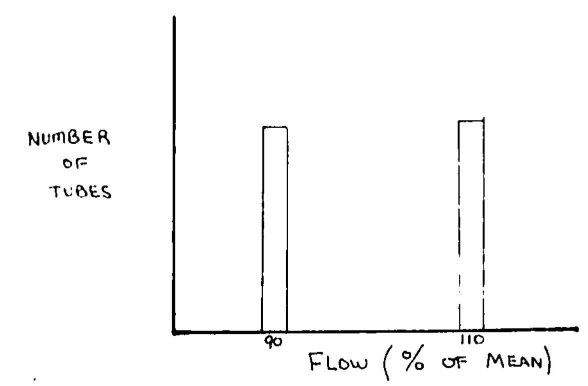


The equation $L'' = K\overline{m}^2$ would apply to this distribution. If one would apply this equation to a distribution such as:

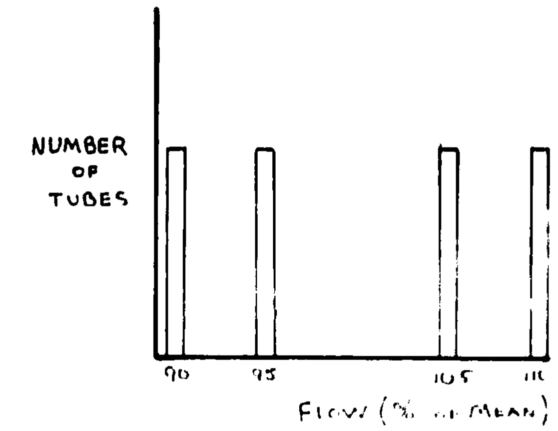


he could say

$$L'' \text{ average} = K(\tfrac{1}{2}\bar{m}_1{}^2 + \tfrac{1}{2}\bar{m}_2{}^2)$$

where $\bar{m}_1 = 10$

$\bar{m}_2 = 5$

Applying this still further to the case of uniform flow distribution due tovariations in tube inside diameter one could write:

where $\bar{m}$ = maximum flow deviation for the mean

$N$ = total number of tubes or discrete flows

$$L'' = K\ 2/N\left[\bar{m}^2 + (\bar{m} - 2\bar{m}/N-1)^2 + (\bar{m} - 2(2\bar{m})/N-1)^2 \right.$$
$$\left. (\bar{m} - 3(2\bar{m})/N-1)^2 + \ldots + (\bar{m} - (N-1/2)(2\bar{m})/N-1)^2\right]$$

or

$$L'' = 2K/N \sum_{i=0}^{\frac{n-1}{2}} \bar{m} - i(2\bar{m})/N-1\ ^2$$

Recall the 15 model exchangers for which maldistribution due to tube inside diameter variation has been neglected. A duty for each has already been calculated. Finding the maximum and minimum flow rates for each of the 15 models and applying the above equation to each one may calculate the loss of exchanger duty and the actual exchanger duty of each. If the actual exchanger duties are summed one will get the total actual exchanger duty. The design duty less this value will be the loss of duty.

If greater accuracy is desired one may go back to page 32 and calculate new shellside flows for each concentric segment using the actual duty. This may be repeated until convergence. Also for greater accuracy one may divide the exchanger into more vertical and concentric segments. One can see the tremendous amount of work necessary for an accurate appraisal of the loss of exchanger duty. If an example can be worked through by the above, one would be able to tell where approximations can be made that would simplify computations.

EXAMPLE DESIGN

A typical ring header for a cryogenic exchanger will now be designed. It will be assumed that the tube bundles have already been designed as arranged in figure 10. A model of the ring header will have to have the dimensions of figure 11 to fit the design of the bundles. The particular stream that will be examined makes up only a small part of the overall exchanger. This stream will be called the feed stream. The feed tubes make up 100% of the exchange area in the C bundle, 35% of the D bundle, and 52% of the E bundle. The remaining tubes in each bundle contain another process stream which is not under consideration and will be assumed to be perfectly distributed. Because of the small heat capacity of the feed stream compared to the shellside flow, it may be assumed that the shellside stream will not be affected by small changes in feed stream flow.

The inlet conditions will first be examined. The following data is available:

Composition at 52°F and 592 psia

| Component | % liquid | % vapor | Total |
|---|---|---|---|
| $N_2$ | .0008 | .012 | .0115 |
| $C_1$ | .1771 | .7355 | .7103 |
| $C_2$ | .1719 | .1450 | .1462 |
| $C_3$ | .2718 | .0766 | .0854 |
| $C_4$ | .2840 | .0279 | .0394 |
| $C_5$ | .0769 | .0029 | .0062 |
| $C_6$ | .0174 | .0002 | .0010 |
| | 1.0000 | 1.0000 | 1.0000 |
| Total moles (%) | 4.506 | 95.494 | 100. |
| Mole wt. (lb/mole) | 43.573 | 21.7154 | 22.7 |
| Density (lb/ft$^3$) | 30.67 | 2.827 | 3.077 |
| Viscosity (cp) | 0.0924 | --- | ---- |
| (lb/ft-hr) | .224 | .027 | ---- |

Surface tension ($\gamma$) of the liquid may be estimated

| Component | $\gamma$ (dynes/cm at 52°F) | | % Composition | |
|---|---|---|---|---|
| $N_2$ | 0 | x | .0008 | = 0 |
| $C_1$ | 0 | x | .1771 | = 0 |
| $C_2$ | 2 | x | .1719 | = 0.344 |
| $C_3$ | 9 | x | .2718 | = 2.44 |
| $C_4$ | 14 | x | .2840 | = 3.98 |
| $C_5$ | 17.5 | x | .0769 | = 1.55 |
| $C_6$ | 20 | x | .0174 | = 0.340 |

Total surface tension 8.442

Total flow rate will be 10478 moles/hr. (molecular weight of mixture = 22.7)

Before estimating the two phase flow pattern the pipe sizes will have to be estimated from the pipe flow chart (1) and table 1. Because of the small amount of liquid assume single phase flow.

Ring header

$T = 10^{\circ}C$
$MW = 22.7$
$\mu_c^{.16}/\rho$ is read from pipe chart as 8.5
$P_G = 40$ atm
$\Delta P_F'/L = .0007$ from table 1
Reference line reads = 7.4
Weight flow (M lbs/hr) = (total moles rate/ 2 streams in ring)(total MW) = 119,000 lb/hr
The inside ring header diameter is estimated as 13 inches.

The ring header will be made from aluminum sheet 0.625 inches thick. Therefore the outside diameter will be 14.25 inches. The nearest piping available is 14 inches and the inside diameter ($D_H$) will be 12.75 inches.

Branch streams (same as ring header)

$T = 10^{\circ}C$
$MW = 22.7$
$P_G = 40$ atm
$\Delta P_F'/L = .0007$
$(\Delta P_F'/L)(P_G) = .028$
Reference = 7.4
Mass flow rate = (total moles per hr/ 8 branch streams)(total MW) = 29,700 lb/hr
Branch inside diameter = 7 inches

The branch piping will be made of schedule 80 XH aluminum. At 8 inches nominal size the inside diameter ($D_B$) = 7.625 inches.

Outlet symmetrical piping at P = 565 psia and $T = -206^{\circ}F$

$\rho V^2 = 1500$ lb/sec$^2$ft$^2$ (based on APCI experience)
$\rho = 30.7$ lb/ft$^2$ at $-206^{\circ}F$
$V = 6.99$ ft/sec $= q/A_p$
where $A_p$ = cross sectional area of pipe
$q$ = volumetric flow (ft$^3$/sec)
$A_p = \pi D_p^2/4$
$D_p = \sqrt{4q_p/\pi V}$

$q$ = (total moles/2 branches)(total MW)(1/$\rho$ of liquid) = 1.075 $ft^3/sec$
$D_p$ = 5.3 inches

The outlet piping will be made of schedule 80 XH aluminum, at 6 inches nominal size the inside diameter ($D_p$) = 5.761 inches.

The first estimation of pipe sizes have been made and results are:

inside diameter of ring header = $D_H$ = 12.75 inches
inside diameter of branches from ring = $D_B$ = 6.725 inches
inside diameter of outlet piping = $D_p$ = 5.761 inches.

The two phase flow patterns at the inlet header now will be examined. The Baker chart (fig. 8) will be used.

$\lambda' = ((\rho_G/.075)(\rho_L/62.3))^{\frac{1}{2}} = 4.31$
where $\rho_G = 2.827$ lb/ft$^3$
$\rho_L = 30.67$ lb/ft$^3$
$\psi = (73/\sigma_L)(\mu_L'(62.3/\rho_L)^2)^{1/3} = 6.3$
where $\sigma_L = 8.442$ dynes/ cm$^2$
$\mu_L = .0924$ cp
$L'/G'$ = (moles liquid/moles gas)(MW liquid/MW gas) = 0.095 lb liquid/lb gas
where $L$ = mass flow rate of liquid (lb/hr.ft$^2$)
$G$ = mass flow rate of gas (lb/hr.ft$^2$)
$A_H = \pi D_H^2/4 = 0.89$ ft$^2$
where $A_H$ = cross-sectional area of ring header (ft$^2$)
$A_B = \pi D_B^2/4 = 0.317$ ft$^2$
where $A_B$ = cross-sectional area of branch stream (ft$^2$)
$G_H'$ = (total mole flow/2 streams)(moles % of gas) (MW of gas)(1/$A_H$) = 122,000 lb/hr.ft$^2$
$(L'/G')\lambda'\psi = 2.57$
$G'/\lambda' = 28,300$

From the Baker chart, the flow is in the annular flow regime for the section of the ring header before the first branch stream. Similar calculations are done for each section of the entire ring header.

If nearly equal flows are assumed out each branch, the flow is annular in all sections except the last which is in the wave region. All four points are placed on figure 8. If the liquid rate ($L'$) in the last section is increased slightly at constant ($G'$), the flow regime will become annular. This will probably occur because of the momentum of entrained liquid drops. Because the liquid volume fraction is small (0.87%) it does not really matter if it is not perfectly distributed. Two phase density, pressure drop, and liquid hold-up are not significantly effected by variations in liquid volume fraction at such a low, non-slip volume fraction. However just the fact that a small amount of liquid is present causes the two phase pressure drop to differ significantly from the gas phase case and necessitates its consideration. Because of the fact that the two phase mixture enters near the dispersed regime and the liquid and gas properties are within an order of magnitude of each other, the annular film in the pipe will be nearly symmetrical and there will be much liquid entrainment in the gas phase. It will be assumed from this that equal gas-liquid ratios occur in each branch. It will also be assumed that no liquid will accumulate in the header because all

**flows are in the annular regime and any excess accumulation of liquid will form waves that will be entrained in the high velocity gas.**

**In the branch streams, assuming near equal flows:**

$G_B' = ((\text{total mole flow rate})/(8 \text{ branch streams}))$
$\quad (\text{gas mole fraction})(\text{MW gas})(1/A_B)$
$G' = 85{,}500 \text{ lb/ft}^2\text{-hr}$
$G'/\lambda = 19{,}800$

**Again from figure 8 annular flow exists. The Baker Plot is not as accurate for vertical flow as horizontal so the flow patterns should be checked by other methods.**

By the Griffith and Wallis Chart (fig. 13):

$Q_L' =$ volumetric flow rate of liquid
$\quad = 0.0233 \text{ ft}^3/\text{sec}$
$Q_G' =$ volumetric flow rate of gas
$\quad = 2.66 \text{ ft}^3/\text{sec}$
$g_c = 32.2 \text{ ft/sec}^2$
$((Q_L' + Q_G')/A_B)^2/g_c D_B = 3.53$
$Q_G'/(Q_L' + Q_G') = 0.992$

Flow is on the border of the slug-annular region.

By the Govier, Radford, and Dunn method (fig. 14):

$V_L = Q_L'/A_B = .0735$
$R_V'' = Q_G'/Q_L' = 114$

Flow is in the froth regime according to this method.

One can see that all three methods give different results because of the limited amount of data used in the correlations. Because of the low liquid flow rate it may be assumed that slug flow will not occur which is what is most important.

Since the branch pipes are vertical, the liquid volume fraction actually existent in the pipe is necessary for pressure drop due to fluid head calculations. By the method of Hughmark on page 18:

$N_{Re} = D_B G_B / 12(R_L' \mu_L + R_G' \mu_g)$
$N_{Re} = 1.87 \times 10^6$
$N_{Fr} = 12540\, q^2_B / D_B^5$
$N_{Fr} = 3.52$
where $D_B = 7.625$ inches
$G_B = 85{,}500$ lb/hr.ft$^2$
$R_L' = .0087$
$R_G' = .9913$
$\mu_L = .224$ lb/hr.ft
$\mu_g = .027$ lb/hr.ft
$q_B = 2.684$ ft$^3$/sec
$N_{Re}$ = two phase Reynold number based on slip

$Z = (NRe)^{1/6}(N_{FR})^{1/8}(R_L)^{-\frac{1}{4}} = 42.3$
from figure 4, $K = .9$
$R_L = 1 - K(R_G')$
$R_L = .11$
$R_G = 1 - R_L$
$R_G = .89$
$N_{Re} = 3.7 \times 10^6$ with new values of $R_L$ and $R_G$
$Z = 39.6$ which is no appreciable change
therefore $R_L = .11$ liquid volume fraction
$R_G = .89$ gas volume fraction

The flow pattern in the tubesheet header (fig. 15) should be examined by the Baker Chart (fig. 8).

$G'$ = (moles flow rate total/number of tube sheets)
(.955 gas mole fraction)(MW gas/$A_{TS}$)
where $D_{TS}$ = diameter of tubesheet = 17.25 inches
$A_{TS}$ = cross-sectional area of tubesheet
= 1.62 ft$^2$
$G' = 17{,}250$
$G'/\lambda' = 4000$
$(L'/G')\lambda'\psi = 2.57$

Flow in the tubesheet headers would be on the border of stratified and wave flow if entrance effects are neglected. However with the design of the header such as it is there will be bubbling and turbulence. It might be assumed that all of the liquid enters the lower one third of the tubes. To say that liquid alone flows in the bottom tubes neglects the entrance effects of bubbling while to say that the liquid is perfectly distributed neglects the steady state characteristics of phase separation.

Two phase pressure drops at various flow rates in both the ring header and branch streams will be needed later on when the pressure drops are added for a particular stream. Since a trial and error solution will be necessary and the calculation of two phase pressure drop is lengthy it would be wise at this point to graph two phase pressure drop ($\Delta P_{TP}$) versus mass flow rate G for both the ring header and branch. The Chenowith - Martin method will be used.

In the ring header

$\Delta P_G^*/L = 4 f_G G_{TP}^2 / 2 g_c \rho_G D_H$
$N_{ReG} = D_H G_{TP}/\mu_G = 5.27 \times 10^6$
$N_{ReL} = D_H G_{TP}/\mu_L = 6.3 \times 10^5$
from Perry's (10)
$\epsilon/D_H = .00014$
$f_G = .0032$
$f_L = .0036$

where $\Delta P_G^*$ = ficticious gas phase pressure drop (psi)
$L$ = length of header (ft)
$G_{TP}$ = total mass flow rate of both liquid and gas ($lb/ft^2$-hr)
$f_G$ = gas phase fanning friction factor based on $G_{TP}$

$D_H$ = head diameter (ft)
$\rho_G$ = gas density ($lb/ft^3$)
$\epsilon$ = roughness coefficient from Perry's Chemical Engineers Handbook [10]

$\Delta P_G^*/L = 6.36 \times 10^{-4}$ psi/ft
$\Delta P_G^*/\Delta P_L^* = f_G \rho_L / f_L \rho_G = 9.7$
$\Delta P_L^*/L = 6.56 \times 10^{-5}$ psi/ft
from figure 5
$\Delta P_{TP}/ P_L^* = 36$
$\Delta P_{TP}/L = 2.4 \times 10^{-3}$ psi/ft at $G_{TP} = 133,600$ $lb/ft^2$-hr

By a similar method the following values can be obtained.

| $\Delta P_{TP}/L$ (psi/ft) | $G_{TP}$ ($lb/ft^2$-hr) |
|---|---|
| $2.36 \times 10^{-3}$ | 133,600 |
| $1.29 \times 10^{-3}$ | 100,000 |
| $8.55 \times 10^{-4}$ | 66,800 |
| $2.10 \times 10^{-4}$ | 33,400 |

These values are plotted in figure 16.

To find $\Delta P_{TP}/L$ for the branch streams the same procedure is used again.

$N_{Reg} = 2.22 \times 10^6$
$N_{ReL} = 2.68 \times 10^5$
$\epsilon/D_H = .000236$
$f_g = .0037$
$f_L = .0042$
where $G_{TP} = 94,500$ $lb/ft^2$-hr (average)
$\Delta P^*_g/\Delta P^*_L = 9.6$
$\Delta P^*_L/L = 4.45 \times 10^5$
$\Delta P_{TP}/L = 0.001555$ psi/ft

Summarizing for branch streams:

| $\Delta P_{TP}/L$ (psi/ft) | $G_{TP}$ ($lbs/ft^2$-hr) |
|---|---|
| .0024 | 124,000 |
| .001555 | 94,500 |
| .000345 | 50,000 |

These values are also plotted in figure 16.

The pressure drop in the tube bundle must now be considered. The cooling curves (enthalpy change versus temperature) for both the feed tubeside flow and the shellside are drawn for each bundle C, D, and E.

The overall heat transfer coefficient times the surface area (UA) is found for intervals of feed stream temperatures by the equation $\Delta H = UA\Delta T_{log\ mean}$. The tube lengths in each bundle are known. If U is assumed constant over a single bundle it can be said that UA is proportional to tube length. A length of a tube segment can now be found for each feed stream temperature interval and a plot of tube length versus temperature can be plotted ( see fig. 17). Next differential pressure drops at particular feed stream temperatures are found. It must be remembered that the liquid-gas ratio is changing because of the heat transfer. A temperature is picked and the liquid fraction without slip is calculated. The differential frictional two phase pressure drop is calculated from Chenowith-Martin as described earlier. Next using Hughmark's slip correlation the actual liquid fraction with slip can be found and the differential pressure drop due to fluid head is found. The pressure change due to velocity change is also calculated. As one can see this is a momentus task and was greatly simplified by partially computerizing it (11). Results of an average case are tabulated in table 2. The differential pressure drops are averaged for each temperature interval and then looking at figure 17 one can find a tube length for that particular interval. To calculate total frictional pressure drop in the tube bundles each tube length is multiplied by the average differential frictional pressure drop in that segment and totaled. To calculate total head pressure drop the vertical height per tube length must be found for each bundle. The product of this ratio times tube length times average differential head pressure is totaled. The velocity head can be found from the velocity in minus the velocity out (see page 12). All pressure drop in the heat exchange part of the bundles has now been accounted for. There is still the pressure drop in the tubes between the tubesheets and bundles and between the separate bundles. By examining figure 10 one can estimate these vertical and longitudinal tube lengths. It is assumed that no heat transfer occurs in these sections. The differential pressures are interpolated in these regions of known temperatures and multiplied by the corresponding lengths. It must be noted and taken into account that the entrance tubesheets are at two different levels; four at each level. The total tube pressure drop is now known at a particular inlet flow rate. When the ring header is designed later a plot of tube pressure drop versus inlet flow will be needed over a narrow flow interval (see fig. 18).

Since pressure drop in the heat exchange tube has just been discussed, it is appropriate that the system is checked for stability at this point. Pressure drops over a large range of flow rates are calculated by the above method. Figure 19 is a plot of this. It can be seen that an unstable region exists between 11.5 and 18 psi. It is unstable in that two different flows may occur at the same pressure drop. The rest of the curve is continuous with an increasing slope and shows no other instabilities. At less than 15,000 lb/ft$^2$-hr. the pressure drop due to fluid head becomes larger than the frictional pressure drop and the pressure drop at no flow is equivalent to having the tubes filled with liquid. The working pressure drop will be at mass flow rates between 185,000 and 190,000 lb/ft$^2$-hr. In this region there will be no instabilities. Also liquid runback will not occur because the working pressure is greater than when the tubes are filled with liquid. Apparently the type of two phase instabilities as presented on page 18 do not exist in this case. This is probably due to the high pressure and the long tube lengths (517 feet).

Tube pulsations will be next examined. An average tube length is 517 feet with cross-sectional area of 0.00083 ft$^2$ the tube volume is therefore 0.43ft$^3$. The average tube pressure drop is 26.8 psi or 3859.2 lb/ft$^2$ as was calculated on page 60. The

**average heat duty per tube is 12 Btu's/sec. Assume 12 Btu's/sec will be transferred at the tube inlet and the entire pressure drop, ($\Delta P = K\rho_2 V_2^2/2g_c$), will occur at the tube outlet. The rest of the tube is adiabatic and frictionless. Fluid properties at the inlet are constant.**

$\rho_1 = 3.067$ lb/ft$^3$


Q = 12 Btu's/sec $\qquad\qquad$ $\Delta P = 3859.2$ lb/ft$^2$

The constant K must first be evaluated from design conditions.

$$\begin{aligned}
\rho_2 &= 30.7 \text{ lb/ft}^3 \\
g_c &= 32.2 \text{ ft/sec}^2 \\
V_2 &= 1.6875 \text{ ft/sec} \\
\Delta P &= 3859.2 \text{ lb/ft}^2 \\
K &= 2\Delta P g_c/\rho_2 V_2^2 = 2848.87
\end{aligned}$$

At time (t) = $0^-$ assume no heat flow (Q = 0).

$$\begin{aligned}
\rho_2 &= \rho_1 = 3.067 \\
V_2^2 &= 2\Delta P g_c/\rho_2 K \\
V_2 &= 5.339 \text{ ft/sec} \\
V_1 &= V_2 \\
m_1 &= V_1\rho_1 A = 0.01349 \text{ lb/sec}
\end{aligned}$$

At time t = 0 (Q = 12 Btu's/sec)

$$\begin{aligned}
\rho_1 V_1 &= \rho_a V_a \\
V_a &= V_2 \\
V_1 &= m_1/\rho_1 A \\
m_1/\rho_a &= V_2 A
\end{aligned}$$

A plot of $m_1/\rho_a$ versus $m_1$ must be made from the following table. Assume $C_p$ constant and equal to 0.69 Btu's/lb°F and $\lambda$ constant and equal to 103 Btu's/lb. See figure 12 for the plot of $m_1/\rho_a$ versus $m_1$.

| $T\,^\circ F$ | $\Delta T$ | $\Delta R_L$ | $(C_p\Delta T + \lambda\Delta R_L) - .891$ | $m_1$ | $\rho_a$ | $m_1/\rho_a$ |
|---|---|---|---|---|---|---|
| 52 | 0 | .00865 | 0 | $\infty$ | 3.068 | $\infty$ |
| 38 | 14 | .0156 | 10.376 | 1.157 | 3.262 | .3547 |
| 25 | 27 | .0226 | 20.069 | .598 | 3.465 | .1726 |
| 11 | 41 | .0316 | 30.654 | .391 | 3.721 | .1051 |
| -2 | 54 | .0414 | 40.633 | .295 | 4.002 | .0737 |
| -16 | 68 | .0535 | 51.34 | .2337 | 4.403 | .0531 |
| -29 | 81 | .0685 | 62.055 | .193 | 4.844 | .0398 |
| -43 | 95 | .0901 | 73.939 | .162 | 5.462 | .0297 |
| -57 | 109 | .12 | 86.679 | .138 | 6.272 | .0220 |
| -70 | 122 | .165 | 100.284 | .12 | 7.445 | .0161 |
| -84 | 136 | .255 | 119.214 | .101 | 9.580 | .0105 |
| -97 | 149 | .456 | 148.887 | .081 | 13.917 | .0058 |
| -111 | 163 | 1. | 214.579 | .056 | 25.012 | .0022 |
| -125 | 177 | 1. | 224.239 | .054 | 26.034 | .00207 |
| -138 | 190 | 1. | 233.209 | .051 | 26.904 | .00190 |
| -152 | 204 | 1. | 242.869 | .049 | 27.776 | .00176 |
| -165 | 217 | 1. | 251.839 | .048 | 28.535 | .00168 |
| -178 | 230 | 1. | 260.809 | .046 | 29.256 | .00157 |
| -192 | 244 | 1. | 270.469 | .044 | 29.994 | .00147 |
| -206 | 258 | 1. | 280.129 | .043 | 30.700 | .00140 |

$m_1/\rho_a = V_2A$
$V_2 = 5.339$ ft/sec
$A = .00083$ ft$^2$
$m_1/\rho_a = .0014$
from figure 19
$m_1/\rho_a = .0044$ when $m_1 = .095$

It takes (tube volume $\rho_a/m_1$) seconds for new density fluid to reach restriction. Summarizing:

| | | |
|---|---|---|
| $\rho_1 = 3.067$ | $\rho_a = 21.136$ | $\rho_2 = 3.067$ |
| $V_1 = 37.319$ | $V_a = 5.339$ | $V_2 = 5.339$ |
| $m_1 = .095$ | $m_a = .095$ | $m_2 = .0135$ |

At t = vol. $\rho_a/m_1$ = vol/$V_2A$ = 98 sec; $\rho_2 = \rho_a = 21.136$

$V_2 = \sqrt{2\Delta P g_c/\rho_2 K} = 2.034$
$m_1/\rho_a = V_2A = .00169$
$m_1 = .048$
$\rho_a = 28.402$

At $t = vol/V_2A + 98 = 352$ sec; $\rho_2 = \rho_a = 28.402$.

$$V_2 = \sqrt{2\Delta P g_c/\rho_2 K} = 1.7544$$
$$m_1/\rho_a = .001456$$
$$m_1 = .044$$
$$\rho_a = 30.219$$

The results are;

| time (sec) | $m_1$ (mass flow in lb/sec) |
|---|---|
| 0- | .0135 |
| 0 | .095 |
| 98 | .048 |
| 352 | .044 |
| 647 | .043 (design) |

Figure 20 is a plot of these values. The pulsations will damp out in at least 10 minutes after startup.

Enough information is now known so that the exact flows in the branch streams may be found by a convergence technique. Referring to figure 11 and pressure drop equations presented in the text, one will get the following equations.

equation number 1

$$\Delta P_{12} = 4.5381\rho(1.8q_2^2/D_2^4 - .36\ q_1q_2/D_1^2D_2^2)$$
$$\Delta p_{12} = .064802$$

where $\rho = 3.077$ lb/ft$^3$

$D_1 = 12.75$ inches

$D_2 = 12.75$ inches

$q_2 = 10.736$ ft$^3$/sec

$q_1 = 21.472$ ft$^3$/sec

Because graphs are drawn as $G$(lb/hr-ft$^2$) versus $\Delta P_{TP}/L$ (psi/ft) and equations are worked in terms of $q$(ft/sec) the following useful relations will be needed.

$$G_H = 12{,}493.42\ q_H$$
$$G_B = 34{,}929.449\ q_B$$
$$G_T = 70{,}042.616\ q_B$$

**where H refers to ring header**
**B refers to branch pipe**
**T refers to tube**

**from** figure 16

$q_H = 10.763$
$G_H = 133{,}624$
$\Delta P_{TP}/L = 0.00225$ psi/ft

from figure 11

$L = 2.02$ ft
$\therefore P_{23} = (\Delta P_{TP}/L)(L)$
$\therefore P_{23} = 0.004545$

equation number 3

$\Delta P_{3a} = 4.5381\,\rho\,(1.8q_a^2/D_B^4 - 0.368q_3q_a/D_H^2D_B^2)$
where $\rho = 3.077$ (lb/ft$^3$)
$D_B = 7.625$ inches
$D_H = 12.75$ inches
$q_3 = 10.763$ (ft$^3$/sec)
$q_a$ = variable (ft$^3$/sec) particular to each branch

$\Delta P_{3a} = .007436q_a^2 - .005837q_a$
similiarly
$\Delta P_{5a} = .007436q_a^2 - .000542q_aq_5$
similiarly
$\Delta P_{7a} = .007436q_a^2 - .000542q_aq_7$
similiarly
$\Delta P_{9a} = .007436q_a^2 - .000542q_aq_9$
where $q_9$ = variable (ft$^3$/sec)

from figure 16

$q_4 = q_3 - q_{B1}$
$G_H = 12{,}493.42\ q_4$

from figure 11

$L = 6.28$ ft
$\Delta P_{45} = (\Delta P_{TP}/L)(L)$
similiarly
$q_6 = q_5 - q_{B2}$
$G_H = 12{,}493.42\ q_8$
$L = 6.28$ ft
$\Delta P_{67} = (\Delta P_{TP}/L)(L)$
similiarly
$q_8 = q_7 - q_{B3}$
$G_H = 12{,}493.42\ q_8$
$L = 6.28$ ft
$\Delta P_{89} = (\Delta P_{TP}/L)(L)$

**equation number 6**

$$\Delta P_{34} = 4.5381(1.36q_4^2/D_4^4 - .64q_3^2/D_3^4 - .72q_3q_4/D_3^2D_4^2)$$

where $= 3.077$

$D_4 = D_3 = 12.75$

$$\Delta P_{34} = .0007186q_4^2 - .0003382q_3^2 - .000384q_3q_4$$

similiarly

$$\Delta P_{56} = .0007186q_6^2 - .0003382q_5^2 - .000384q_6q_5$$

similiarly

$$\Delta P_{78} = .0007186q_8^2 - .0003382q_7^2 - .000384q_7q_8$$

from figure 16

$G_{B1} = 34{,}929.449\ q_{B1}$

from figure 11

$L_1 = 3.9322$ feet

$\Delta P_{ab1}$ (friction) $= (\Delta P_{TP}/L)(L)$

similiarly

$G_{B2} = 34{,}929.449q_{B2}$

$L_2 = 1.4322$ feet

$\Delta P_{ab2}$ (friction) $= (\Delta P_{TP}/L)(L)$

similiarly

$G_{B3} = 34{,}929.449q_{B3}$

$L_3 = 3.9322$ feet

$\Delta P_{ab3}$ (friction) $= (\Delta P_{TP}/L)(L)$

similiarly

$G_{B4} = 34{,}929.449q_{B4}$

$L_4 = 1.4322$ feet

$\Delta P_{ab4}$ (friction) $= (\Delta P_{TP}/L)(L)$

In the branch streams which are vertical the gas velocity is greater than the liquid velocity. This is known as slip. Hence the density of fluid in these branches is greater than the density at the inlet.

$$\rho_{TP}(\text{slip}) = R_L\rho_L + R_G\rho_G$$
$$= 0.11(30.67) + .89(2.827)$$
$$= 5.89 \text{ lb/ft}^3$$

where $R_L$ = volume fraction of liquid

$R_G$ = volume fraction of gas

from page 8

$\Delta P_{ab1}$ (head) $= \rho_{TP}(\text{slip})L_{B1}/144$

$\Delta P_{ab1}$ (head) $= 0.160837$ psi

where $L_{B1} = L_{B3} = 3.9322$ feet

similiarly

$\Delta P_{ab2}(\text{head}) = \rho_{TP}(\text{slip})L_{B2}/144$
$= 0.058581$ psi

where $L_{B2} = L_{B4} = 1.4322$ feet

$\Delta P_{ab3}$ (head) $= 0.160837$ psi

$\Delta P_{ab4}$ (head) $= 0.058581$ psi

equation number 4

$\Delta P_{bc1} = 3.6283((K_e - 1)q_{B1}^2/D_B^4 + q_{B1}^2/D_{TSH}^4)$

where $q_B$ = flow in branch ($ft^3$/sec) variable
$D_B$ = inside diameter of branch (inches)
= 7.625 inches
$D_{TSH}$ = inside diameter of tube sheet header (inches)
= 17.25 inches

$N_{Re}' = 3.7 \times 10^6$ as calculated earlier

using graphs in McCabe and Smith[4]

$D_B^2/D_{TSH}^2 = 0.1954$

$K_e = 0.65$ (this value will not appreciably change for the branch streams and will be considered constant)

$\Delta P_{bc1} = -.00103\, q_{B1}^2$

similiarly

$\Delta P_{bc2} = -.00103 q_{B2}^2$

$\Delta P_{bc3} = -.00103 q_{B3}^2$

$\Delta P_{bc4} = -.00103 q_{B4}^2$

equation number 5

$\Delta P_{cd} = 3.6283(((K_c + 1)q_T^2/D_T^4 - q_{B1}^2/D_{TSH}^4)$

where $q_T$ = flow through a single tube (ft/sec)
$= 8q_B/N_T$
$N_T$ = total number of tubes = 1525
$D_T$ = inside diameter of tube = 0.39 inches

from McCabe and Smith[4]

$(N_T/8)D_T^2/D_{TSH}^2 = 0.09744$

$N_{Re} = 10^6$

$K_c = 0.4$ (this value will be assumed constant in the branches)

$\Delta P_{cd1} = 0.018466 q_{B1}^2$

$\Delta P_{cd2} = 0.018466 q_{B2}^2$

$\Delta P_{cd3} = 0.018466 q_{B3}^2$

$\Delta P_{cd4} = 0.018466 q_{B4}^2$

from figure 18

$G_T = 70{,}042.616 q_B$

$\Delta P_{de1} = \Delta P_{de}$ (upper tubesheet)

$\Delta P_{de2} = \Delta P_{de}$ (lower tubesheet)

$\Delta P_{de3} = \Delta P_{de}$ (upper tubesheet)

$\Delta P_{de4} = \Delta P_{de}$ (lower tubesheet)

**equation number 4**

$$\Delta P_{ef} = 3.6283\rho((K_e - 1)q_T^2/D_T^4 + q_p^2/D_{TSH}^4)$$

**This is at the exit end of the exchanger. The fluid is all liquid.** Because of the randomness of **tubes in** the bundle each exit tubesheet will be **at the same** pressure and carry the same flow.

$q_p$ = flow in each outlet pipe
$= 1.076\ ft^3/sec$
$\rho = 30.7\ lb/ft^3$
$D_T = 0.39$ inches
$D_{TSH} = 31.5$ inches
$q_T = 2q_p/NT$
$NT = 1525$
$N_{Re} = 10^6$
$(NT/2)(D_T^2/D_{TSH}^2) = .117$
$K_e = .79$ from McCabe and Smith (4)
$\Delta P_{ef} = -0.002013$ psi

equation number 5

$$\Delta P_{fg} = 3.6283\rho((K_c + 1)/D_p^4 - 1/D_{TSH}^4)q_p^2$$

where $q_p = 1.076\ ft^3/sec$
$\rho = 30.7\ lb/ft^3$
$D_{TSH} = 31.5$ inches
$N_{Re} = 9 \times 10^5$
$D_p = 5.761$ inches
from McCabe and Smith (4)
$D_p^2/D_{TSH}^2 = 0.0334$
$K_c = 0.45$
$\Delta P_{fg} = 0.169632$ psi

equation number 2

$$\Delta P_{(gh + ij)} = 174fq^2L\rho/D_p^5$$

where $L = 14.1145$ feet
$N_{Re} = 9 \times 10^5$
from Perry's (1)
$\epsilon/D_2 = .00031$
$f_2 = .0039$
$\Delta P_{gh + ij} = 0.053648$ psi

**equation number 10**

$$\Delta P_{hi} = 5.4457\rho q_p^2/D_p^4 = 0.175722\ psi$$

equation number 11

$$\Delta P_{jk} = 4.5381\,(2(2q_p)^2/D_k^4 - .4q_p^2/D_p^4 - .82q_p^2/D_p^2D_k^2)$$

where $D_p = D_k = 5.761$ inches

$$\Delta P_{jk} = 0.992831$$

Equal flows in each branch stream will first be assumed ($q_p = 2.684$). The pressure drop equations are solved and the results are presented in tabular form.

TRIAL 1

| Branch number | 1 | 2 | 3 | 4 |
|---|---|---|---|---|
| $q_H$ | 10.736 | 8.052 | 5.368 | 2.684 |
| $q_B$ | 2.684 | 2.684 | 2.684 | 2.684 |
| $L_H$ | 2.02 | 6.28 | 6.28 | 6.28 |
| $L_B$ | 3.9322 | 1.4322 | 3.9322 | 1.4322 |
| $G_H$ | 134,130 | 100,597 | 67,065 | 33,532 |
| $G_B$ | 93,750 | 93,750 | 93,750 | 93,750 |
| $G_T$ | 187,994 | 187,994 | 187,994 | 187,994 |
| | | | | |
| $\Delta P_{12}$ | .064802 | .064802 | .064802 | .064802 |
| $\Delta P_{3a}$ | .037901 | ---- | ---- | ---- |
| $\Delta P_{23}$ | .004545 | .004545 | .004545 | .004545 |
| $\Delta P_{5a}$ | ---- | .041854 | ---- | ---- |
| $\Delta P_{7a}$ | ---- | ---- | .045758 | ---- |
| $\Delta P_{9a}$ | ---- | ---- | ---- | .049663 |
| $\Delta P_{45}$ | ---- | .008541 | .008541 | .008541 |
| $\Delta P_{67}$ | ---- | ---- | .005150 | .005150 |
| $\Delta P_{89}$ | ---- | ---- | ---- | .001790 |
| $\Delta P_{34}$ | ---- | -.025587 | -.025587 | -.025587 |
| $\Delta P_{56}$ | ---- | ---- | -.017818 | -.017818 |
| $\Delta P_{78}$ | ---- | ---- | ---- | -.010101 |
| $\Delta P_{ab}$ (friction) | .006056 | .002206 | .006056 | .002206 |
| (head) | .160837 | .058581 | .160837 | .058581 |
| $\Delta P_{bc}$ | -.00742 | -.00742 | -.00742 | -.00742 |
| $\Delta P_{cd}$ | .133026 | .133026 | .133026 | .133026 |
| $\Delta P_{de}$ | 26.420 | 26.942 | 26.420 | 26.942 |
| $\Delta P_{ef}$ | -.002013 | -.002013 | -.002013 | -.002013 |
| $\Delta P_{fg}$ | .169630 | .169630 | .169630 | .169630 |
| $\Delta P_{gh}$ + ij | .053648 | .053648 | .053648 | .053648 |
| $\Delta P_{hi}$ | .175722 | .175722 | .175722 | .175722 |
| $\Delta P_{jk}$ | .992831 | .992831 | .992831 | .992831 |
| $\Delta P_{total}$ (1k) | 28.2095 | 28.6123 | 28.1877 | 28.5992 |

$\Delta P = Kq^2$

$\partial \Delta P = 2K \partial q$

$\partial q_B = \partial \Delta P_B (q_{B\ average} / 2 \Delta P_{B\ average})$

$\Delta P_{average} = (\Delta P_{B1} + \Delta P_{B2} + \Delta P_{B3} + \Delta P_{B4})/4 = 28.4022$

$q_{average} = 2.684$

$\partial q_B = q_{B\ average} - q_B$

$\partial \Delta P_B = \Delta P_{B\ average} - \Delta P_B$

TRIAL 2

| Branch number | | 1 | 2 | 3 | 4 |
|---|---|---|---|---|---|
| $\partial \Delta P_B$ | | .1927 | -.2101 | .2145 | -.1970 |
| $\partial q$ | | .00913 | -.00995 | .01016 | -.00933 |
| $q_B$ | | 2.69313 | 2.67405 | 2.69416 | 2.67404 |
| $q_H$ | | 10.736 | 8.04287 | 5.34871 | 2.67405 |
| $L_H$ | | 2.02 | 6.28 | 6.28 | 6.28 |
| $L_B$ | | 3.9322 | 1.4322 | 3.9322 | 1.4322 |
| $G_H$ | | 134,130 | 100,483 | 66,824 | 33,408 |
| $G_B$ | | 94,070 | 93,403 | 94,106 | 93,403 |
| $G_T$ | | 188,634 | 187,297 | 188,706 | 187,297 |
| | | | | | |
| $\Delta P_{13}$ | | .069347 | .069347 | .069347 | .069347 |
| $\Delta P_{3a}$ | | .038262 | ---- | ---- | ---- |
| $\Delta P_{5a}$ | | ---- | .041515 | ---- | ---- |
| $\Delta P_{7a}$ | | ---- | ---- | .046164 | ---- |
| $\Delta P_{9a}$ | | ---- | ----- | ---- | .049296 |
| $\Delta P_{45}$ | | ---- | .008509 | .008509 | .008509 |
| $\Delta P_{67}$ | | ---- | ---- | .005118 | .005118 |
| $\Delta P_{89}$ | | ---- | ---- | ---- | .001790 |
| $\Delta P_{34}$ | | ---- | -.025655 | -.025655 | -.025655 |
| $\Delta P_{56}$ | | ---- | ---- | -.017838 | -.017838 |
| $\Delta P_{78}$ | | ---- | ---- | ---- | -.010029 |
| $\Delta P_{ab}$ | (friction) | .006095 | .002191 | .006095 | .002191 |
| | (head) | .160837 | .058581 | .160837 | .058581 |
| $\Delta P_{bc}$ | | -.007471 | -.007365 | -.007476 | -.007365 |
| $\Delta P_{cd}$ | | .133933 | .132042 | .134035 | .132041 |
| $\Delta P_{de}$ | | 26.522 | 26.827 | 26.535 | 26.827 |
| $\Delta P_{ek}$ | | 1.3898 | 1.3898 | 1.3898 | 1.3898 |
| | | 28.3128 | 28.4960 | 28.3039 | 28.4828 |

$\Delta P_{average} = 28.39888$

$\partial q_B = \partial \Delta P_B (2.684/2(28.39888)) = \partial \Delta P_B (.0419735)$

## TRIAL 3

| Branch number | 1 | 2 | 3 | 4 |
|---|---|---|---|---|
| $\partial \Delta P_B$ | .18938 | -.21342 | .21118 | -.200032 |
| $\partial q_B$ | .00795 | -.00896 | .00886 | -.0084 |
| $q_B$ | 2.7010 | 2.66509 | 2.70302 | 2.66627 |
| $q_H$ | 10.736 | 8.035 | 5.36991 | 2.66627 |
| $G_H$ | 134,129 | 100,385 | 67,089 | 33,311 |
| $G_B$ | 94,344 | 93,090 | 94,415 | 93,131 |
| $G_T$ | 189,185 | 186,670 | 189,327 | 186,753 |

| | | | | |
|---|---|---|---|---|
| $\Delta P_{13}$ | .069347 | .069347 | .069347 | .069347 |
| $\Delta P_{3a}$ | .038532 | ---- | ---- | ---- |
| $\Delta P_{5a}$ | ---- | .041209 | ---- | ---- |
| $\Delta P_{7a}$ | ---- | ---- | .046463 | ---- |
| $\Delta P_{9a}$ | ---- | ---- | ---- | .049009 |
| $\Delta P_{45}$ | ---- | .008509 | .008509 | .008509 |
| $\Delta P_{67}$ | ---- | ---- | .005118 | .005118 |
| $\Delta P_{89}$ | ---- | ---- | ---- | .001790 |
| $\Delta P_{34}$ | ---- | -.025713 | -.025713 | -.025713 |
| $\Delta P_{56}$ | ---- | ---- | -.017682 | -.017682 |
| $\Delta P_{78}$ | ---- | ---- | ---- | -.010142 |
| $\Delta P_{ab}$ (friction) | .006095 | .002184 | .006095 | .002184 |
| (head) | .160837 | .058581 | .160837 | .058581 |
| $\Delta P_{bc}$ | -.007514 | -.007316 | -.007526 | -.007322 |
| $\Delta P_{cd}$ | .134717 | .131159 | .134918 | .131275 |
| $\Delta P_{de}$ | 26.612 | 26.725 | 26.632 | 26.742 |
| $\Delta P_{ek}$ | 1.3898 | 1.3898 | 1.3898 | 1.3898 |
| | 28.4038 | 28.3927 | 28.4022 | 28.3968 |

$\Delta P_{average} = 28.39888$
$\partial q_B = .0419735 \, \partial \Delta P_B$

FINAL RESULTS

| Branch number | 1 | 2 | 3 | 4 |
|---|---|---|---|---|
| $\partial \Delta P_B$ | -.0049 | .0062 | -.0033 | .0021 |
| $\partial q_B$ | -.00021 | .00026 | -.00014 | .00009 |
| $q_B$ | 2.7009 | 2.6655 | 2.7030 | 2.6665 |

**These are flow results accurate to four decimal places.**

**Pressure drops are accurate to two decimal places.**

Now that flow rates for the branch streams from the ring header have been established and the system has been checked for instabilities, the loss of exchanger duty must be calculated. The exchanger will be divided into three concentric segments each with an equal number of tubes. It will be assumed that the liquid phase enters separate tubes uniformly distributed in the innermost segment and gas phase only enters all other tubes. Variations in tubesheet pressures and tube lengths will cause sixteen discrete flows through the exchanger which will be calculated. After finding the number of plugged tubes and where they exist one may calculate the number of tubes carrying each discrete flow. Assuming a constant overall U, a UA for each of the sixteen flows may be found. It will be assumed that the shellside flow is uniformly distributed. Cooling curves for each discrete flow will be drawn maintaining a fixed UA and the enthalpy change of each flow will be found. The loss of duty for each flow due to variations in tube inside diameter will be calculated and the actual exchanger duty can be found by adding the sixteen enthalpy changes.

The number of plugged tubes in each segment will be found. Since the feed stream tubes are continuous through all three bundles (C, D, and E)

**the maximum number of tubes plugged in the three bundles will be lost to all three bundles. The number of plugged tubes are reported for each tube layer, therefore the number of layers per segment for each bundle must first be found.**

<u>C Bundle</u>

inside diameter = 120.75 inches
outside diameter = 144.5 inches
effective tube length = 44.35 feet
total surface area = 8850 feet squared

Because the C Bundle is wound on top of another bundle and not on the mandrel it has no plugged tubes.

<u>D Bundle</u>

inside diameter = 30 inches
outside diameter = 143.54 inches
effective tube length = 107.1 feet
total number of layers = 86
total surface area = 21,370 $ft^2$
outside diameter of inside segment = $((O.D.^2 - I.D.^2)/3 + I.D.^2)^{\frac{1}{2}}$ = 86.4 inches
layers in inside segment = $86(86.4 - 30)/(143.54 - 30)$ = 43

There are 12 plugged tubes in the first segment and none in the other two. [12]

<u>E Bundle</u>

inside diameter = 30 inches
outside diameter = 143.54 inches
effective tube length = 134.5 feet
tube layers = 62
total surface area = 26,870 $ft^2$
outside diameter of insider (No. 1) segment = $((O.D.^2 - I.D.^2)/3 + I.D.^2)^{\frac{1}{2}}$ = 66.6 inches
layers in segment 1 = $62(66.6 - 30)/(143.54 - 30)$ = 29

There are 18 plugged tubes in the first segment and none in the other two. [12]

From an analysis of the three bundles, the maximum number of tubes plugged is eighteen. This means that eighteen tubes will be lost in each bundle. To be conservative it will be assumed that all the plugged tubes are in the first segment of each bundle.

Surface area lost per bundle = (effective length) (number of plugged tubes)$\pi$(tube outside diameter)

| Bundle | Surface area lost ($ft^2$) |
|---|---|
| C | 104.95 |
| D | 252.34 |
| E | 316.91 |
| Total | 674.20 |

The effect of plugging the eighteen tubes will cause the G rate to increase in the other tubes by 18/1525 = 1.18%. By checking figure 18 this increase in flow rate will increase the total bundle pressure drop by 0.355 psi. This small increase in bundle pressure drop will not appreciably effect the flow distribution that has already been calculated in the ring header.

An average tube length in each of the three concentric segments must now be found. Since tubes are wrapped around the mandrel in each bundle, the tubes lose their identity in the circumferential direction. Also since tubes of one bundle are randomly connected to tubes of another bundle in the same segment, one may assume that all tubes at a particular radius are the same length. The tube lengths in any particular bundle are all equal. It is between the bundle that the lengths differ and a definite trend allows one to predict an average tube length in concentric

**segments. By actual observance of the bundle winding operations it was noticed that all tubes of a particular radial distance maintain their identity in corresponding** radial distances throughout the entire circuit. In other words tubes on the outside periphery tend to stay on the outside while tubes on the inside tend to follow nearest the mandrel the entire distance. This might be better illustrated by looking at figure 10. Sections A, B, C, D, and E are drawn in figure 10. An explanation of the diagrams of each section as will be used in this analysis is presented on pages 27 - 30.

DIAGRAM OF SECTION A

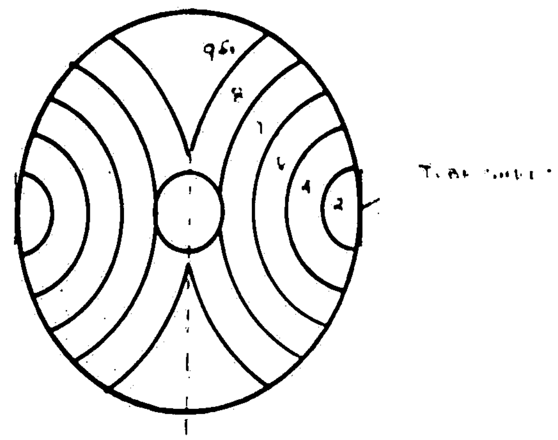

The above diagram illustrates the relative distance tubes from a particular position must extend to be connected to the tubesheet. The fact that tubes nearest the mandrel are connected to the top of the circular tubesheet has been taken into account. Divide the above diagram into three concentric equal areas. Find the average excess tube length in each concentric segment by a mathematical summation of particular excess tube lengths times the fraction of total tubes in the segment that are associated with the particular excess length. It is then desired to have the second concentric segment have the design excess tube length which will have zero variation of tube lengths. Concentric segments one and three are adjusted to show variations of tube length from the design case. The resultant diagram will be called the tube length variations of concentric segment of section A.

<u>TUBE LENGTH VARIATIONS OF CONCENTRIC SEGMENTS OF SECTION A</u>

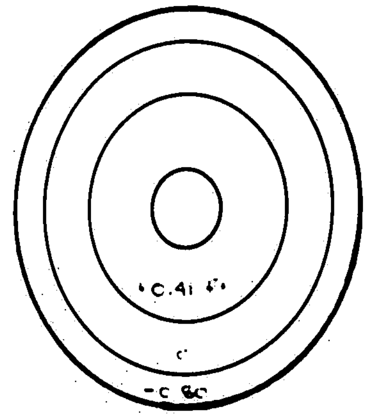

Sections B and C are directly transformable into the diagrams below.

<u>TUBE LENGTH VARIATIONS OF CONCENTRIC SEGMENTS OF SECTION B</u>

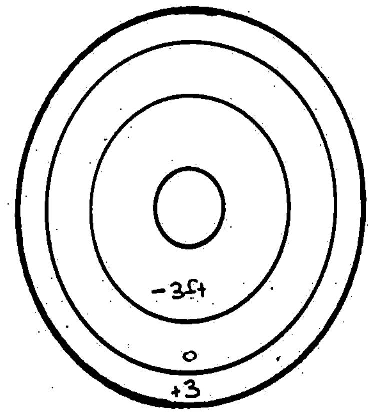

## TUBE LENGTH VARIATIONS OF CONCENTRIC SEGMENTS OF SECTION C

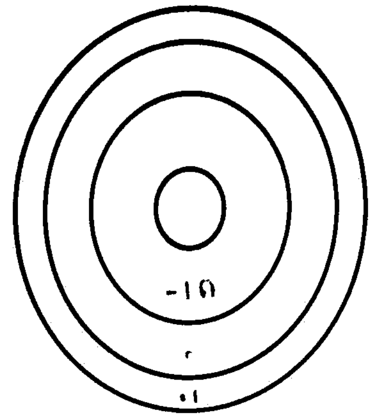


In section D the tubes are drawn from the top of Bundle C into eight tightly packed columns. Tube length variation in this case is very slight. Proceeding by the same method as for section A the following diagrams result.

DIAGRAM OF SECTION D

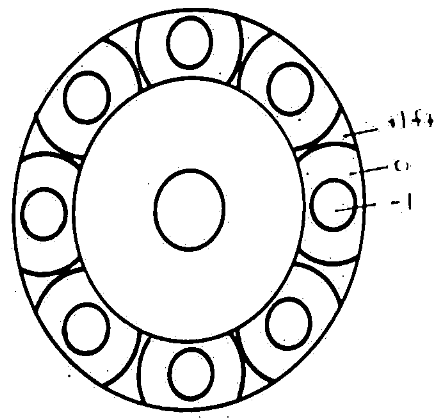


TUBE LENGTH VARIATIONS OF CONCENTRIC SEGMENTS OF SECTION D

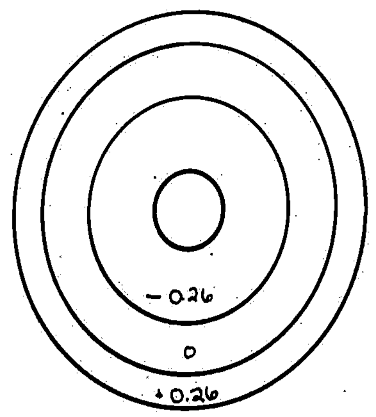

**Similiarly,**

**DIAGRAM OF SECTION E**

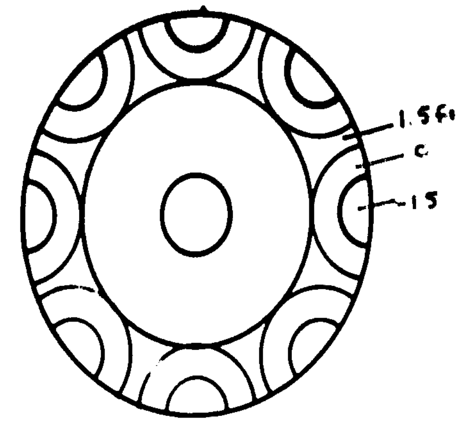


TUBE LENGTH VARIATIONS OF CONCENTRIC SEGMENTS OF SECTION E

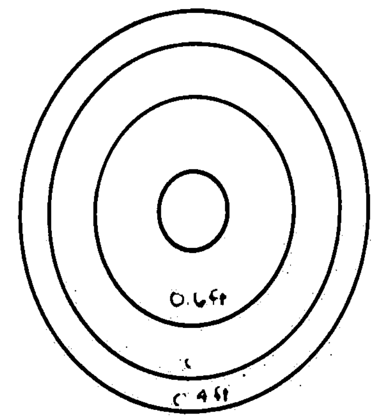


The tube length variations for each segment are directly additive for each of the five sections.

FINAL RESULT OF THE TUBE LENGTH VARIATIONS OF CONCENTRIC SEGMENTS FOR SECTIONS A, B, C, D, AND E

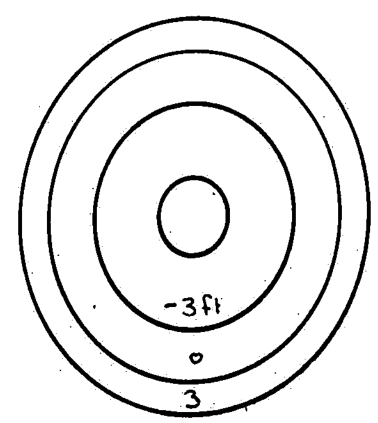

It can be seen that the tube lengths in segment 1 nearest the mandrel are three feet less than design and the tubes in segment 3 furthermost from the mandrel are roughly three feet over design. This will lead to maldistribution problems.

Pressure drop versus flow rate for each segment must be plotted. It has been stated that in certain tubes of segment 1 all liquid enters while gas phase enters all other tubes. Pressure drops were calculated for various liquid flows in segment 1, also for various gas rates in segments 1, 2, and 3. Results are presented in table 3 and plotted in figure 21. Given a pressure drop and segment number one can now find a gas or liquid flow rate. Pressure drops caused by variations of tubesheet pressures were calculated on page 60. It must be remembered that the plugging of eighteen tubes has increased these pressure drops by 0.355 psi. With these pressure drops and referring to figure 21 the following sixteen discrete flow rates may be tabulated:

| Tube sheet number | 1 | 2 | 3 | 4 |
|---|---|---|---|---|
| Pressure drop in bundle (with plugged tubes) | 26.967 | 27.080 | 26.987 | 27.097 |
| Flow rate G(lb/hr.ft$^2$) from figure 21 | | | | |
| liquid in seg.1 | 256,500 | 237,000 | 257,000 | 238,000 |
| gas in seg. 1 | 186,900 | 186,400 | 187,000 | 186,550 |
| gas in seg. 2 | 187,600 | 187,200 | 187,700 | 187,300 |
| gas in seg. 3 | 188,050 | 187,550 | 188,150 | 187,700 |

The number of tubes that liquid enters will vary with flow rate. If the liquid flow rate $G_L$ is low more tubes will be filled with liquid. If the liquid flow rate $G_L$ is high less tubes will be filled. Therefore, the area that is to be allotted to each flow is actually dependent upon the flow rate. $G_{TP}$ is constant.

$$\text{Number of tubes carrying liquid} = \frac{\text{M lbs/hr. of liquid}}{(G_L \text{ lb/hr.- ft}^2)(\text{A ft}^2\text{/tube})}$$

Where M = 5143 lb/hr. of liquid

| Tube sheet number | 1 | 2 | 3 | 4 | Total |
|---|---|---|---|---|---|
| Number of tubes | 381.25 | 381.25 | 381.25 | 381.25 | 1,525 |
| liquid in seg. 1 | 24.17 | 28.16 | 24.12 | 28.05 | |
| gas in - seg. 1 | 98.41 | 94.42 | 98.46 | 94.53 | |
| seg. 2 | 127.08 | 127.08 | 127.08 | 127.08 | |
| seg. 3 | 127.08 | 127.08 | 127.08 | 127.08 | |
| Flow (lb/hr) M | | | | | |
| liquid in seg. 1 | 4,953.42 | 5,332.39 | 4,952.81 | 5,333.98 | 20,572.59 |
| gas in - seg. 1 | 15,206.08 | 14,550.55 | 15,221.95 | 14,579.22 | 59,558.00 |
| seg. 2 | 19,709.50 | 19,667.48 | 19,720.00 | 19,677.98 | 78,775.96 |
| seg. 3 | 19,756.78 | 19,704.25 | 19,767.29 | 19,720.01 | 78,949.33 |
| | 54,672.36 | 53,922.28 | 54,709.24 | 53,977.22 | 237,853. |

If greater accuracy is desired use the new values for M lb/hr. and go back and recalculate the number of tubes carrying each flow. Repeat this until the values no longer change.

The UA for each discrete flow can be found noting that UA is proportional to the number of tubes and that the total UA after taking into account the loss of tubes due to plugging is 3,963,051 $\frac{\text{Btu's}}{\text{hr.}^\circ\text{F}}$. The flow rate in moles of feed per hour is simply found by dividing the flow in (lb/hr.) by the molecular weight of the flow (MW gas = 21.7169; MW liquid = 43.5786).

| Tube sheet number | 1 | 2 | 3 | 4 | Total |
|---|---|---|---|---|---|
| UA (Btu's/hr.°F) | | | | | |
| liquid seg. 1 | 63,560 | 74,053 | 63,492 | 73,764 | 274,869 |
| gas seg. 1 | 258,802 | 248,309 | 258,870 | 248,598 | 1,014,579 |
| gas seg. 2 | 334,201 | 334,201 | 334,201 | 334,201 | 1,336,805 |
| gas seg. 3 | 334,201 | 334,201 | 334,201 | 334,201 | 1,336,805 |
| Total | 990,764 | 990,764 | 990,764 | 990,764 | 3,963,058 |
| Flow (moles/hr.) | | | | | |
| liquid seg. 1 | 113.679 | 122.377 | 113.665 | 122.413 | 472.134 |
| gas seg. 1 | 700.196 | 670.011 | 700.926 | 671.331 | 2,742.464 |
| gas seg. 2 | 907.565 | 905.630 | 908.049 | 906.114 | 3,627.358 |
| gas seg. 3 | 909.742 | 907.323 | 910.226 | 908.049 | 3,635.340 |
| | | | | | 10,478 |

To be accurate one would construct cooling curves for each of the sixteen flows, fix the inlet conditions and UA, and calculate the duty of each. This could probably be worked out on the computer. By graphical methods the accuracy decreases and several flows may be combined without appreciable error. The gas flows in segments 1, 2, and 3 differ only by 0.9% and may be combined; also liquid in tube sheet 1 and 3, and liquid in tube

**sheet 2 and 4. Only three cooling curves will now have to be drawn.**

| Flow No. | Description | Flow (Moles/hr.) | UA (Btu's/M°F) |
|---|---|---|---|
| 1. | Liquid, segment 1 (tube sheet 1 and 3) | 227.344 | 127.052 |
| 2. | Liquid, segment 1 (tube sheet 2 and 4) | 244.810 | 147.817 |
| 3. | Gas, segments 1, 2, 3 (tube sheets 1, 2, 3, 4) | 10,005.861 | 3,688.189 |
| | Total | 10,478.015 | 3,963.058 |

The duty (Btu's/hr.) was determined from enthalpy data (Btu's/mole) times the flow rate (moles/hr.) Table 4 lists the temperature enthalpy data that has been calculated for each of the three flow rates that are described above. Shellside flow has been divided proportional to the surface area of each of the three tubeside flows and enthalpy data listed in table 5. The cooling curves were plotted in figures 22, 23, and 24. The UA of each was found by dividing the cooling curves into incremental segments and calculating UA = $\sum \Delta H/\Delta T$ log mean.

$$\text{Where: } \Delta T \text{ log mean} = \frac{\Delta T \text{ high} - \Delta T \text{ low}}{\log \dfrac{\Delta T \text{ high}}{\Delta T \text{ low}}}$$

The calculated value of UA was compared to the actual UA as listed on page 71. If the UA was lower the cooling stream was shifted to the left, if the calculate UA was higher the cooling stream was shifted to the right slightly.

A new UA was calculated. The curve was shifted until the calculated UA equaled the actual UA and the $\Delta H$ observed. The final cooling curves with the actual UA are drawn on figures 22, 23, and 24. The results are listed below.

| Flow No. | Duty Btu's/hr. |
|---|---|
| 1 | 1,350,327 |
| 2 | 1,484,161 |
| 3 | 61,642,653 |
| Total | 64,477,141 |

The design duty was 66,110,000 Btu's per hour so one can see that already 2.45% of the duty has been lost and the loss due to variation in tube inside diameter has not yet been considered.

To calculate the loss of duty caused by variations in tube inside diameter, the maximum and minimum flow rates must first be found. The following figures were obtained from the tube vendors:

Average tube I.D. = 0.390"
Maximum tube I.D. = 0.401"
Minimum tube I.D. = 0.379"

The effect of tube I.D. on the liquid flows may be found with the use of equation #2, $\Delta P = \frac{174\ fq^2 \rho L}{D^5}$. Since pressure drop, density, and length are not a function of tube I.D., the following relationship can be developed:

$$\frac{f_1 q_1^2}{D_1^5} = \frac{f_2 q_2^2}{D_2^5}$$

Liquid will flow at about $G = 250,000\ lb/ft^2$-hr. and the friction factor ratio will be found at this flow rate.

$$N_{Re} = GD/\mu \qquad \text{let } \mu = 0.224 \text{ lb/hr.ft}^2$$

$N_{Re}$ (max dia) = $3.730 \times 10^4$
$N_{Re}$ (ave dia) = $3.627 \times 10^4$
$N_{Re}$ (min dia) = $3.525 \times 10^4$

$$f = .0014 + .125/N_{Re}^{.32} \quad \text{(for turbulent region)}$$ 13

$f$ (max dia) = .003450
$f$ (ave dia) = .003474
$f$ (min dia) = .003490

$$\left(\frac{q_1}{q_2}\right)^2 = \left(\frac{f_2}{f_1}\right)\left(\frac{D_1}{D_2}\right)^5$$

$$\frac{M\ max}{M\ ave} = \frac{q\ max}{q\ ave} = 1.076 \qquad \frac{M\ min}{M\ ave} = \frac{q\ min}{q\ ave} = 0.929$$

Flow No. 1
M ave = 227.34 mole/hr. from page 67
M max = 244.62
M min = 211.20

Flow No. 2
M ave = 249.80 moles/hr. from page 67
M max = 263.40
M min = 237.42

The cooling curves for the high and low flow rates are plotted on figures 22 and 23 keeping UA fixed at the design case. Because of the nature of the curves there is a pinch at the cold end. Thus, when the high and low flow duties are averaged, the loss of duty is so small that it cannot be determined graphically. It can, therefore, be said that variations in tube I.D. causes negligible loss of duty in the liquid flows (no. 1 and 2).

The effect of tube I.D. variations on the gas stream (flow no. 3) will be examined next. First the

**maximum** and minimum maldistribution of flow must be found. Assume at $G = 185{,}000$ lb/hr.-ft$^2$ the pressure drop through tubes of maximum and minimum diameter are equal. Calculate the maximum and minimum flows under this assumption

$G = 185{,}000$ lb/hr.-ft$^2$

| Tube I.D. (ft) | X-Sect. Area (ft$^2$) | M (lb/hr. - tube) |
|---|---|---|
| .033417 | .0008770 | 162.2524 |
| .032500 | .0008296 | 153.4705 |
| .031583 | .0007834 | 144.9327 |

Next the assumption of equal pressure drops are checked as on pages 44 and 45 and the flows corrected for equal $\Delta P$.

| Tube I.D. (ft) | $\Delta P$ (psi) |
|---|---|
| .033417 | 25.8483 |
| .032500 | 26.3333 |
| .031583 | 26.5154 |

$$\delta\Delta P/2\Delta P_{ave} = \delta M/M_{ave}$$

where $\Delta P_{ave} = 26.3333$ psi

$M_{ave} = 153.4705$

$\delta\Delta P = \Delta P - \Delta P_{ave}$

$\delta M = M - M_{ave}$

$$\delta M = \delta\Delta P M_{ave}/2\Delta P_{ave}$$

$\delta M_{(max\ I.\ D.)} = -1.41329$

$\delta M_{(min\ I.\ D.)} = 0.5306$

| Tube I. D. (ft) | Corrected flow M(lb/hr-tube) | Flow (moles/hr) |
|---|---|---|
| .033417 | 160.73 | 10,506.15 |
| .031583 | 145.46 | 9,505.67 |

The cooling curve for these maximum and minimum flows due to variation of tube I. D. are plotted in figure 24

**with fixed UA. This is the same as having two equal area exchangers, one with all small diameter tubes and one with all large diameter tubes. The duty of each is calculated and the two are averaged. The result is the duty considering maldistribution. Results are tabulated below.**

| UA | $\Delta H$ | Flow (moles/hr) |
|---|---|---|
| 3,588,000 | 61,521,453 | 10,005.86 |
| 4,017,300 | 61,921,453 | 10,005.86 |
| 2,857,400 | 62,521,966 | 10,506.15 |
| 4,571,500 | 63,521,966 | 10,506.15 |
| 3,221,470 | 59,521,966 | 9,505.67 |
| 4,346,800 | 60,521,966 | 9,505.67 |

Since the design UA = 3,688,000 for this gas flow, the duty is found by extrapolation and tabulated below for each flow rate. It should be noted that when extrapolating linearity is assumed which is not the case here. For better accuracy more trials should be made perferably on the computer.

Flow #3

$\Delta H$(average) = 61,642,653 Btu's/hr

$\Delta H$(max. dia.) = 63,006,575

$\Delta H$(min. dia.) = 59,936,000

$\Delta H$(maldistribution) = $(\Delta H_{max.\,dia.} - \Delta H_{min.\,dia.})(M_{max})/(M_{min} + M_{max}) + \Delta H_{min.\,dia.}$ = 61,532,699

Loss of duty = $\Delta H_{design} - \Delta H_{mal}$ = 110,000 Btu's/hr

% loss of duty = 0.178%

This value for loss of duty is conservative. For a truer value the equation $L' = 2K/N \sum_{i=0}^{\frac{n-1}{2}} (\bar{m} - 12\bar{m}/(N - 1))^2$ should be used. However, in this case i is the number of tubes and would be equal to 1403. Since the loss of duty (0.178%) is so small it would be useless to be very accurate.

The actual duties for each of the three flows considering all types of maldistribution that could exist in the exchanger have now been calculated. The results are slightly conservative.

| | Duty (Btu's/hr.) |
|---|---|
| Flow #1 (liquid in segment 1, tubesheet 1 and 3) | 1,484,160 |
| Flow #2 (liquid in segment 1, tubesheet 2 and 4) | 1,350,327 |
| Flow #3 (gas in segment 1, 2, 3, tubesheet 1, 2, 3, 4) | 61,532,699 |
| Total exchanger duty (ACTUAL) | 64,367,186 |
| Total exchanger duty (DESIGN) | 66,110,000 |
| Loss of exchanger duty | 1,742,814 |
| % loss of exchanger duty | 2.63% |

The results of maldistribution from the different causes may be broken down as follows:

| Cause of Maldistribution | % Loss of Duty |
|---|---|
| Liquid-vapor separation | 1.805 |
| Variation in tubesheet pressures | negligible |
| Variation in tube I.D. | 0.178 |
| Variation in tube lengths | negligible |
| Plugged tubes | 0.645 |
| | 2.628 |

It can be seen that phase separation is by far the most critical condition and great care should be taken to keep a dispersed or homogeneous fluid in the tubesheet header. With the ring header design that has been assumed the loss of duty due to maldistribution of flow caused by the unsymmetric ring header is negligible. To get an exact answer the use of a computer would be required.

Variations in tube I.D. causes a slight loss of duty in the tubes carrying gas phase. For this particular example variations in tube lengths produces no visable effects. Again a computer would be needed to arrive at a duty loss. Of course, plugged tubes cause appreciable loss of duty due to loss of surface area.

The ring header design that was chosen appears to be adequate. If it is desired to reduce the ring header diameters to cut costs, the procedure would have to be repeated and loss of duty recalculated. Cost due to loss of production, increased pressure drop, and ring header should be minimized. If a new header design is assumed several shortcuts can be made. The loss of duty caused by liquid-vapor separation, variation in tube I.D., variations in tube length, and plugged tubes will remain relatively constant. It does appear, however, that the cost of increased pressure drop of a new design will dominate the total cost rather than the cost due to loss of duty and perhaps loss of duty need not be recalculated.

APPENDIX

FIGURE #1

BUTTONHOOK HEADERS

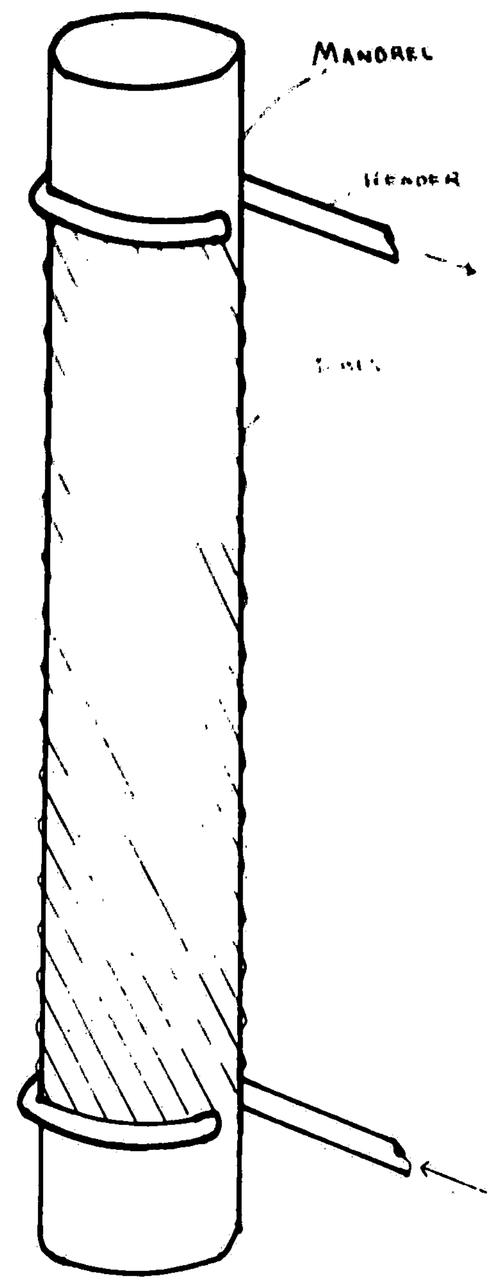

FIGURE #2

TYPICAL COIL WOUND EXCHANGER

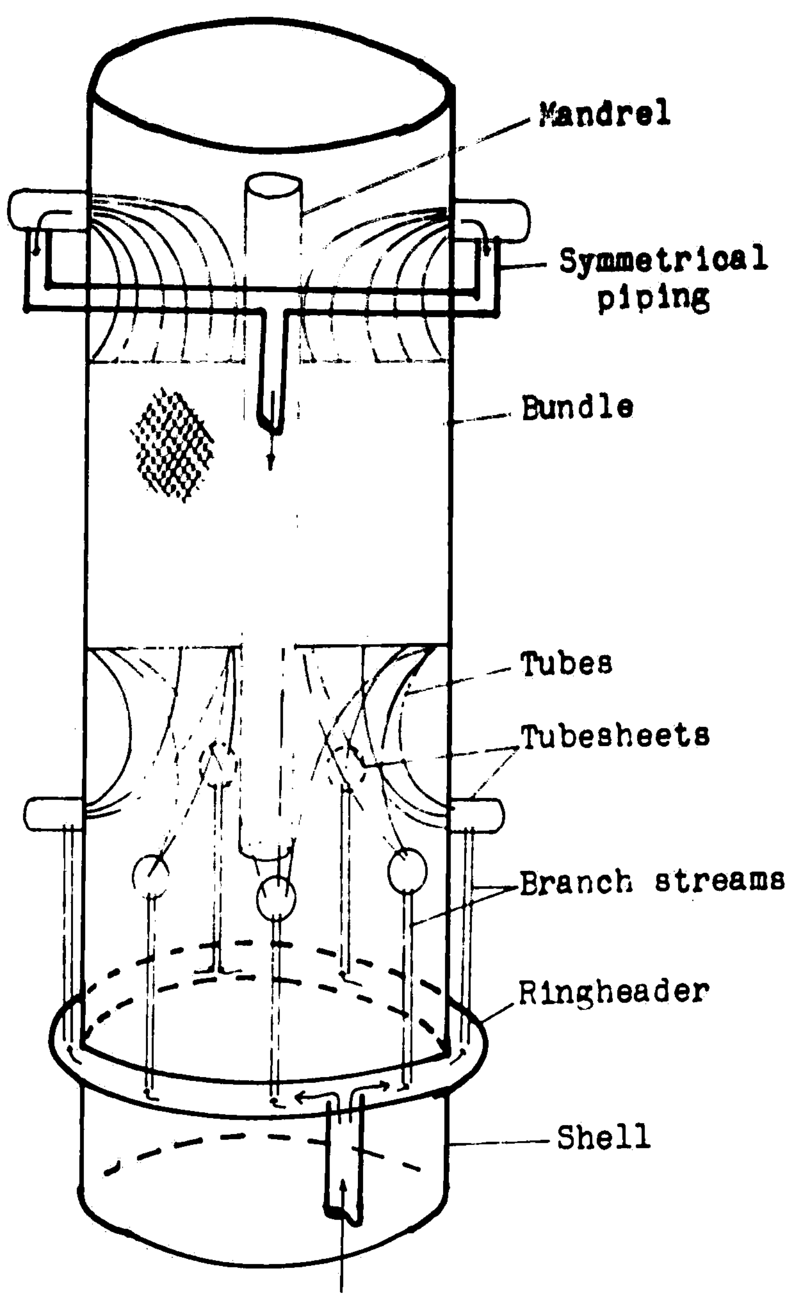

**FIGURE #3**

**PLATE-FIN or CORE EXCHANGERS**

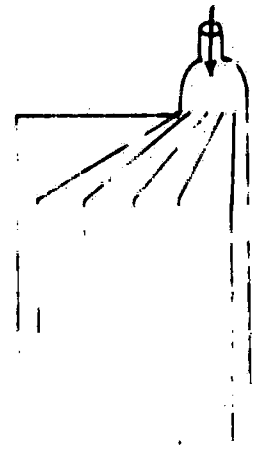

Core inlet

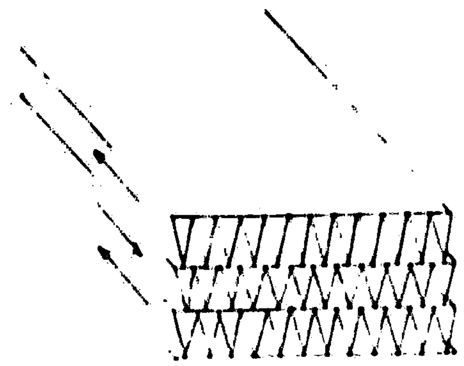

Flow passages

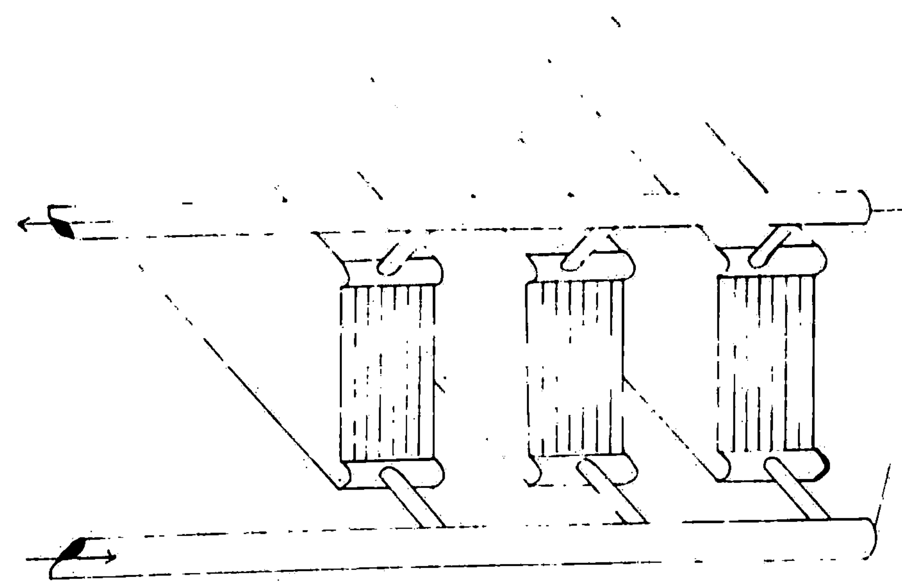


Cores in parallel

FIGURE #4

Correlation for Hughmark's Flow Parameter Z

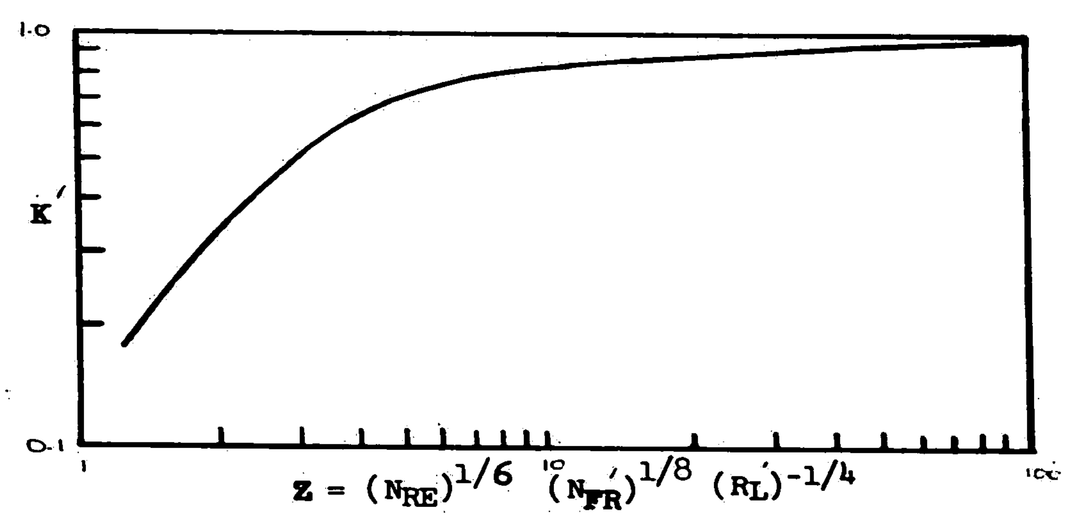


**Coordinate Points For**

**Fig. # 4**

| Z | K' |
|---|---|
| 1.3 | 0.185 |
| 1.5 | 0.225 |
| 2.0 | 0.325 |
| 3.0 | 0.49 |
| 4.0 | 0.605 |
| 5.0 | 0.675 |
| 6.0 | 0.72 |
| 8.0 | 0.767 |
| 10.0 | 0.78 |
| 15.0 | 0.808 |
| 20.0 | 0.83 |
| 40.0 | 0.88 |
| 70.0 | 0.93 |
| 130.0 | 0.98 |

**FIGURE #5**

**CHENOWITH - MARTIN**

**TWO PHASE PRESSURE DROP CORRELATION**

**(Extended by Lapin and Bauer)**

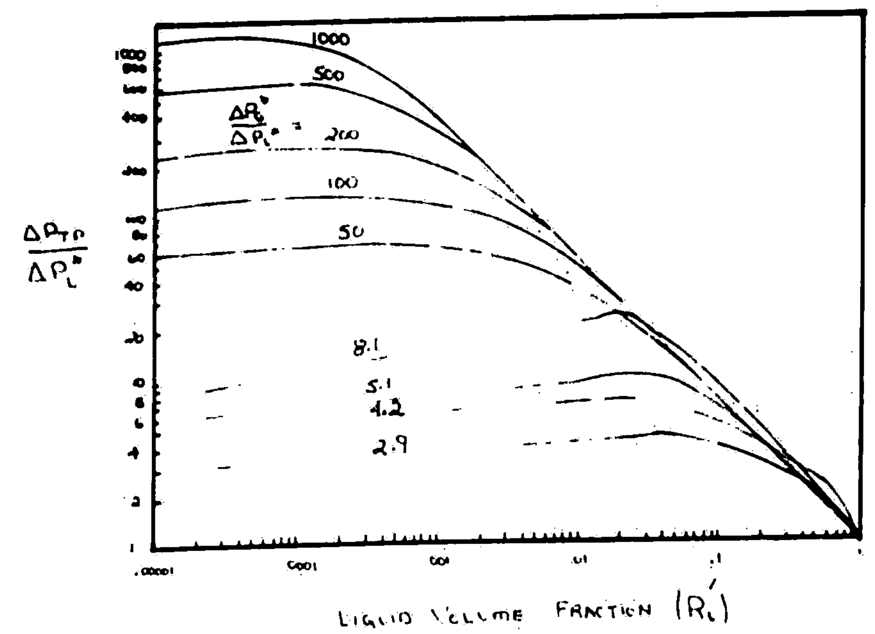

**FIGURE # 6**

**Coefficient, Loss From Sudden Enlargement of Cross Section** (4)

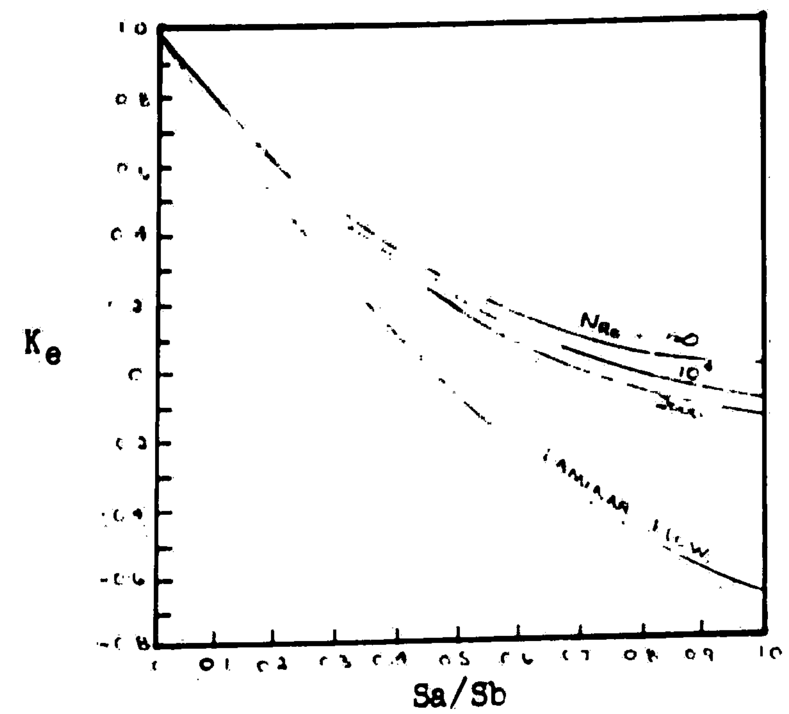


FIGURE #7

Coefficient, Loss From Sudden Contraction of Cross Section (4)

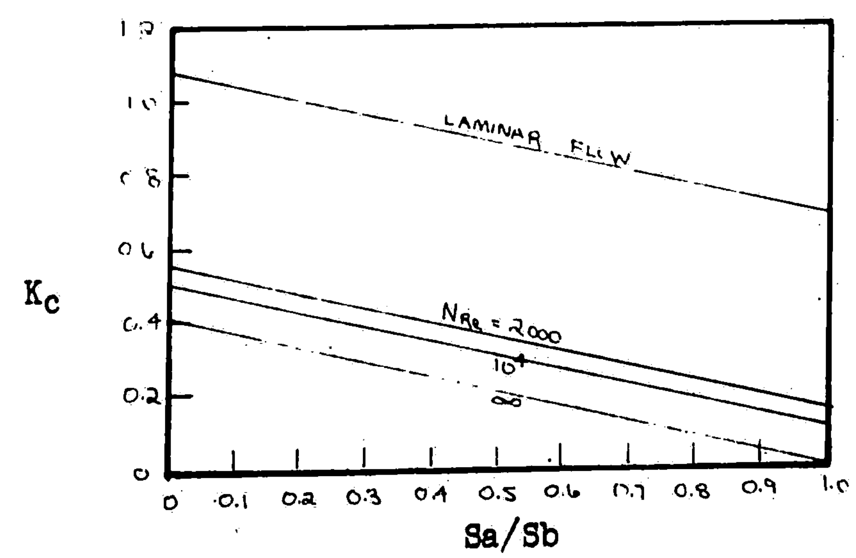

## FIGURE 8

Baker Chart
(for prediction of Flow Patterns)

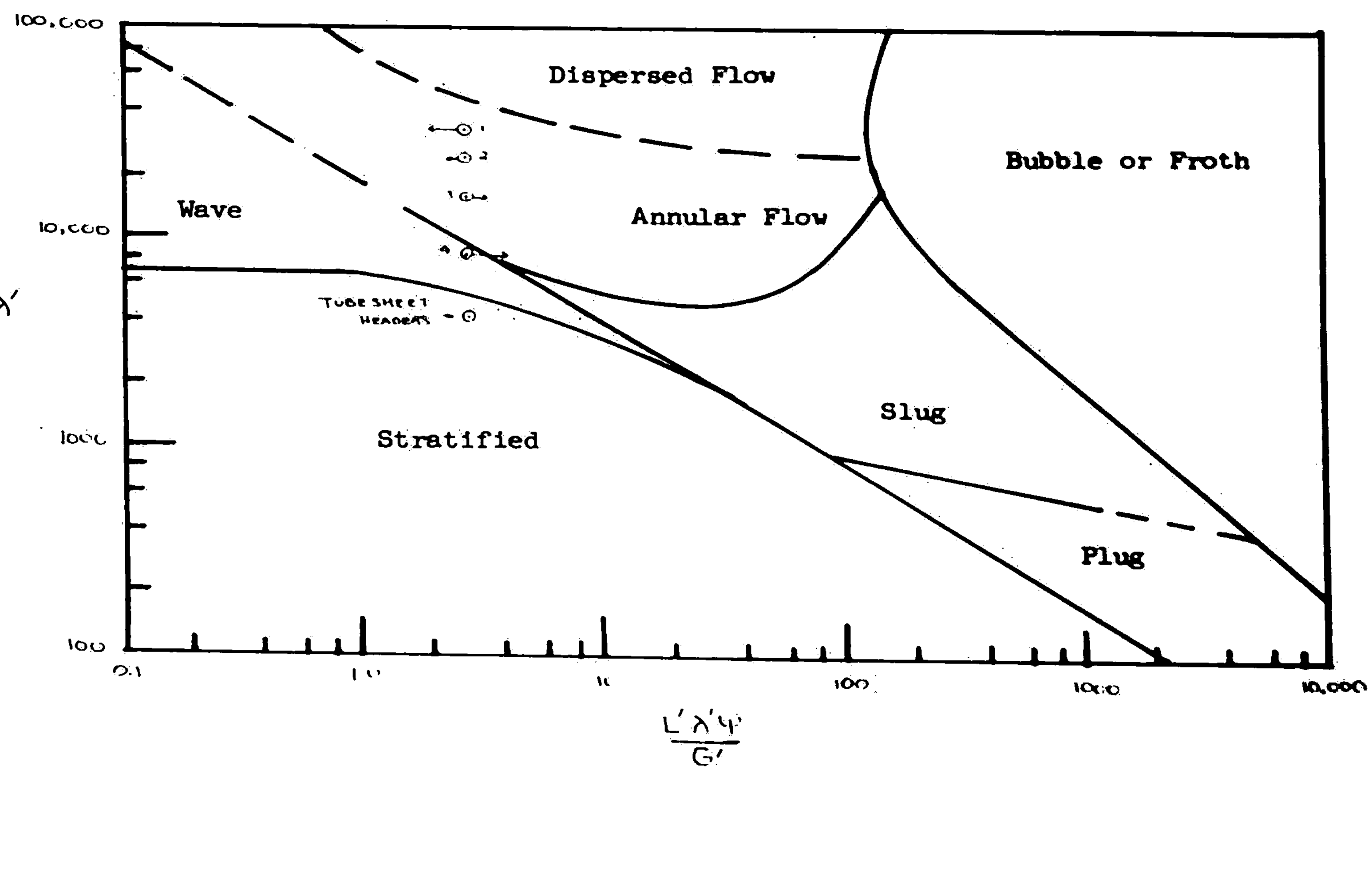

FIGURE #9

DISTRIBUTION OF TWO PHASE ANNULAR FLOW

IN TUBE SHEET HEADER

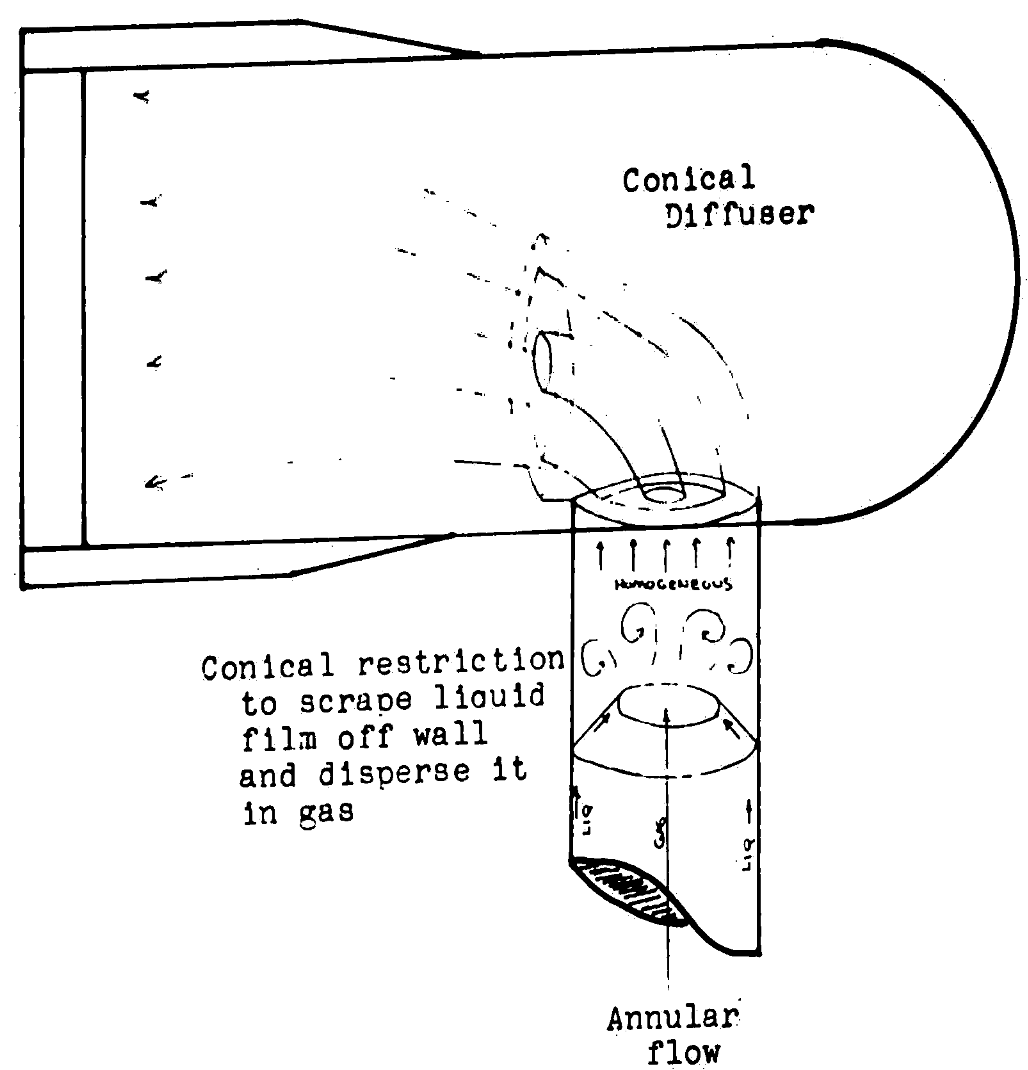

**FIGURE # 10**

**EXAMPLE HEAT EXCHANGER**
**(Feed stream only is shown)**

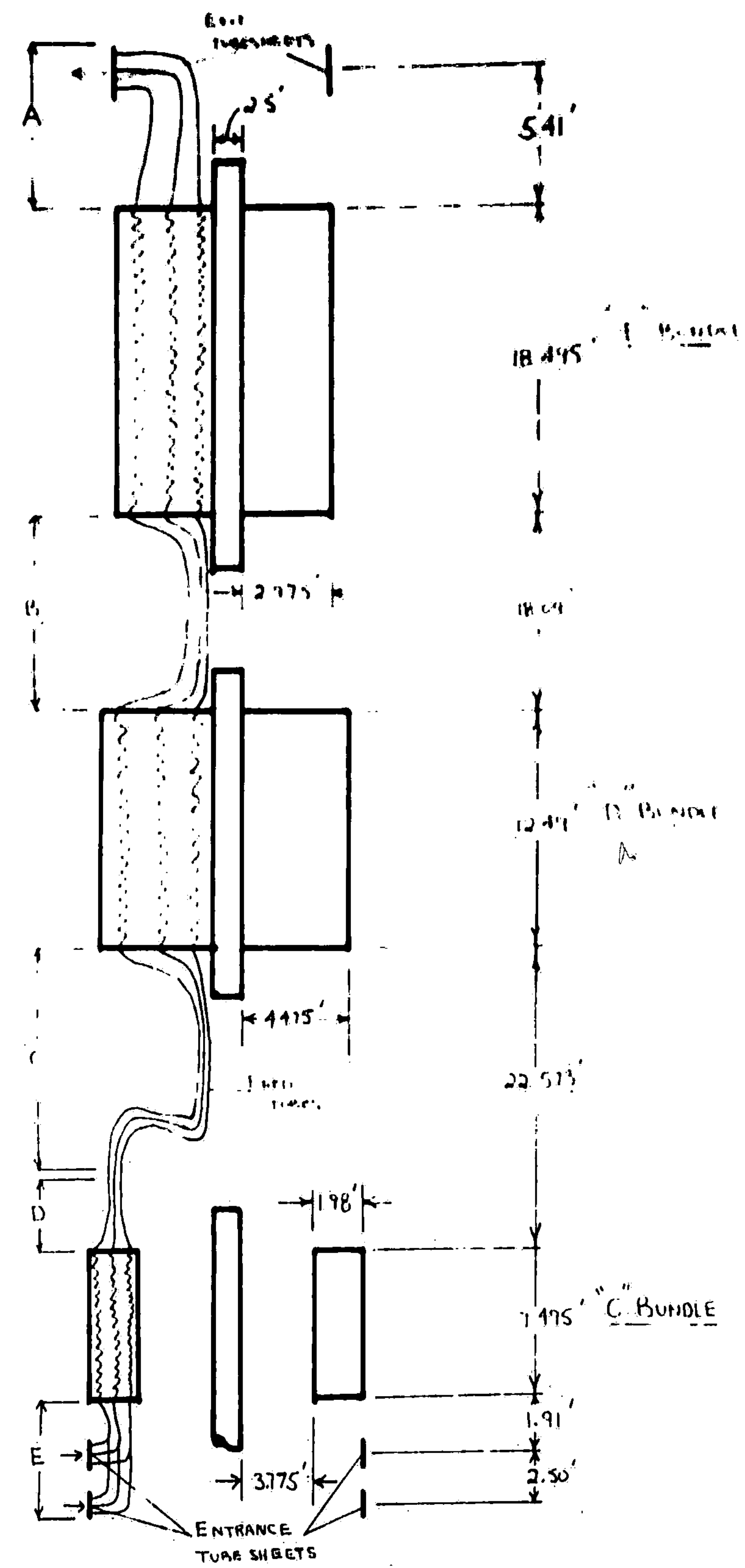

88.

FIGURE #11

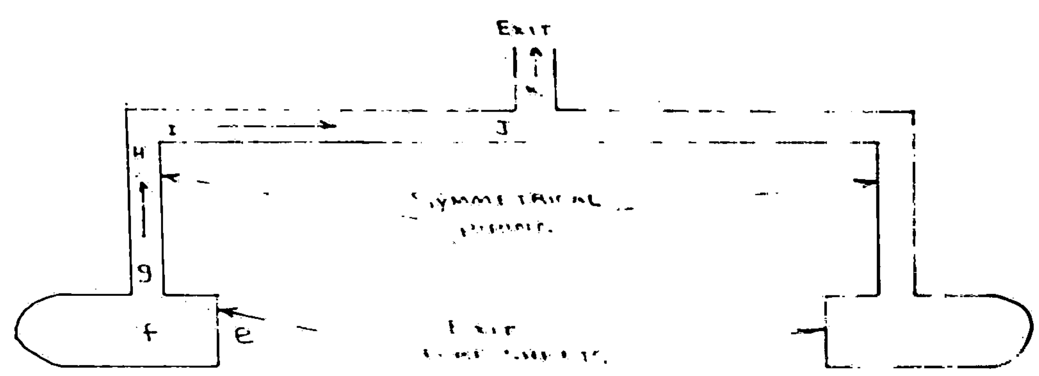


Tube Bundle

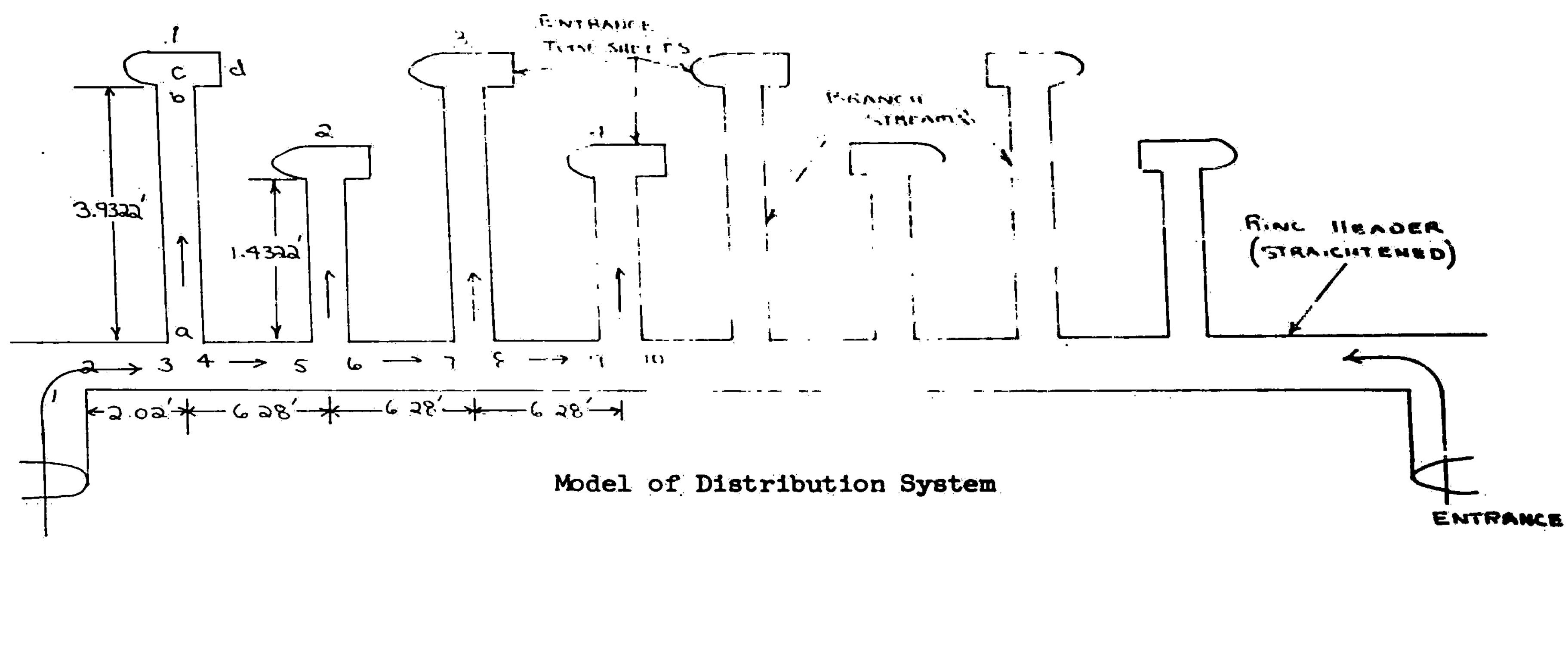


Model of Distribution System

FIGURE #12

Mass Flow versus Volumetric Flow Entering

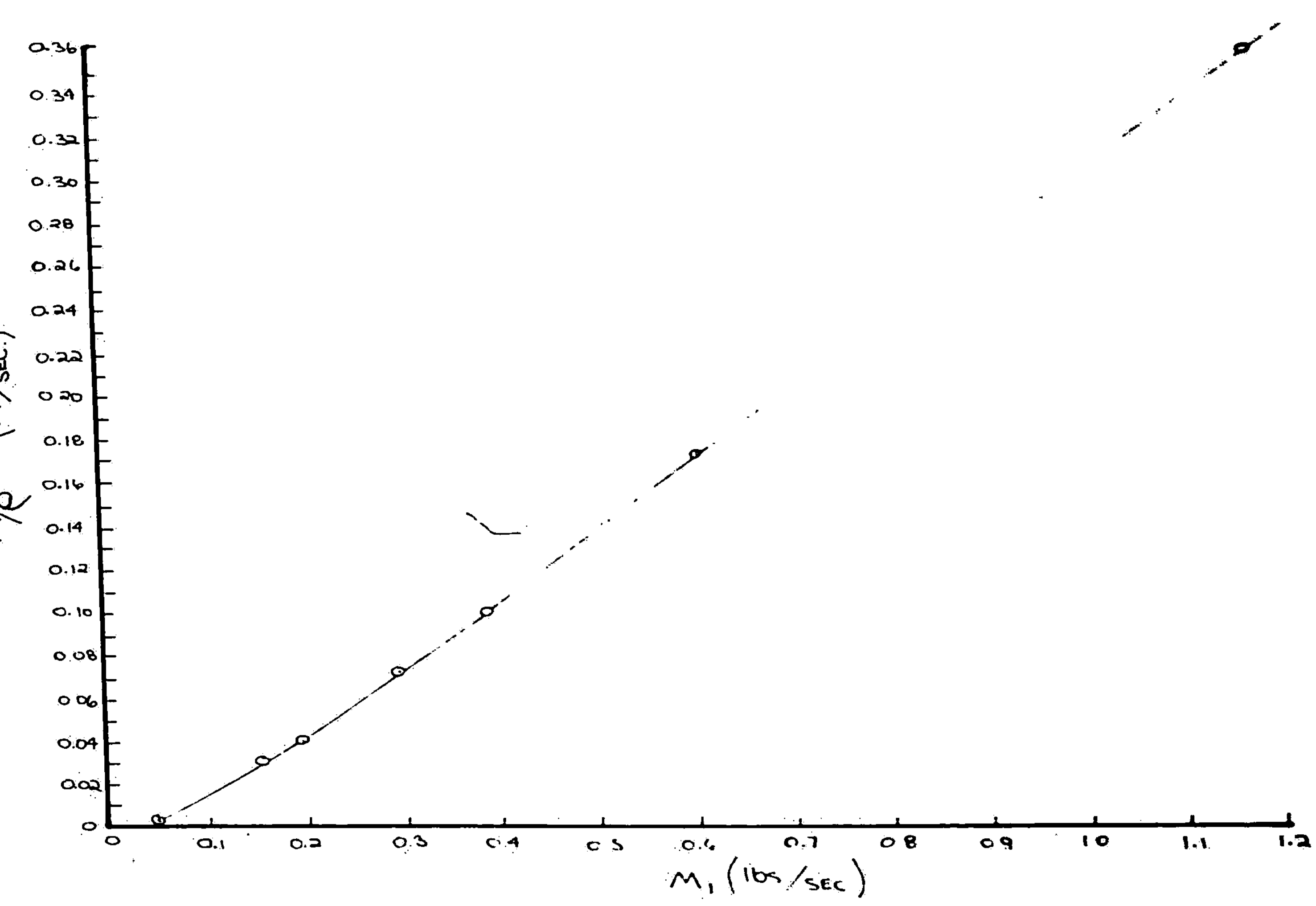

FIGURE # 13

FLOW PATTERN PREDICTION CHART FOR VERTICAL FLOW
(Griffith and Wallis)

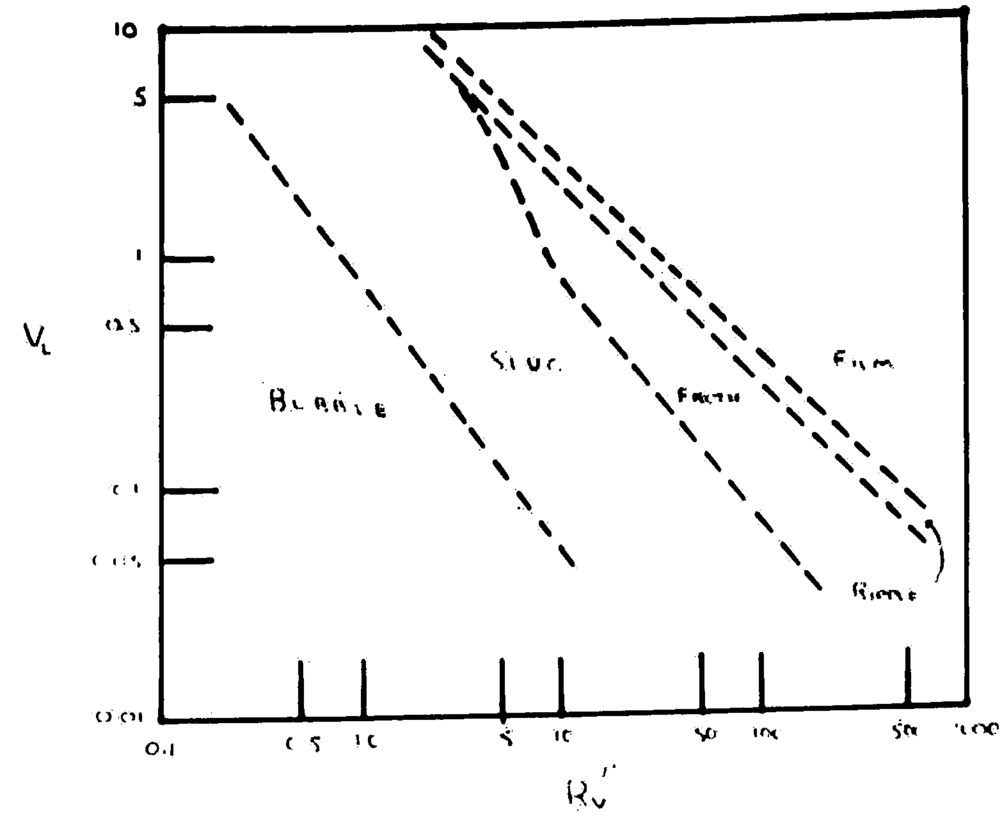


FIGURE # 14

FLOW PATTERN PREDICTION CHART FOR VERTICAL FLOW
(Govier, Radford, and Dunn)

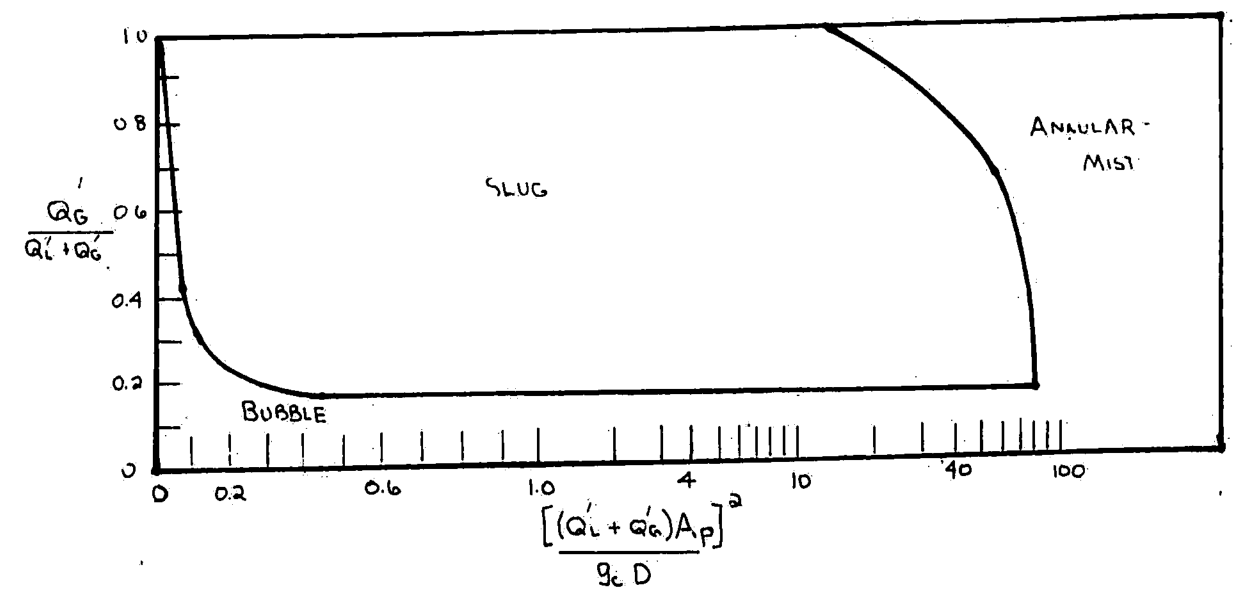

**FIGURE # 15**

**TUBE SHEET HEADER**

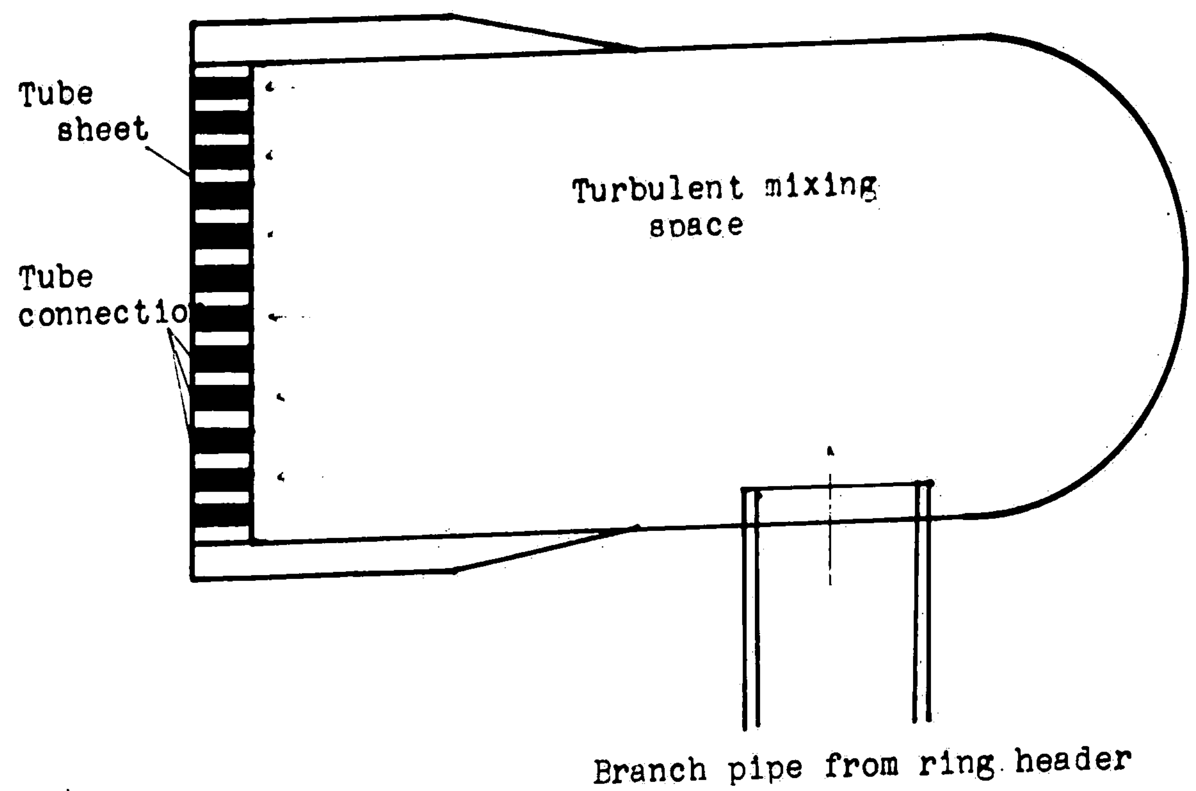

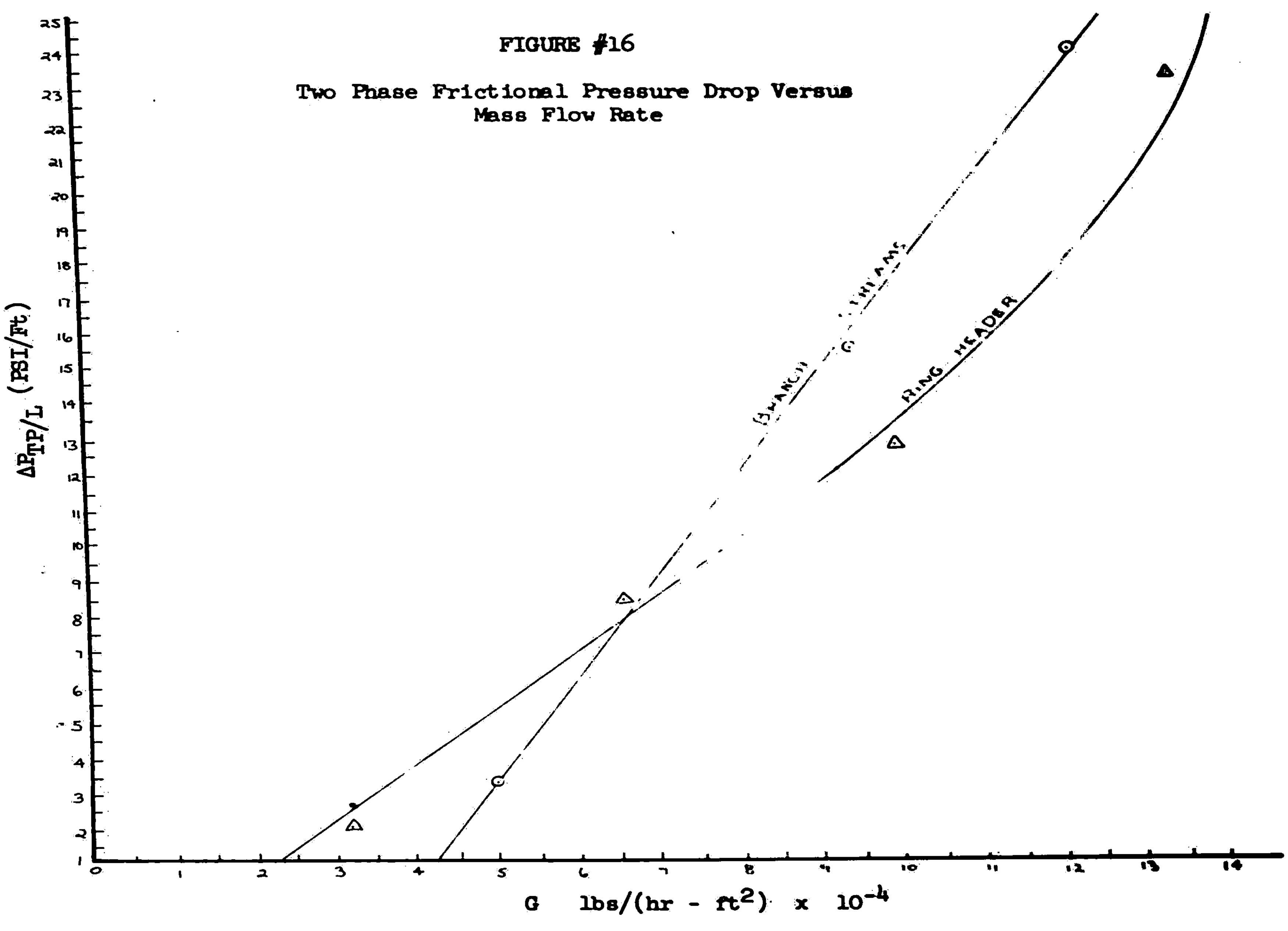


FIGURE #16

Two Phase Frictional Pressure Drop Versus Mass Flow Rate

FIGURE #17

Temperature Versus Tube Length

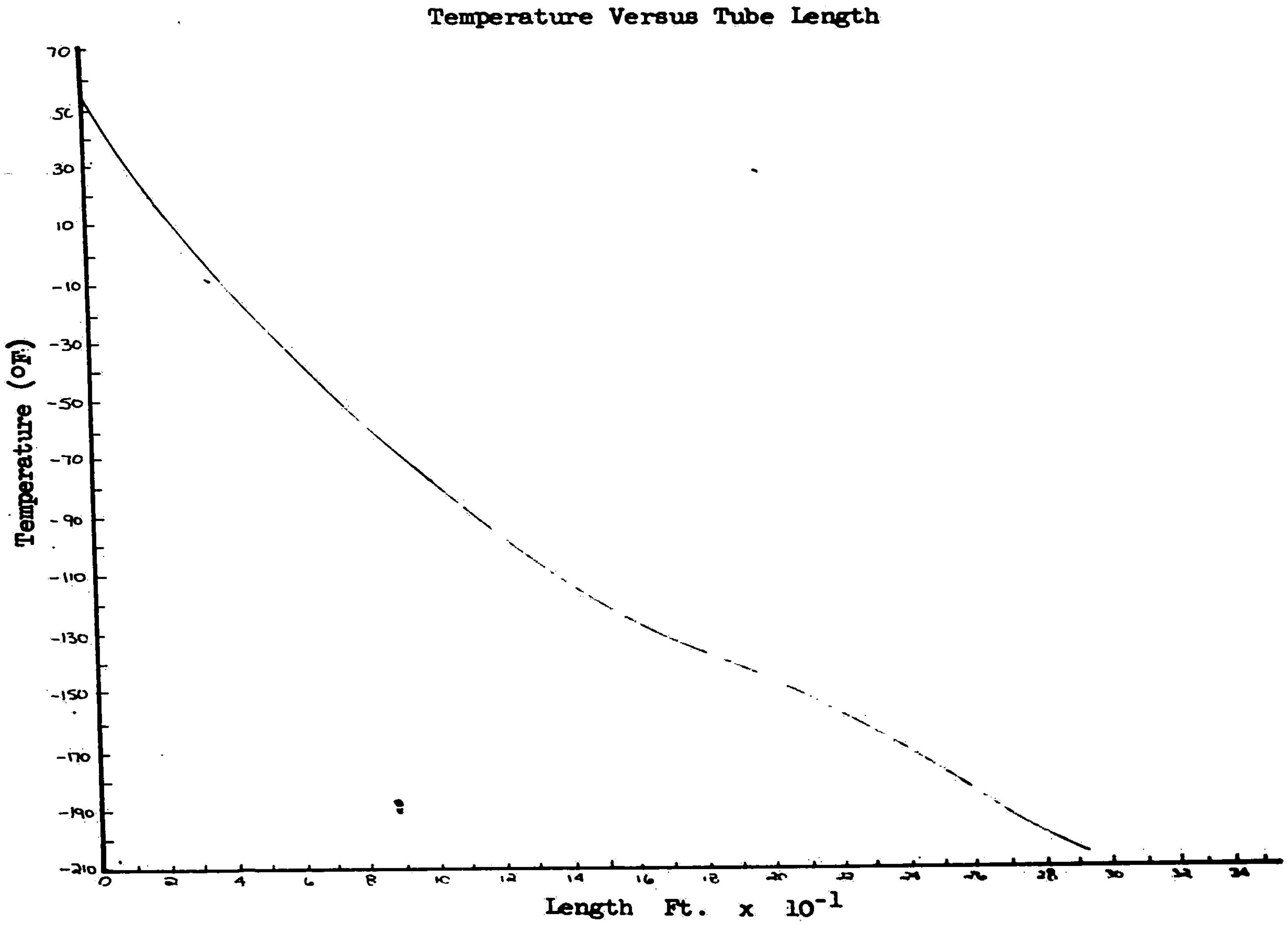

FIGURE #18

Pressure Drop versus Flow Rate in Bundle

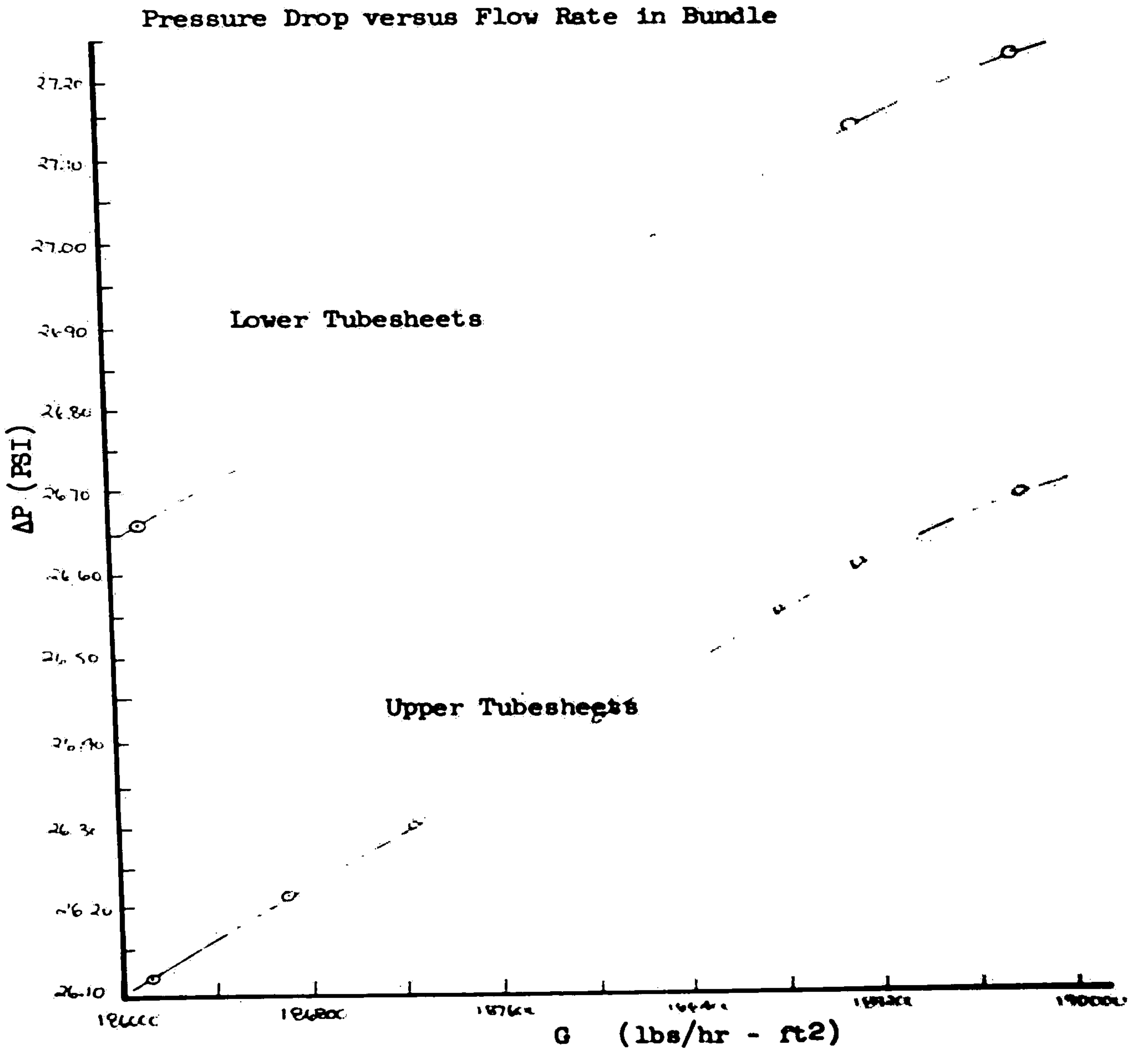

FIGURE #19

Pressure Drop in Tube Bundles

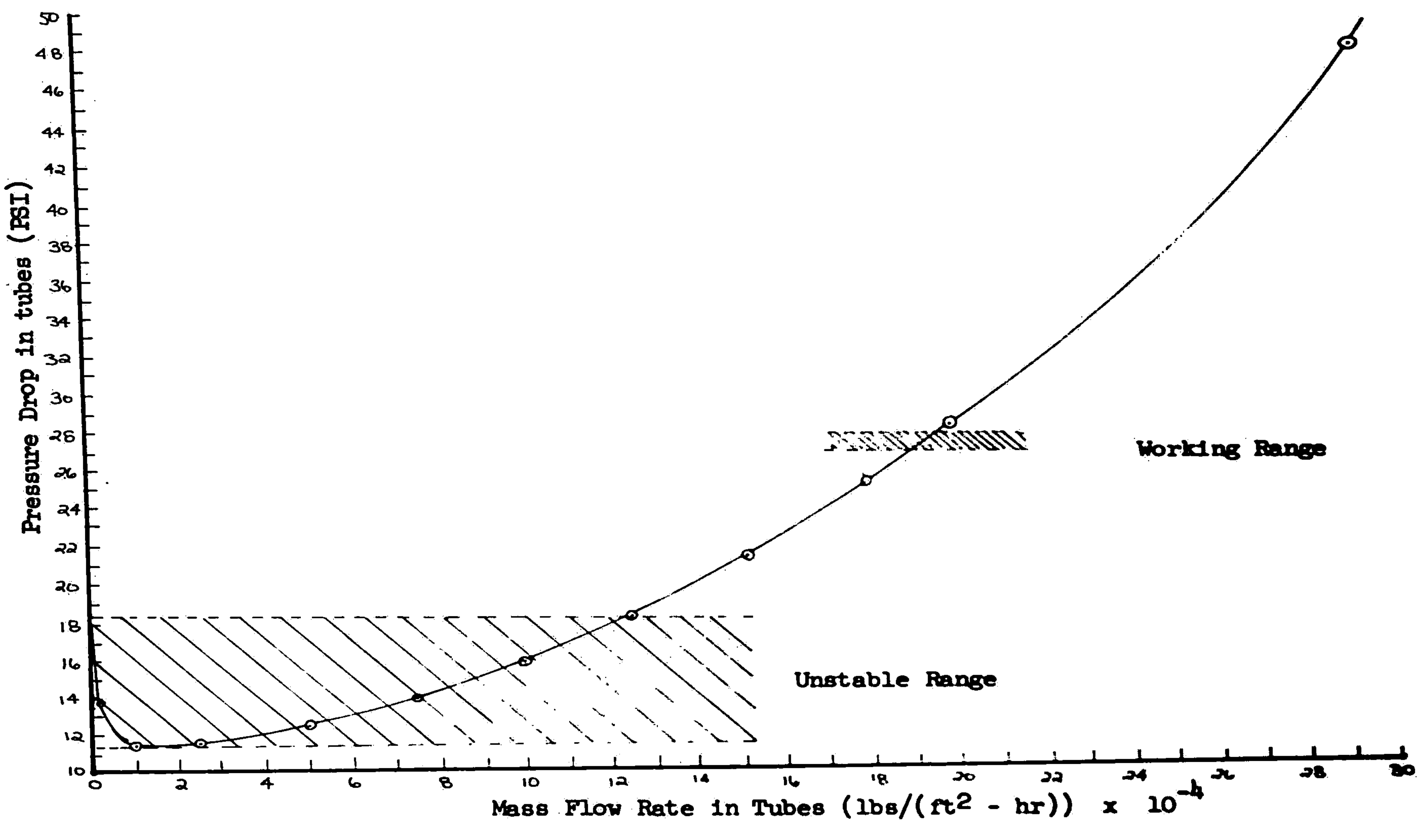

**FIGURE #20**

**Tube Pulsations at Start-up**

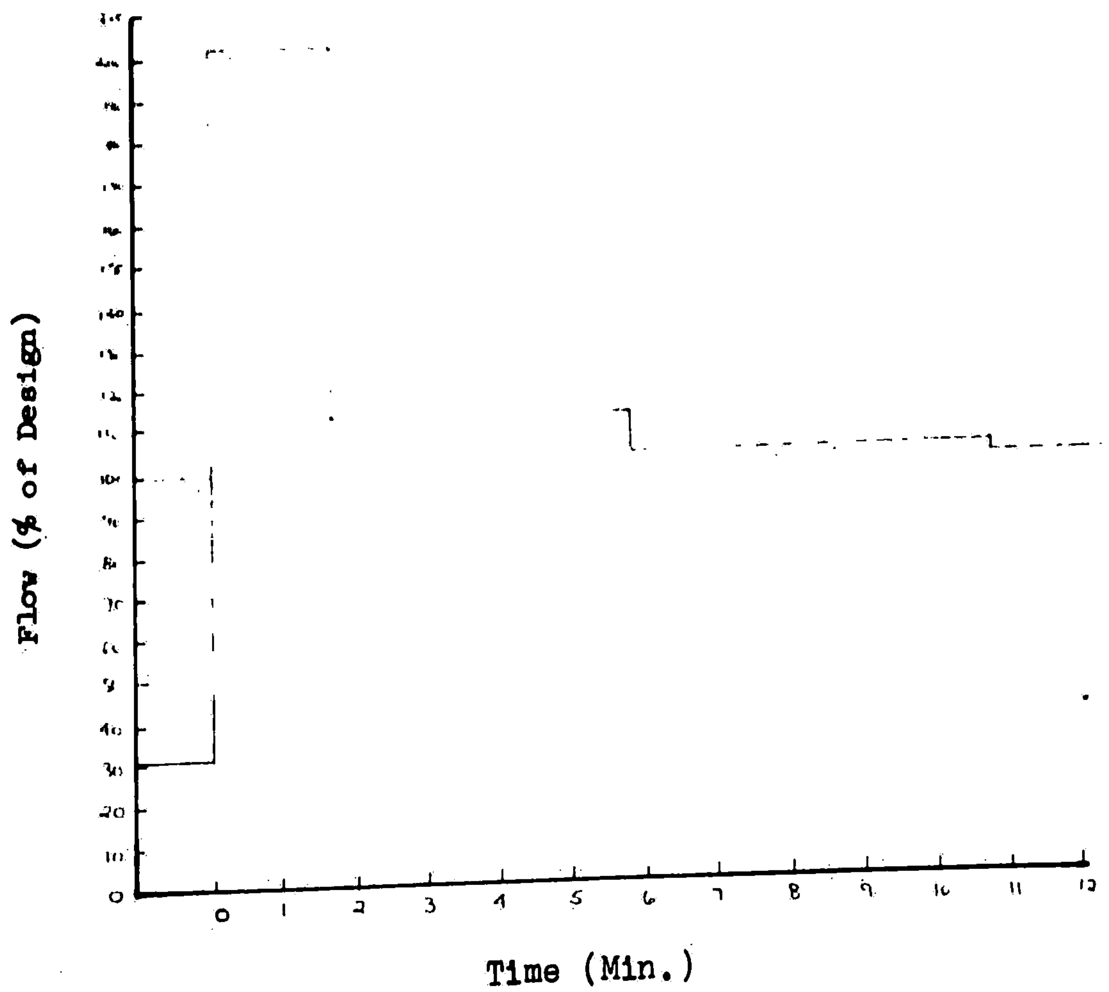

FIGURE #21

Pressure Drop versus Flow Rate in Bundle
For Discrete Flows

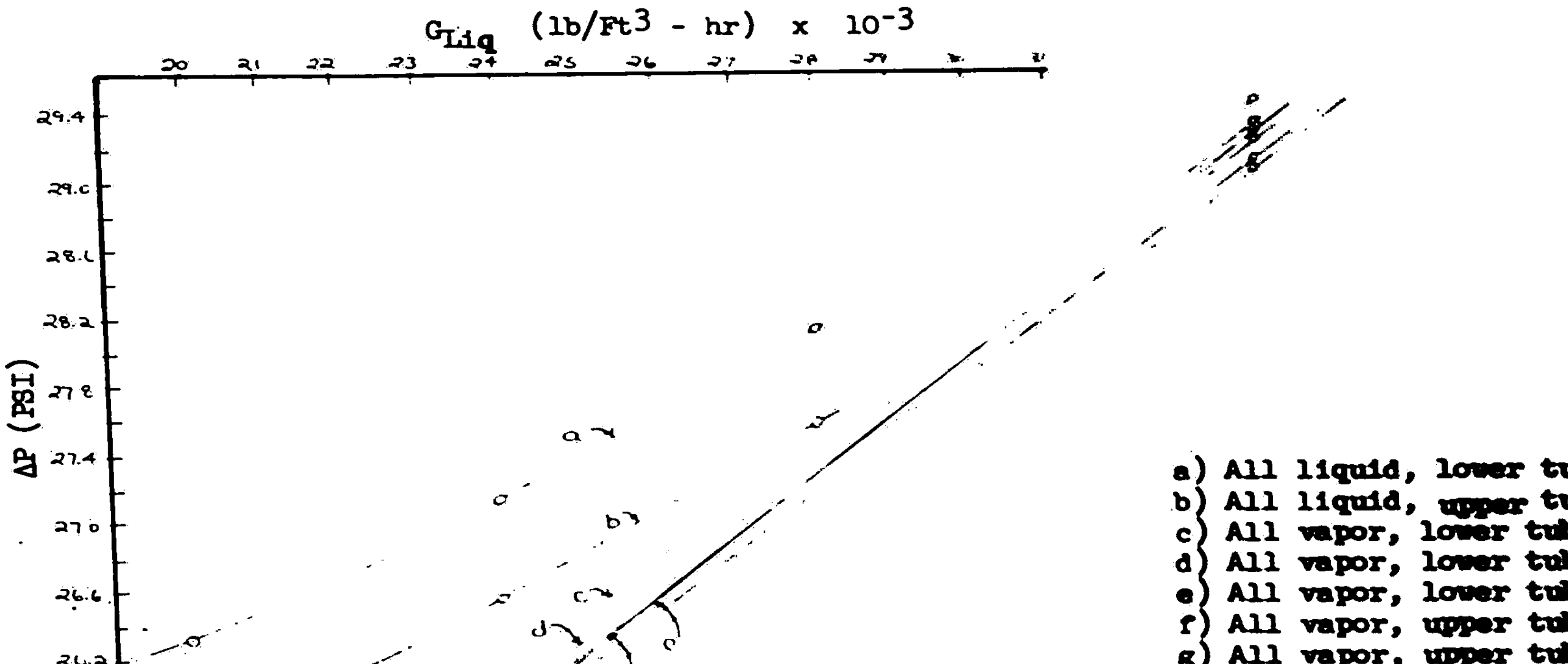


a) All liquid, lower tube sheets, Segment #
b) All liquid, upper tube sheets, Segment #
c) All vapor, lower tube sheets, Segment #1
d) All vapor, lower tube sheets, Segment #
e) All vapor, lower tube sheets, Segment #
f) All vapor, upper tube sheets, Segment #1
g) All vapor, upper tube sheets, Segment #
h) All vapor, upper tube sheets, Segment #

FIGURE #22
Cooling Curve for Flow #1

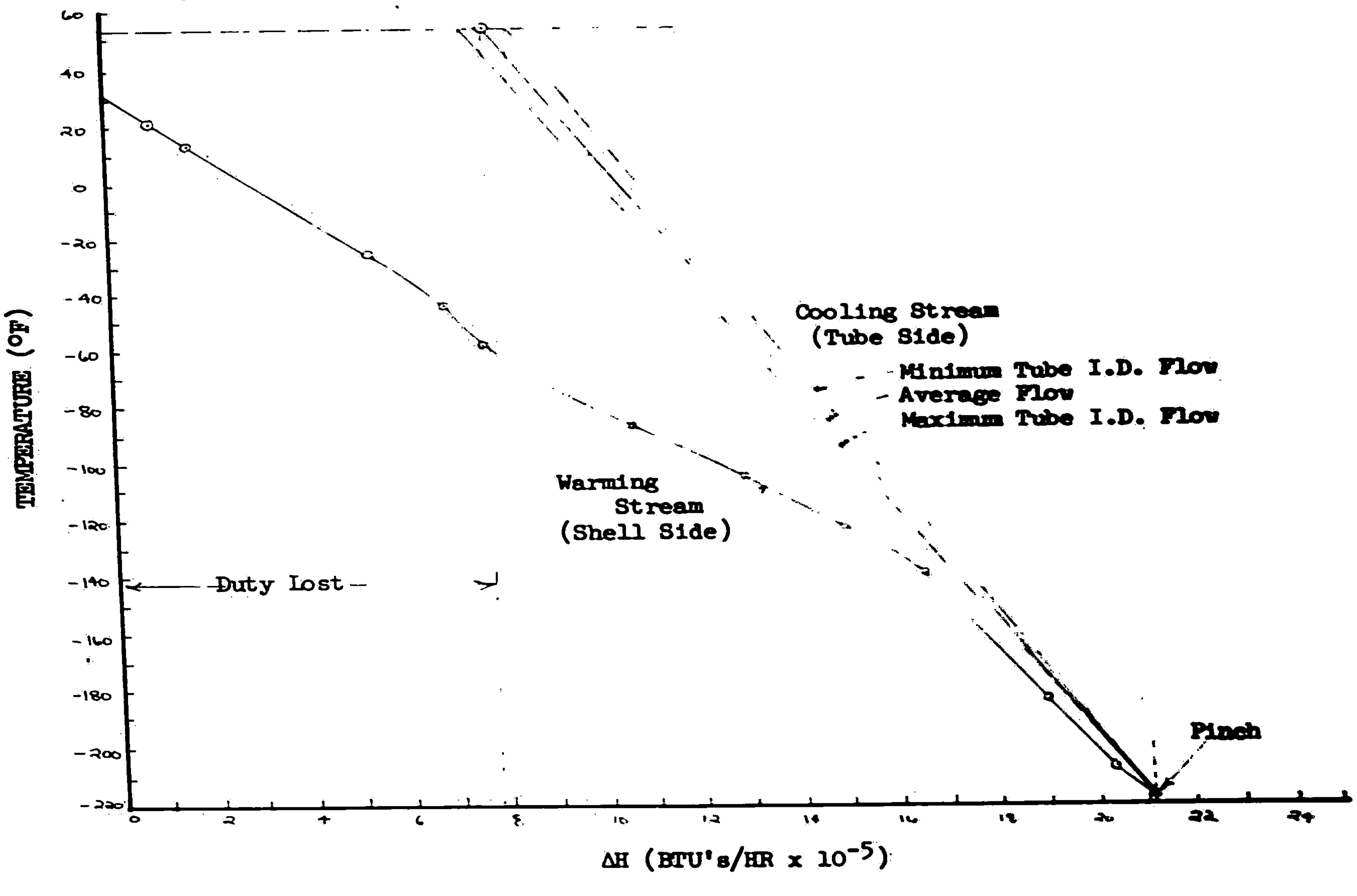

FIGURE #23
Cooling Curve for Flow #2

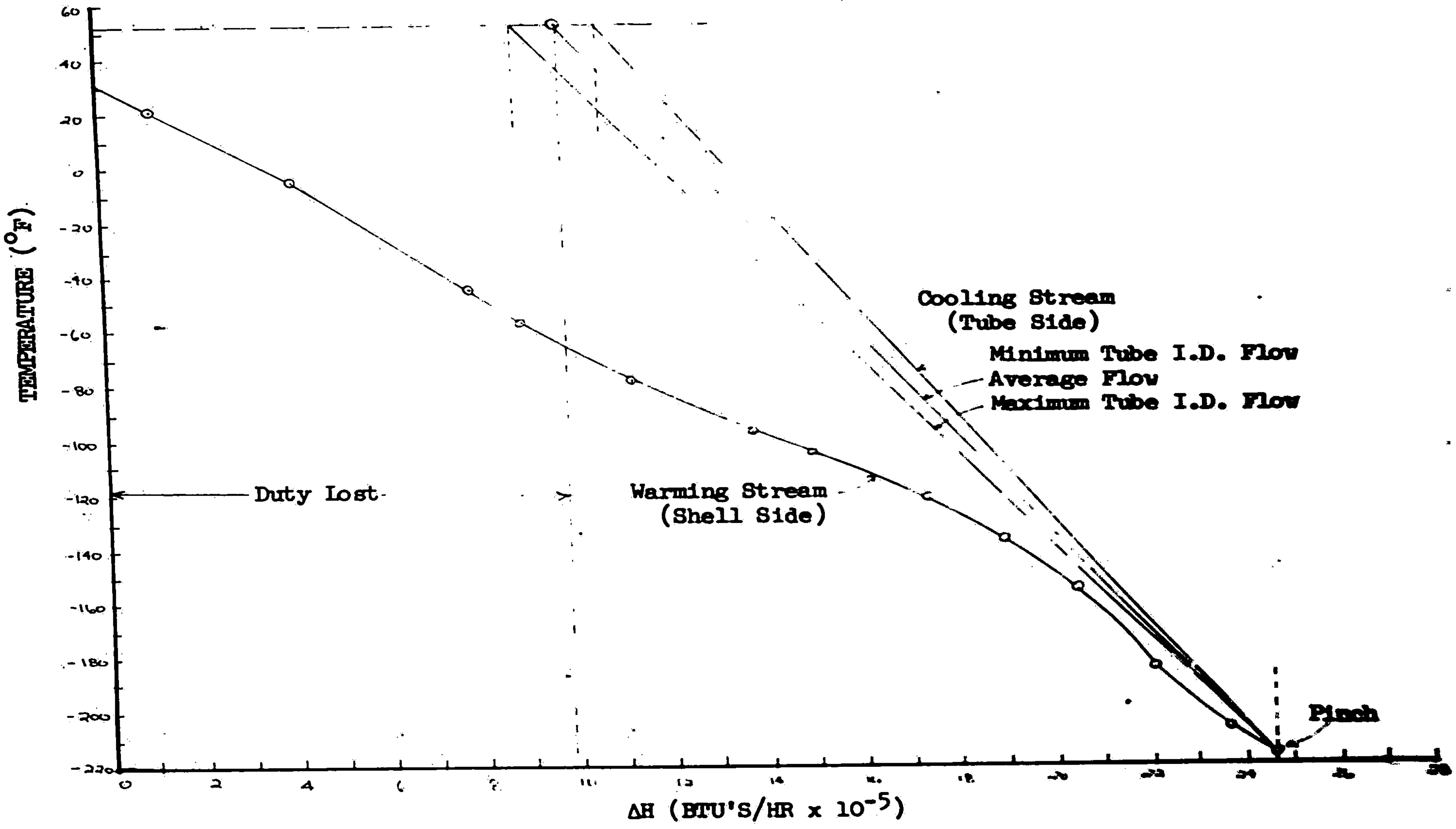

FIGURE #24
Cooling Curve for Flow #3

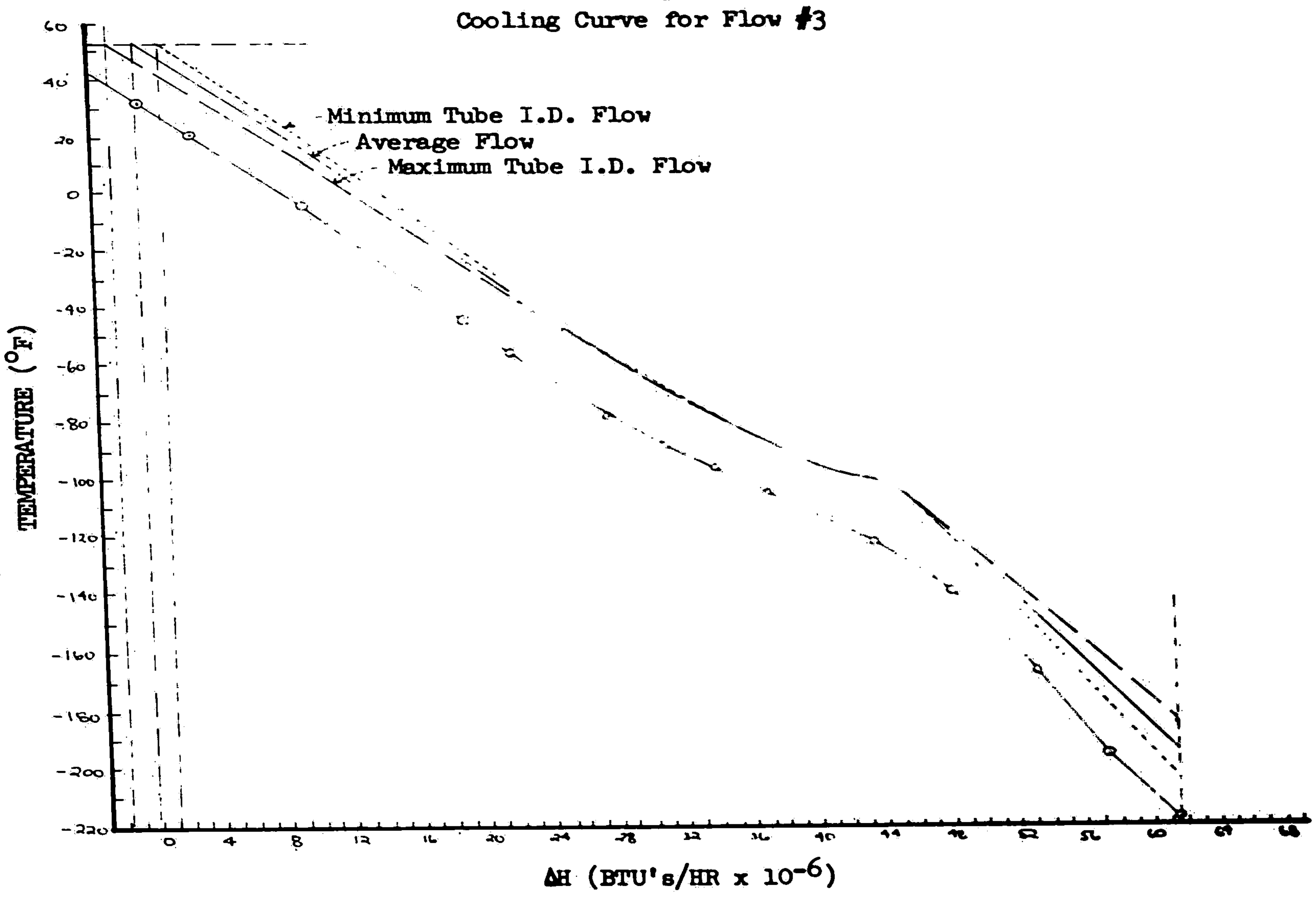

.00

**TABLE - 1**

**Pressure Drop Factors to be used with Perry's ① Pipe Flow Chart**

| $P_G$ (atm) | $\Delta P/L$ (psi/1,000 ft.) Manifold Inlet | Ordinary Piping |
|---|---|---|
| < 1 | < .1 | < 1 |
| 2 - 4 | .1 | 1 |
| 4 - 7 | .2 | 2 |
| 7 - 13 | .3 | 3 |
| 13 - 34 | .4 | 4 |
| 34 - 68 | .7 | 7 |
| 68 - 204 | 1 | 10 |

## TABLE - 2

## COMPUTER OUTPUT

### COOLING CURVE SUMMARY

| Pressure | Temperature | Enthalpy, Btu | Delta H |
|---|---|---|---|
| 592.0000 | 52.0000 | 0.56380E 06 | 0.0 |
| 590.6001 | 38.0000 | 0.52941E 06 | 0.34395E 05 |
| 589.2000 | 25.0000 | 0.49796E 06 | 0.65841E 05 |
| 587.7000 | 11.0000 | 0.46338E 06 | 0.10043E 06 |
| 586.3000 | -2.0000 | 0.43126E 06 | 0.13254E 06 |
| 584.8999 | -16.0000 | 0.39727E 06 | 0.16654E 06 |
| 583.5000 | -29.0000 | 0.36431E 06 | 0.19950E 06 |
| 582.1001 | -43.0000 | 0.32809E 06 | 0.23571E 06 |
| 580.6001 | -57.0000 | 0.29115E 06 | 0.27265E 06 |
| 579.2000 | -70.0000 | 0.25376E 06 | 0.31005E 06 |
| 577.8000 | -84.0000 | 0.20877E 06 | 0.35503E 06 |
| 576.3999 | -97.0000 | 0.15907E 06 | 0.40473E 06 |
| 574.8999 | -111.0000 | 0.10342E 06 | 0.46038E 06 |
| 573.5000 | -125.0000 | 0.78802E 05 | 0.48500E 06 |
| 572.1001 | -138.0000 | 0.55420E 05 | 0.50838E 06 |
| 570.7000 | -152.0000 | 0.29880E 05 | 0.53392E 06 |
| 569.3000 | -165.0000 | 0.60681E 04 | 0.55774E 06 |
| 567.8000 | -178.0000 | -0.17605E 05 | 0.58141E 06 |
| 566.3999 | -192.0000 | -0.42635E 05 | 0.60644E 06 |
| 565.0000 | -206.0000 | -0.66733E 05 | 0.63054E 06 |

### TRANSPORT PROPERTIES

### LIQUID PHASE

| Temperature Degree F | Viscosity lb/ft hr | Conductivity Btu/hr ft Deg F | Density lb/ft 3 | Specific Heat Btu/lb Deg F |
|---|---|---|---|---|
| 52.0000 | 0.22395E 00 | 0.52106E-01 | 0.30672E 02 | 0.59457E 00 |
| 38.0000 | 0.22309E 00 | 0.53045E-01 | 0.30471E 02 | 0.58618E 00 |
| 25.0000 | 0.22355E 00 | 0.54023E-01 | 0.30345E 02 | 0.57936E 00 |
| 11.0000 | 0.22262E 00 | 0.55034E-01 | 0.30138E 02 | 0.57390E 00 |
| -2.0000 | 0.22105E 00 | 0.55973E-01 | 0.29904E 02 | 0.57042E 00 |
| -16.0000 | 0.21956E 00 | 0.57053E-01 | 0.29654E 02 | 0.57015E 00 |
| -29.0000 | 0.21557E 00 | 0.57937E-01 | 0.29281E 02 | 0.57430E 00 |
| -43.0000 | 0.20970E 00 | 0.58827E-01 | 0.28784E 02 | 0.58414E 00 |
| -57.0000 | 0.20306E 00 | 0.59711E-01 | 0.28224E 02 | 0.60135E 00 |
| -70.0000 | 0.19410E 00 | 0.60354E-01 | 0.27527E 02 | 0.62622E 00 |
| -84.0000 | 0.18233E 00 | 0.60891E-01 | 0.26612E 02 | 0.66371E 00 |
| -97.0000 | 0.16982E 00 | 0.61228E-01 | 0.25615E 02 | 0.71118E 00 |
| -111.0000 | 0.16434E 00 | 0.62398E-01 | 0.25012E 02 | 0.76251E 00 |
| -125.0000 | 0.18688E 00 | 0.66751E-01 | 0.26034E 02 | 0.78560E 00 |
| -138.0000 | 0.20932E 00 | 0.70827E-01 | 0.26904E 02 | 0.79921E 00 |
| -152.0000 | 0.23537E 00 | 0.75282E-01 | 0.27776E 02 | 0.80771E 00 |
| -165.0000 | 0.26155E 00 | 0.79500E-01 | 0.28535E 02 | 0.80559E 00 |
| -178.0000 | 0.28992E 00 | 0.83814E-01 | 0.29256E 02 | 0.79775E 00 |
| -192.0000 | 0.32323E 00 | 0.88581E-01 | 0.29994E 02 | 0.77501E 00 |
| -206.0000 | 0.35978E 00 | 0.93489E-01 | 0.30700E 02 | 0.73711E 00 |

## TABLE - 2, continued

### COMPUTER OUTPUT

### TRANSPORT PROPERTIES

### VAPOR PHASE

| Temperature Degree F | Viscosity lb/ft hr | Conductivity Btu/hr ft DegF | Density lb/ft 3 | Specific Heat Btu/lb Deg F |
|---|---|---|---|---|
| 52.0000 | 0.27073E-01 | 0.17582E-01 | 0.28270E 01 | 0.61035E 00 |
| 38.0000 | 0.26714E-01 | 0.17384E-01 | 0.28305E 01 | 0.61743E 00 |
| 25.0000 | 0.26377E-01 | 0.17203E-01 | 0.28435E 01 | 0.62646E 00 |
| 11.0000 | 0.26014E-01 | 0.17027E-01 | 0.28592E 01 | 0.63794E 00 |
| -2.0000 | 0.25677E-01 | 0.16873E-01 | 0.28835E 01 | 0.65088E 00 |
| -16.0000 | 0.25318E-01 | 0.16711E-01 | 0.29298E 01 | 0.66968E 00 |
| -29.0000 | 0.24991E-01 | 0.16582E-01 | 0.29762E 01 | 0.68921E 00 |
| -43.0000 | 0.24651E-01 | 0.16458E-01 | 0.30472E 01 | 0.71680E 00 |
| -57.0000 | 0.24338E-01 | 0.16347E-01 | 0.31529E 01 | 0.75415E 00 |
| -70.0000 | 0.24085E-01 | 0.16275E-01 | 0.32790E 01 | 0.80029E 00 |
| -84.0000 | 0.23900E-01 | 0.16239E-01 | 0.34764E 01 | 0.87366E 00 |
| -97.0000 | 0.23887E-01 | 0.16271E-01 | 0.37503E 01 | 0.98592E 00 |
| -111.0000 | 0.0 | 0.0 | 0.0 | 0.0 |
| -125.0000 | 0.0 | 0.0 | 0.0 | 0.0 |
| -138.0000 | 0.0 | 0.0 | 0.0 | 0.0 |
| -152.0000 | 0.0 | 0.0 | 0.0 | 0.0 |
| -165.0000 | 0.0 | 0.0 | 0.0 | 0.0 |
| -178.0000 | 0.0 | 0.0 | 0.0 | 0.0 |
| -192.0000 | 0.0 | 0.0 | 0.0 | 0.0 |
| -206.0000 | 0.0 | 0.0 | 0.0 | 0.0 |

| Temperature | Pseudo Latent Heat Btu/lb | Btu/mole | Prandtl No. Liquid | Vapor |
|---|---|---|---|---|
| 52.0000 | 0.11171E 03 | 0.45418E 04 | 0.2556E 01 | 0.9398E 00 |
| 38.0000 | 0.11334E 03 | 0.42404E 04 | 0.2465E 01 | 0.9488E 00 |
| 25.0000 | 0.11421E 03 | 0.39671E 04 | 0.2397E 01 | 0.9605E 00 |
| 11.0000 | 0.11471E 03 | 0.36361E 04 | 0.2322E 01 | 0.9746E 00 |
| -2.0000 | 0.11454E 03 | 0.33306E 04 | 0.2253E 01 | 0.9905E 00 |
| -16.0000 | 0.11316E 03 | 0.30026E 04 | 0.2194E 01 | 0.1015E 01 |
| -29.0000 | 0.11141E 03 | 0.27026E 04 | 0.2137E 01 | 0.1039E 01 |
| -43.0000 | 0.10816E 03 | 0.23754E 04 | 0.2082E 01 | 0.1074E 01 |
| -57.0000 | 0.10486E 03 | 0.21059E 04 | 0.2045E 01 | 0.1123E 01 |
| -70.0000 | 0.10128E 03 | 0.18924E 04 | 0.2014E 01 | 0.1184E 01 |
| -84.0000 | 0.98921E 02 | 0.17351E 04 | 0.1987E 01 | 0.1286E 01 |
| -97.0000 | 0.96003E 02 | 0.16278E 04 | 0.1973E 01 | 0.1447E 01 |
| -111.0000 | 0.0 | 0.0 | 0.2008E 01 | 0.0 |
| -125.0000 | 0.0 | 0.0 | 0.2199E 01 | 0.0 |
| -138.0000 | 0.0 | 0.0 | 0.2362E 01 | 0.0 |
| -152.0000 | 0.0 | 0.0 | 0.2525E 01 | 0.0 |
| -165.0000 | 0.0 | 0.0 | 0.2650E 01 | 0.0 |
| -178.0000 | 0.0 | 0.0 | 0.2759E 01 | 0.0 |
| -192.0000 | 0.0 | 0.0 | 0.2828E 01 | 0.0 |
| -206.0000 | 0.0 | 0.0 | 0.2837E 01 | 0.0 |

TABLE - 2, continued

COMPUTER OUTPUT

TUBE PRESSURE DROP

| Inside Diameter-Ft | Roughness-Ft | Flow Rate-Lb/Hr Ft2 |
|---|---|---|
| 0.32500E-01 | 0.50000E-05 | 0.18801E 06 |

| Temp Deg F | Reynolds No. Vapor | Reynolds No. Liquid | Liquid Volume Fraction No Slip | Liquid Volume Fraction Slip | Pressure Differentials Friction lb/ft2/ft | Pressure Differentials Head lb/ft2/vert |
|---|---|---|---|---|---|---|
| 52.00 | 0.23E 06 | 0.27E 05 | 0.865E-02 | 0.114E 00 | 0.231E 02 | 0.600E 01 |
| 38.00 | 0.23E 06 | 0.27E 05 | 0.156E-01 | 0.135E 00 | 0.229E 02 | 0.656E 01 |
| 25.00 | 0.23E 06 | 0.27E 05 | 0.226E-01 | 0.151E 00 | 0.219E 02 | 0.700E 01 |
| 11.00 | 0.23E 06 | 0.27E 05 | 0.316E-01 | 0.168E 00 | 0.202E 02 | 0.744E 01 |
| -2.00 | 0.24E 06 | 0.28E 05 | 0.414E-01 | 0.183E 00 | 0.173E 02 | 0.784E 01 |
| -16.00 | 0.24E 06 | 0.28E 05 | 0.535E-01 | 0.201E 00 | 0.144E 02 | 0.829E 01 |
| -29.00 | 0.24E 06 | 0.28E 05 | 0.685E-01 | 0.220E 00 | 0.118E 02 | 0.875E 01 |
| -43.00 | 0.25E 06 | 0.29E 05 | 0.901E-01 | 0.245E 00 | 0.915E 01 | 0.935E 01 |
| -57.00 | 0.25E 06 | 0.30E 05 | 0.120E 00 | 0.277E 00 | 0.749E 01 | 0.101E 02 |
| -70.00 | 0.25E 06 | 0.31E 05 | 0.165E 00 | 0.320E 00 | 0.633E 01 | 0.110E 02 |
| -84.00 | 0.26E 06 | 0.34E 05 | 0.255E 00 | 0.402E 00 | 0.495E 01 | 0.128E 02 |
| -97.00 | 0.26E 06 | 0.36E 05 | 0.456E 00 | 0.573E 00 | 0.323E 01 | 0.163E 02 |
| -111.00 | 0.0 | 0.37E 05 | 0.100E 01 | 0.100E 01 | 0.117E 01 | 0.250E 02 |
| -125.00 | 0.0 | 0.33E 05 | 0.100E 01 | 0.100E 01 | 0.115E 01 | 0.260E 02 |
| -138.00 | 0.0 | 0.29E 05 | 0.100E 01 | 0.100E 01 | 0.114E 01 | 0.269E 02 |
| -152.00 | 0.0 | 0.26E 05 | 0.100E 01 | 0.100E 01 | 0.114E 01 | 0.278E 02 |
| -165.00 | 0.0 | 0.23E 05 | 0.100E 01 | 0.100E 01 | 0.114E 01 | 0.285E 02 |
| -178.00 | 0.0 | 0.21E 05 | 0.100E 01 | 0.100E 01 | 0.114E 01 | 0.293E 02 |
| -192.00 | 0.0 | 0.19E 05 | 0.100E 01 | 0.100E 01 | 0.114E 01 | 0.300E 02 |
| -206.00 | 0.0 | 0.17E 05 | 0.100E 01 | 0.100E 01 | 0.115E 01 | 0.307E 02 |

## TABLE - 3

ΔP versus G by Segments

| Phase | Entrance Tubesheet Position | Segment | $P_{bundle}$ (psi) | G (lb/hr ft$^2$) |
|---|---|---|---|---|
| liquid | lower | 1 | 26.32 | 200,000 |
| liquid | lower | 1 | 27.14 | 240,000 |
| liquid | lower | 1 | 28.17 | 280,000 |
| liquid | upper | 1 | 25.77 | 200,000 |
| liquid | upper | 1 | 26.57 | 240,000 |
| liquid | upper | 1 | 27.60 | 280,000 |
| gas | lower | 1 | 25.17 | 175,000 |
| gas | lower | 1 | 25.99 | 180,000 |
| gas | lower | 1 | 29.38 | 200,000 |
| gas | upper | 1 | 25.00 | 175,000 |
| gas | upper | 1 | 25.81 | 180,000 |
| gas | upper | 1 | 29.17 | 200,000 |
| gas | lower | 2 | 25.30 | 175,000 |
| gas | lower | 2 | 25.85 | 180,000 |
| gas | lower | 2 | 29.27 | 200,000 |
| gas | upper | 2 | 24.86 | 175,000 |
| gas | upper | 2 | 25.67 | 180,000 |
| gas | upper | 2 | 29.07 | 200,000 |
| gas | lower | 3 | 24.94 | 175,000 |
| gas | lower | 3 | 25.77 | 180,000 |
| gas | lower | 3 | 29.22 | 200,000 |
| gas | upper | 3 | 24.77 | 175,000 |
| gas | upper | 3 | 25.59 | 180,000 |
| gas | upper | 3 | 29.01 | 200,000 |

TABLE - 4

TUBESIDE TEMPERATURE - DUTY DATA

| Temperature ($^oF$) | $\Delta H$ (Btu's/hr.) Flow 1 | Flow 2 | Flow 3 |
|---|---|---|---|
| 52 | 0 | 0 | 0 |
| 38 | 79,902 | 87,821 | 3,183,665 |
| 25 | 152,557 | 167,678 | 6,203,733 |
| 11 | 229,394 | 252,130 | 9,572,606 |
| - 2 | 299,689 | 329,392 | 12,726,453 |
| - 16 | 374,461 | 411,575 | 16,080,418 |
| - 29 | 443,197 | 487,123 | 19,345,330 |
| - 43 | 516,655 | 567,861 | 22,936,433 |
| - 57 | 589,689 | 648,134 | 26,587,571 |
| - 70 | 657,222 | 722,361 | 30,268,727 |
| - 84 | 729,767 | 802,095 | 34,660,299 |
| - 97 | 797,011 | 876,004 | 39,486,125 |
| -111 | 869,288 | 955,444 | 46,334,136 |
| -125 | 941,454 | 1,034,763 | 48,831,599 |
| -138 | 1,008,274 | 1,108,206 | 51,140,951 |
| -152 | 1,079,950 | 1,186,986 | 53,665,430 |
| -165 | 1,146,124 | 1,259,719 | 56,020,809 |
| -178 | 1,211,764 | 1,331,864 | 58,361,180 |
| -192 | 1,281,636 | 1,408,661 | 60,836,629 |
| -206 | 1,350,327 | 1,484,161 | 63,216,023 |

**TABLE - 5**

**SHELLSIDE TEMPERATURE - DUTY DATA**

| Temperature ($^{o}F$) | ΔH (Btu's/hr.) Flow 1 | Flow 2 | Flow 3 |
|---|---|---|---|
| | 0 | 0 | 0 |
| 31.034 | 15,456 | 17,967 | 449,474 |
| 29.59 | 101,083 | 117,509 | 2,939,628 |
| 20.90 | 181,260 | 210,715 | 5,271,276 |
| 12.95 | 261,551 | 304,053 | 7,606,239 |
| 4.35 | 347,962 | 404,506 | 10,119,163 |
| - 5.90 | 432,470 | 502,746 | 12,576,769 |
| - 16.76 | 513,881 | 597,386 | 14,944,289 |
| - 27.14 | 584,320 | 679,272 | 16,992,756 |
| - 36.32 | 672,826 | 782,160 | 19,566,613 |
| - 46.10 | 768,409 | 893,275 | 22,346,293 |
| - 58.00 | 868,704 | 1,009,869 | 25,263,012 |
| - 69.11 | 968,734 | 1,126,154 | 28,172,004 |
| - 79.36 | 1,071,774 | 1,245,938 | 31,168,536 |
| - 89.16 | 1,174,521 | 1,365,381 | 34,156,538 |
| - 98.34 | 1,279,073 | 1,486,923 | 37,197,053 |
| -105.98 | 1,385,542 | 1,610,692 | 40,293,280 |
| -113.80 | 1,495,680 | 1,738,728 | 43,496,239 |
| -122.89 | 1,591,360 | 1,849,956 | 46,278,738 |
| -132.12 | 1,646,387 | 1,913,924 | 47,878,982 |
| -139.83 | 1,703,290 | 1,980,074 | 49,533,794 |
| -146.72 | 1,764,866 | 2,051,656 | 51,324,499 |
| -155.69 | 1,833,043 | 2,130,912 | 53,307,175 |
| -168.39 | 1,903,791 | 2,213,157 | 55,364,621 |
| -183.94 | 1,970,693 | 2,290,930 | 57,310,203 |
| -197.26 | 2,035,633 | 2,366,424 | 59,198,764 |
| -207.97 | 2,089,862 | 2,429,465 | 60,775,812 |
| -215.15 | 2,115,520 | 2,459,292 | 61,521,966 |
| -218.18 | | | |

## FOOTNOTES

1. J. H. Perry, Chemical Engineers Handbook, 4th ed. (New York, 1963), p. 5-23.

2. F. A. Zenz, "Minimize Manifold Pressure Drop", Hydrocarbon Processing and Petroleum Refiner, XLI, no. 12 (1962), 126.

3. Perry, 5-19

4. W. L. McCabe and J. C. Smith, Unit Operations of Chemical Engineering, (New York, 1963), pp. 75-78.

5. G. A. Hughmark, "Holdup in Gas - Liquid Flow", CEP, LVIII, no. 4 (1962), 63.

6. K. D. Timmerhaus, Advances in Cryogenic Engineering (New York, 1967), XII, 417.

7. W. L. McCabe and J. C. Smith, 76.

8. W. L. McCabe and J. C. Smith, 78.

9. O. Baker, "Multiphase Flow in Pipelines", The Oil and Gas Journal, LVI( 1958), 159.

10. Perry, 5-19, 20.

11. S. M. Morris, "Computer Program for Two Phase Cooling Curve, Transport Properties, and Pressure Drops (360 Hetran Program No. D2B010", (July 1966), pp. 1-20.

12. B. W. Taylor, "Esso Libya Bundle Tests" (June 13, 1967).

13. W. L. McCabe and J. C. Smith, 67.

## BIBLIOGRAPHY

### BOOKS


Barron, R. Cryogenic Systems, New York: McGraw-Hill Book Co., 1966, pp. 129 - 161, 514 - 530.

Fraas, A. P. and Ozisik, M. N. Heat Exchange Design, New York: John Wiley and Sons Inc. , 1965, pp. 98 - 116.

Katz, O. L. Handbook of Natural Gas Engineering, New York: McGraw-Hill Book Co., 1954, p. 127.

McCabe, W. L. and Sumith, J. C. Unit Operations of Chemical Engineering, New York: McGraw-Hill Book Co., 1956, pp. 74 - 78.

Perry, J. H. Chemical Engineers Handbook. 4th ed. New York: McGraw-Hill Book Co., 1963, pp. 5-19, 20, 23, 38, 40, 6-45, 46.

Scott, R. B. Cryogenic Engineering, New York: D. Van Nostrand Co., Inc., 1959, pp. 249 - 50.

Timmerhaus, K. D. Advances in Cryogenic Engineering, vol. 12 New York: Plenum Press, 1967, pp. 409 - 427.

Vance, R. W. Cryogenic Technology, New York: John Wiley and Sons Inc., 1963, pp. 170 - 176.


### ARTICLES


Acrivos, A., Babcock, B. D., and Pigford, R. L. "Flow Distributions in Manifolds," Chem. Eng. Science, vol. 10 (1959), pp. 112 - 124.

Alves, G. E. "Cocurrent Liquid-Gas Flow in a Pipe-line Contactor," CEP, vol. 50, no. 9 (1954), pp. 449 - 456.

Anderson, G. H., and Mantzouranis, B. G. "Two Phase Flow Phenomena - I," Chem. Eng. Science, vol. 12 (1960), pp. 109 - 126.

Anderson, J. D., Bollinger, R. E., and Lamb, D. E. "Gas Phase Controlled Mass Transfer in Two Phase Annular Horizontal Flow," A. I. Ch. E. Journal, vol. 10, no. 5 (1964), pp. 640-645.

Anderson, R. J. and Russel T. W. F. "Designing for Two-Phase Flow," Chemical Engineering, December 6 (1965), pp. 139 - 144, December 20 (1965), pp. 99 - 104, January 3 (1966), pp. 87 - 90.

Baker, O. "Multiphase Flow in Pipelines," The Oil and Gas Journal, vol. 56 (1958), pp. 156 - 167.

Baker, O. "Simultaneous Flow of Oil and Gas," The Oil and Gas Journal, vol. 53 (1954), pp. 185 - 195.

Bankoff, S. G. "A Variable Density Single-Fluid Model for Two-Phase Flow with Particular Reference to Steam-Water Flow," Journal of Heat Transfer, Transactions of the ASME, November (1960), pp. 265 - 272.

Brown, R. A. S. "The Mechanic of Large Gas Bubbles in Tubes," Canadian Journal of Chemical Engineering, October (1965), pp. 217 - 230.

Cady, P. D. "How to Stop Slug Flow in Condenser Outlet Piping," Hydrocarbon Processing and Petroleum Refiner, vol. 42, no. 9 (1963), pp. 192 - 194.

Calvert, S., and Williams, B. "Upwards Cocurrent Annular Flow of Air and Water in Smooth Tubes," A. I. Ch. E. Journal, vol.1, no. 1 (1955), pp. 78 - 86.

Chenoweth, J. M. and Martin, M. W. "Turbulent Two-Phase Flow," Petroleum Refiner, vol. 34, pp. 151 - 155.

Cichelli, M. T. and Boucher, D. F. "Design of Heat Exchanger Heads for Low Holdup," CEP, vol. 52, no. 5 (1956), pp. 213 - 218.

Collier, J. G. and Hewitt, G. F. "Experimental Techniques in Two-Phase Flow," British Chemical Engineering, vol. 11, no. 12 (1966), pp. 1526 - 1531.

Collier, J. F., Lacey, P. M. C., Pulling, D. J. "Heat Transfer to Two-Phase Gas-Liquid Systems," *Trans. Instn. Chem. Engrs.*, vol. 42 (1964), pp. 127 - 139.

Collier, J. G. and Hewitt, G. F. "Measurement of Liquid Entrainment," *British Chemical Engineering*, vol. 11, no. 12 (1966), pp. 1526 - 1531.

Davis, E. J. and David, M. M. "Two-Phase Gas-Liquid Convection Heat Transfer," *Canadian Journal of Chemical Engineering*, June 1961, p. 99.

Dengler, C. E. and Addoms, J. N. "Heat Transfer Mechanism for Vaporization of Water in a Vertical Tube," *CEP Symposium Series*, vol. 52, no. 18 (1956), pp. 95 - 103.

Dukler, A. E., Wicks, M., and Cleveland, R. G. "Frictional Pressure Drop in Two-Phase Flow," *A. I. Ch. E. Journal*, vol 10, no. 1 (1964), pp. 38 - 51.

Govier, G. W., Radford, B. A., and Dunn, J. S. C. "The Upwards Vertical Flow of Air-Water Mixtures," *The Canadian Journal of Chemical Engineering*, August (1957), pp. 58 - 70.

Greene, J. L. "Symmetrical Piping Arrangement Solves Two-Phase Flow Distribution Problems," *Hydrcarbon Processing*, vol. 46, no. 2 (1967), pp. 141 - 143.

Griffith, P. and Wallis, G. B. "Two-Phase Slug Flow," *Journal of Heat Transfer, Transactions of the ASME*, August (1961), pp. 307 - 320.

Hewitt, G. F., King, I., and Lovegrove, P. C. "Holdup and Pressure Drop Measurements in the Two-Phase Annular Flow of Air-Water Mixtures," *British Chemical Engineering*, vol. 8, no. 5 (1963), pp. 311 - 317.

Hinze, J. O. "Fundamentals of the Hydrodynamic Mechanism of Splitting in Dispersion Processes," *A. I. Ch. E. Journal*, vol. 1, no. 3 (1955), pp. 289 - 295.

Hoopes, J. W., Ssakoff, S. E., Clark, J. J., and Drew, T. B. "Friction Losses in Screwed Iron Tees," *CEP*, vol. 44, no. 9 (1948), pp. 691 - 696.

Hughmark, G. A. "Holdup in Gas-Liquid Flow," CEP, vol. 58, no. 4 (1962), pp. 62 - 65.

Hughmark, G. A. "Pressure Drop in Horizontal and Vertical Cocurrent Gas-Liquid Flow," J. & E. C. Fundamentals, vol. 2, no. 4 (1963), pp. 315 - 321.

Keller, J. D. "The Manifold Problem," Journal of Applied Mechanics, March (1949), pp. 77 - 85.

Kordyban, E. S. "A Flow Model for Two-Phase Slug Flow in Horizontal Tubes," Journal of Basic Engineering, Transactions of the ASME, December (1961), pp. 613 - 618.

Levy, S. "Prediction of Two-Phase Annular Flow with Liquid Entrainment," Int. J. Heat Mass Transfer, vol. 9 (1966), pp. 171 - 188.

Lockhart, N. W. and Martinelli, R. C. "Proposed Correlation of Data for Isothermal Two-Phase, Two Component Flow in Pipes," CEP, vol. 45, no. 1 (1949), pp. 39 - 48.

McDonald, J. S. and Eng, K. Y. "Tubeside Flow Distribution Effects on Heat Exchanger Performance," CEP Symposium Series, vol. 59, no. 41, pp. 11 - 17.

Nicklin, D. J. "Two Phase Bubble Flow," Chemical Engineering Science, vol. 17 (1962), pp. 693 - 702.

Nicklin, D. J., Wilkes, J. O., and Davidson, J. F. "Two-Phase Flow in Vertical Tubes," Trans. Instn. Chem. Engrs., vol. 40 (1962), pp. 61 - 68.

Quandt, E. "Analysis of Gas-Liquid Flow Patterns," CEP Symposium Series, vol. 61, no. 57 (1966), pp. 128 - 135.

Reid, R. C., Reynolds, A. B., Diglis, A. J., Spiewak, I., Klipstein, D. H. "Two-Phase Pressure Drops in Large Diameter Pipes," A. I. Ch. E. Journal, vol. 3, no. 3 (1957), pp. 321 - 324.

Rippel, G. R., Eidt, C. M., and Jordon H. B. "Two-Phase Flow in a Coiled Tubes," I. & E. C. Process Design and Development, vol. 5, no. 1 (1966), pp. 32 - 39.

Russel, T. W. F. and Lamb, D. E. "Flow Mechanism of Two-Phase Annular Flow," The Canadian Journal of Chemical Engineering, October (1965), pp. 237 - 245.

Tsuyana, M. and Taga, M. " On the Flow of the Air-Water Mixture in the Branch Pipe," Bulletin of the Japan Society of Mechanical Engineers, vol. 2, no. 5 (1959), pp. 151 - 156.

Vazsonyi, A. "Pressure Loss in Elbows and Duct Branches," Transactions of the ASME, April 1944, pp. 177 - 183.

Wicks, M. and Dukler, A. E. "Entrainment and Pressure Drop in Concurrent Gas-Liquid Flow: I. Air-Water in Horizontal Flow," A. I. Ch. E. Journal, vol. 6, no. 3 (1960), pp. 463 - 468.

Zenz, F. A. "Minimize Manifold Pressure Drop," Hydrocarbon Processing and Petroleum Refiner, vol. 41, no. 12 (1962), pp. 125 - 130.

## REPORTS

McManus, H. N. Local Liquid Distribution and Pressure Drops in Annular Two-Phase Flow. ASME paper 61-HYD-20, New York: 1961, pp. 1 - 13.

## UNPUBLISHED MATERIAL

Fleming, R. B. "The Effect of Flow Distribution in Parallel Channels of Counterflow Heat Exchangers." Paper No. R-8 presented at the 1966 Cryogenic Engineering Conference at Boulder, Colorado, June 13 - 15, pp. 1 - 18.

Kinard, G. E. "Effects of Plugged Tubes and Tube Ruptures on Plant Performance." Property of Air Products and Chemicals, Inc., June 19, 1967.

Morris, S. M. "Computer Program for Two Phase Cooling Curve, Transport Properties, and Pressure Drops (360 Hetran Program No. D2B010)." Property of Air Products and Chemicals, Inc., July 1966, pp. 1 - 20.

Taylor, B. W. "Esso Libya Bundle Tests." Property of Air Products and Chemicals, Inc., June 13, 1967.

Wilson, K. "Maldistribution in Esso - Libya Exchanger." Property of Air Products and Chemicals, Inc., June 10, 1966.

VITA

Donald W. Woodward was born January 20, 1943 to Dr. & Mrs. Albert T. Woodward of West Chester, Pennsylvania. He attended West Chester Public Schools and received a Bachelor of Science Degree in Chemical Engineering from the Pennsylvania State University in 1964. For two and one-half years following graduation he was employed by the Agri Chem Division of Swift and Company of Chicago, Illinois, as a research engineer. He attended the graduate school of Lehigh University during 1966-67 while working part-time in process design at Air Products. Don is married to the former Virginia Brown and has a daughter, Pamela Sue. He is a member of the American Institute of Chemical Engineers.